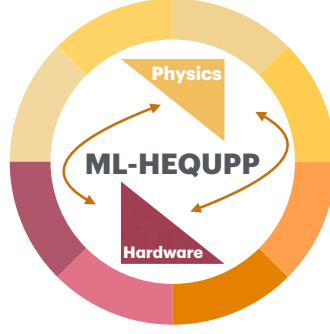


# Machine Learning on Heterogeneous, Edge, and QUantum Hardware for Particle Physics (ML-HEQUPP)



**Editors:** Julia Gonski<sup>1†</sup>, Jenni Ott<sup>2†</sup>, Shiva Abbaszadeh<sup>3</sup>, Sagar Addepalli<sup>1</sup>, Matteo Cremonesi<sup>4</sup>, Jennet Dickinson<sup>5</sup>, Giuseppe Di Guglielmo<sup>6,7</sup>, Erdem Yigit Ertorer<sup>4</sup>, Lindsey Gray<sup>6</sup>, Ryan Herbst<sup>1</sup>, Christian Herwig<sup>8</sup>, Tae Min Hong<sup>9</sup>, Benedikt Maier<sup>10</sup>, Maryam Bayat Makou<sup>11</sup>, David Miller<sup>12</sup>, Mark S. Neubauer<sup>13</sup>, Cristián Peña<sup>6</sup>, Dylan Rankin<sup>14</sup>, Seon-Hee (Sunny) Seo<sup>6</sup>, Giordon Stark<sup>15</sup>, Alexander Tapper<sup>10</sup>, Audrey Corbeil Therrien<sup>16</sup>, Ioannis Xiotidis<sup>17</sup>, Keisuke Yoshihara<sup>2</sup>

**Contributors:** G Abarajithan<sup>18</sup>, Sagar Addepalli<sup>1</sup>, Nural Akchurin<sup>19</sup>, Carlos Argüelles<sup>20</sup>, Saptaparna Bhattacharya<sup>11</sup>, Lorenzo Borella<sup>21,22</sup>, Christian Boutan<sup>23</sup>, Tom Braine<sup>23</sup>, James Brau<sup>24</sup>, Martin Breidenbach<sup>1</sup>, Antonio Chahine<sup>10</sup>, Talal Ahmed Chowdhury<sup>25</sup>, Yuan-Tang Chou<sup>26</sup>, Seokju Chung<sup>27</sup>, Alberto Coppi<sup>21,22</sup>, Mariarosaria D'Alfonso<sup>28</sup>, Abhilasha Dave<sup>1</sup>, Chance Desmet<sup>23</sup>, Angela Di Fulvio<sup>29</sup>, Karri DiPetrillo<sup>12</sup>, Javier Duarte<sup>18</sup>, Auralee Edelen<sup>1</sup>, Jan Eysermans<sup>28</sup>, Yongbin Feng<sup>19</sup>, Emmett Forrestel<sup>31</sup>, Dolores Garcia<sup>17</sup>, Loredana Gastaldo<sup>32</sup>, Julián García Pardiñas<sup>28</sup>, Lino Gerlach<sup>33</sup>, Loukas Gouskos<sup>31</sup>, Katya Govorkova<sup>28</sup>, Carl Grace<sup>34</sup>, Christopher Grant<sup>35</sup>, Philip Harris<sup>28</sup>, Ciaran Hasnip<sup>17</sup>, Timon Heim<sup>34</sup>, Abraham Holtermann<sup>28</sup>, Tae Min Hong<sup>9</sup>, Gian Michele Innocenti<sup>28</sup>, Koji Ishidoshiro<sup>36</sup>, Miao Chen Jin<sup>20</sup>, Jyothisraj Johnson<sup>34</sup>, Stephen Jones<sup>23</sup>, Andreas Jung<sup>37</sup>, Georgia Karagiorgi<sup>27</sup>, Ryan Kastner<sup>18</sup>, Nicholas Kamp<sup>20</sup>, Doojin Kim<sup>38</sup>, Kyoungchul Kong<sup>25</sup>, Katie Kudela<sup>28</sup>, Jelena Lalic<sup>28</sup>, Bo-Cheng Lai<sup>39</sup>, Yun-Tsung Lai<sup>33</sup>, Tommy Lam<sup>40</sup>, Jeffrey Lazar<sup>41</sup>, Aobo Li<sup>18</sup>, Zepeng Li<sup>2</sup>, Haoyun Liu<sup>10</sup>, Vladimir Lončar<sup>28</sup>, Luca Macchiarulo<sup>42</sup>, Christopher Madrid<sup>19</sup>, Benedikt Maier<sup>10</sup>, Zhenghua Ma<sup>18</sup>, Prashansa Mukim<sup>43</sup>, Mark S. Neubauer<sup>13</sup>, Victoria Nguyen<sup>28</sup>, Sungbin Oh<sup>6</sup>, Isobel Ojalvo<sup>44</sup>, Hideyoshi Ozaki<sup>45</sup>, Simone Pagan Griso<sup>34</sup>, Myeonghun Park<sup>46</sup>, Christoph Paus<sup>28</sup>, Santosh Parajuli<sup>13</sup>, Benjamin Parpillon<sup>6</sup>, Sara Pozzi<sup>8</sup>, Ema Puljak<sup>17</sup>, Benjamin Ramhorst<sup>47</sup>, Amy Roberts<sup>48</sup>, Larry Ruckman<sup>1</sup>, Kate Scholberg<sup>49</sup>, Sebastian Schmitt<sup>28</sup>, Noah Singer<sup>37</sup>, Eluned Anne Smith<sup>28</sup>, Alexandre Sousa<sup>50</sup>, Michael Spannowsky<sup>51</sup>, Sioni Summers<sup>17</sup>, Yanwen Sun<sup>1</sup>, Daniel Tapia Takaki<sup>25</sup>, Antonino Tumeo<sup>23</sup>, Caterina Vernieri<sup>1</sup>, Belina von Krosigk<sup>52</sup>, Yash Vora<sup>31</sup>, Linyan Wan<sup>6</sup>, Michael H.L. S. Wang<sup>6</sup>, Amanda Weinstein<sup>53</sup>, Andy White<sup>7</sup>, Simon Williams<sup>51</sup>, Felix Yu<sup>20</sup>

† coordinator

<sup>1</sup> SLAC National Accelerator Laboratory, Menlo Park CA, US <sup>2</sup> University of Hawai'i Mānoa, Honolulu HI, US  
<sup>3</sup> Santa Cruz Institute for Particle Physics, UC Santa Cruz, Santa Cruz, US <sup>4</sup> Carnegie Mellon University,  
Pittsburgh, PA, US <sup>5</sup> Cornell University, Ithaca NY, US <sup>6</sup> Fermi National Accelerator Laboratory, Batavia IL,  
US <sup>7</sup> Northwestern University, Evanston IL, US <sup>8</sup> University of Michigan, Ann Arbor, MI, US <sup>9</sup> University of  
Pittsburgh, Pittsburgh PA, US <sup>10</sup> Imperial College London, London, GB <sup>11</sup> Southern Methodist University,  
University Park TX, US <sup>12</sup> University of Chicago, Chicago IL, US <sup>13</sup> University of Illinois, Urbana-Champaign,  
US <sup>14</sup> University of Pennsylvania, Philadelphia PA, US <sup>15</sup> University of California Santa Cruz, Santa Cruz CA,  
US <sup>16</sup> Université de Sherbrooke, Sherbrooke, Québec, CA <sup>17</sup> CERN, Geneva, CH <sup>18</sup> University of California San  
Diego, California, US <sup>19</sup> Texas Tech University, Lubbock TX, US <sup>20</sup> Harvard University, Cambridge MA, US <sup>21</sup>  
Istituto Nazionale di Fisica Nucleare (INFN), Padova, IT <sup>22</sup> University of Padua, Padova, IT <sup>23</sup> Pacific  
Northwest National Laboratory, Richland WA, US <sup>24</sup> University of Oregon, Eugene OR, US <sup>25</sup> University of  
Kansas, Lawrence KS, US <sup>26</sup> University of Washington, Seattle WA, US <sup>27</sup> Columbia University, New York NY,  
US <sup>28</sup> Massachusetts Institute of Technology, Cambridge MA, US <sup>29</sup> University of Pisa, Pisa, IT <sup>30</sup> (affiliation  
needed for Karri DiPetrillo) <sup>31</sup> Brown University, Providence RI, US <sup>32</sup> Kirchhoff Institute for Physics,  
Heidelberg University, Heidelberg, 69120, DE <sup>33</sup> High Energy Accelerator Research Organization, JP <sup>34</sup>  
Lawrence Berkeley National Laboratory, Berkeley CA, US <sup>35</sup> Boston University, Boston MA, US <sup>36</sup> Tohoku  
University, Sendai, Miyagi 980-8577, JP <sup>37</sup> Purdue University, West Lafayette IN, US <sup>38</sup> University of South  
Dakota, Vermillion SD, US <sup>39</sup> National Yang Ming Chiao Tung University, Taiwan, TW <sup>40</sup> Virginia Tech,  
Blacksburg VA, US <sup>41</sup> Université catholique de Louvain, Louvain-la-Neuve, BE <sup>42</sup> Nalu Scientific LLC, US <sup>43</sup>  
Brookhaven National Laboratory, Upton NY, US <sup>44</sup> Princeton University, Princeton, NJ 08544, US <sup>45</sup> Tokyo  
University of Science, Shinjuku City, Tokyo 162-8601, JP <sup>46</sup> Seoul National University of Science and  
Technology, KR <sup>47</sup> ETH Zurich, CH <sup>48</sup> University of Colorado Denver, Denver CO, US <sup>49</sup> Duke University,  
Durham NC, US <sup>50</sup> Cincinnati University, Cincinnati OH, US <sup>51</sup> Durham University, Durham, GB <sup>52</sup>  
Heidelberg University, Heidelberg, DE <sup>53</sup> Iowa State University, Ames IA, US

## Abstract

The next generation of particle physics experiments will face a new era of challenges in data acquisition, due to unprecedented data rates and volumes along with extreme environments and operational constraints. Harnessing this data for scientific discovery demands real-time inference and decision-making, intelligent data reduction, and efficient processing architectures beyond current capabilities. Crucial to the success of this experimental paradigm are several emerging technologies, such as artificial intelligence and machine learning (AI/ML) and silicon microelectronics, and the advent of quantum algorithms and processing. Their intersection includes areas of research such as low-power and low-latency devices for edge computing, heterogeneous accelerator systems, reconfigurable hardware, novel codesign and synthesis strategies, readout for cryogenic or high-radiation environments, and analog computing. This white paper presents a community-driven vision to identify and prioritize research and development opportunities in hardware-based ML systems and corresponding physics applications, contributing towards a successful transition to the new data frontier of fundamental science.

# Contents

|          |   |           |
|----------|---|-----------|
| <b>1</b> | <b>Introduction</b>   | <b>4</b>  |
| <b>2</b> | <b>Technology</b>   | <b>7</b>  |
| 2.1      | ASICs . . . . .   | 7         |
| 2.1.1    | Co-design of artificial neural networks for real-time feature extraction in AIML65P1 ASIC . . . . .                           | 8         |
| 2.1.2    | In-pixel integration of signal processing and machine learning based data filtering for particle tracking detectors . . . . . | 9         |
| 2.1.3    | Analog Neural Networks for Signal Processing Embedded in the Detector Front-End Electronics . . . . .                         | 10        |
| 2.2      | FPGAs . . . . .   | 12        |
| 2.2.1    | hls4ml project . . . . .  | 13        |
| 2.2.2    | CGRA4ML project . . . . .   | 14        |
| 2.2.3    | SLAC Neural network Language (SNL) . . . . .  | 15        |
| 2.2.4    | Decision Forests for Efficient Edge Inference . . . . .   | 18        |
| 2.3      | Quantum Algorithms, Processors, and Networks . . . . .  | 21        |
| 2.3.1    | Overview of Current Quantum Processor Technologies . . . . .  | 21        |
| 2.3.2    | Quantum Algorithms . . . . .  | 23        |
| 2.3.3    | Quantum Networking, Distributed Quantum Computing and Sensing . . . . .   | 27        |
| 2.4      | Novel Paradigms . . . . .   | 28        |
| 2.4.1    | Embedded FPGAs . . . . .  | 29        |
| 2.4.2    | Analog Compute . . . . .  | 32        |
| 2.4.3    | Open Source Tools for Hardware-Software Co-Design . . . . .   | 35        |
| 2.4.4    | Heterogeneous Pipelines . . . . .   | 37        |
| 2.5      | Analysis Facilities . . . . .   | 38        |
| 2.5.1    | Training Infrastructure for Edge Deployment . . . . .   | 39        |
| 2.5.2    | Model Optimization Workflows . . . . .  | 40        |
| 2.5.3    | Analysis Facility Landscape . . . . .   | 40        |
| 2.5.4    | Data Access Infrastructure . . . . .  | 41        |
| 2.5.5    | Bridging Analysis Facilities and Front-End Deployment . . . . .   | 42        |
| 2.5.6    | Recommendations for Optimal Analysis Facilities . . . . .   | 44        |
| 2.5.7    | Future Directions: Quantum Computing Integration . . . . .  | 44        |
| <b>3</b> | <b>Physics Applications</b>   | <b>46</b> |
| 3.1      | Collider Physics . . . . .  | 46        |
| 3.1.1    | Applications to Vertex Detectors . . . . .  | 46        |
| 3.1.2    | Applications to Tracking Detectors . . . . .  | 49        |
| 3.1.3    | Applications to Calorimetry . . . . .   | 50        |
| 3.1.4    | Applications to Triggers . . . . .  | 56        |
| 3.1.5    | SuperKEKB/Belle II . . . . .  | 59        |
| 3.2      | Dark Matter . . . . .   | 62        |
| 3.2.1    | Hardware AI/ML at the Dark Matter Frontier . . . . .  | 62        |
| 3.2.2    | Exploring AI/ML tools for axion dark matter detection . . . . .   | 64        |
| 3.3      | Neutrino Physics . . . . .  | 65        |
| 3.3.1    | Applications in LArTPCs and DUNE . . . . .  | 65        |
| 3.3.2    | Low-Latency Machine-Learning-Based Supernova Burst Pointing in DUNE . . . . .   | 66        |

|          |   |            |
|----------|---|------------|
| 3.3.3    | Capturing Neutrinos and New Physics at ProtoDUNE with a Machine Learning Online Trigger Algorithm . . . . .       | 67         |
| 3.3.4    | Real-time Anomaly Detection in DUNE . . . . .   | 69         |
| 3.3.5    | Real-time AI for Data Selection in DUNE . . . . .   | 70         |
| 3.3.6    | Smart Time Projection Chamber . . . . .   | 72         |
| 3.3.7    | LArTPC Calibration Using Pre-Trigger Data . . . . .   | 72         |
| 3.3.8    | ML-based self-trigger for the COHERENT experiment for supernova burst and BSM searches . . . . .                  | 73         |
| 3.3.9    | Real-Time, Low-Power Machine Learning for Neutrino Telescopes . . . . .   | 74         |
| 3.3.10   | Efficient Neural Network Architectures for Real-Time Neutrino Telescope Data Processing . . . . .                 | 76         |
| 3.3.11   | Accelerating KamLAND2-Zen’s Search for Majorana Neutrino with Hardware AI Codesign . . . . .                      | 78         |
| 3.4      | Quantum Sensors & Experiments . . . . .   | 80         |
| 3.4.1    | Continuous-variable photonic quantum extreme learning machines for fast collider-data selection . . . . .         | 80         |
| 3.4.2    | Particle Tracking and Active Particle Sensing via Quantum Devices . . . . .                                       | 81         |
| 3.4.3    | Quantum-Enhanced Graph Neural Networks for Particle Tracking in High-Energy Physics . . . . .                     | 83         |
| 3.4.4    | Quantum Sensing Radiative Decays of Neutrinos and Dark Matter Particles . . . . .                                 | 84         |
| 3.4.5    | Axion DM Searches: Quantum Amplifier auto-tuning . . . . .  | 85         |
| 3.4.6    | The Advent of Superconducting Microwire Single Particle Detectors . . . . .                                       | 86         |
| 3.5      | Accelerators . . . . .  | 88         |
| 3.5.1    | Physics-Informed AI for Ultrafast X-Ray Diffraction at SLAC’s LCLS . . . . .                                      | 88         |
| 3.5.2    | AI/ML for Beam Optimization at the UH Accelerator and FEL Facility . . . . .                                      | 89         |
| 3.5.3    | Combining System Models and ML-based Control to Enable New Capabilities in Beam Tuning for Accelerators . . . . . | 90         |
| <b>4</b> | <b>Community &amp; Education</b>  | <b>93</b>  |
| 4.1      | Related Organizations and Initiatives . . . . .   | 93         |
| 4.1.1    | Accelerated AI Algorithms for Data-Driven Discovery (A3D3) . . . . .  | 93         |
| 4.1.2    | Next Generation Triggers (NGT) . . . . .  | 94         |
| 4.1.3    | FastML Community . . . . .  | 95         |
| 4.1.4    | U.S. Higgs Factory Circular Collider Organization . . . . .   | 96         |
| 4.1.5    | Quantum Computing for High-Energy Physics . . . . .   | 97         |
| 4.2      | Workforce Development . . . . .   | 97         |
| 4.3      | Interdisciplinary Impacts . . . . .   | 98         |
| <b>5</b> | <b>Key R&amp;D Topics</b>   | <b>101</b> |
| <b>6</b> | <b>Conclusions</b>  | <b>102</b> |

# 1 Introduction

The scientific ambitions of particle physics over the coming decades, covering precision measurements and discovery-driven experiments across a huge range of energy scales, are tightly coupled to advances in detector instrumentation and computing. The potential impacts of basic research at the most fundamental level are vast and transformational, with the promise of a more detailed understanding of the evolution and fate of the universe. The technological advancements

required for this research also leads to breakthroughs such as magnetic resonance imaging and the World Wide Web, transforming society and improving lives. What’s more, research at the most fundamental level of physics represents a pursuit of inherent human curiosity, arguably responsible for the most broad and enduring advances in scientific understanding and technological innovation.

In recent years, the US particle physics community has sought to articulate these scientific goals and potential enabling technologies through a variety of strategic planning processes, such as the 2021 Snowmass process [1], the 2023 Particle Physics Project Prioritization Panel (P5) report [2], the Department of Energy (DOE) Basic Research Needs (BRN) reports for detector R&D [3], and the AI-native HEP ecosystem vision [4]. These studies collectively point to a new era of experiments which face unprecedented data rates, growing detector complexity, and real-time decision-making requirements, all under increasingly stringent constraints on power, cost, and facility resources. Enabling continued discovery in this environment demands new computing paradigms that maximize physics reach while making efficient use of limited resources.

Advancing to the next stage of fundamental physics requires the integration of several critical emerging technologies. **Artificial intelligence (AI) and machine learning (ML)** are essential, due to their ability to extract complex patterns from high dimensional data, enabling the scaling of human insight to regimes of data volume and complexity that are otherwise inaccessible. In parallel, novel **silicon microelectronics** technologies can improve modern scientific data acquisition systems, determining achievable bandwidth, latency, power efficiency, and reliability from the detector front-end through downstream processing. The integration of AI/ML directly into advanced microelectronics enables real-time inference at the “edge” (i.e. at the source of data), transforming data acquisition (DAQ) from a passive readout into an active, intelligent component of the experiment. **Quantum sensors, networks, and processors** have the potential to fundamentally reshape precision measurement and information processing, enabling new classes of data acquisition and inference beyond the reach of classical systems, while simultaneously serving as platforms for fundamental physics measurements in their own right. Optimal use of these technologies motivates the study of data acquisition architectures that optimize data flow across **heterogeneous computing platforms**, ensuring efficient movement, transformation, and processing of information across classical, accelerated, and quantum resources. The dedicated R&D of these technologies under consideration of particle physics drivers, and the study of their benefits and implementation opportunities into particle physics experiments, is a unique area of study defined here as **Machine Learning on Heterogenous, Edge, and QUantum hardware for Particle Physics (ML-HEQUPP)** (Figure 1).

Achieving the full potential of ML-HEQUPP requires a co-design philosophy that tightly integrates algorithms, hardware, firmware, and systems, as well as close collaboration between physicists and engineers. Rather than treating machine learning models and computing platforms as independent layers, a holistic approach to system design is necessary to optimize performance, latency, power consumption, and reliability.

Investment in ML-HEQUPP technologies for particle physics aligns with U.S. mission priorities in AI/ML and microelectronics, supporting technology transfer, cross-sector partnerships, and international competitiveness. It also strengthens workforce development at the intersection of particle physics, machine learning, and hardware engineering, building specialized talent in high demand sectors across government, academia, national labs, and industry. Furthermore, this program offers a risk-balanced portfolio spanning varying investment timescales: near-term deployment of edge ML capabilities in operating experiments; mid-term design and optimization of future experiments with heterogeneous platforms; and longer-term exploratory work in novel electronics and quantum/hybrid workflows for unprecedented physics reach. The 2025 U.S.

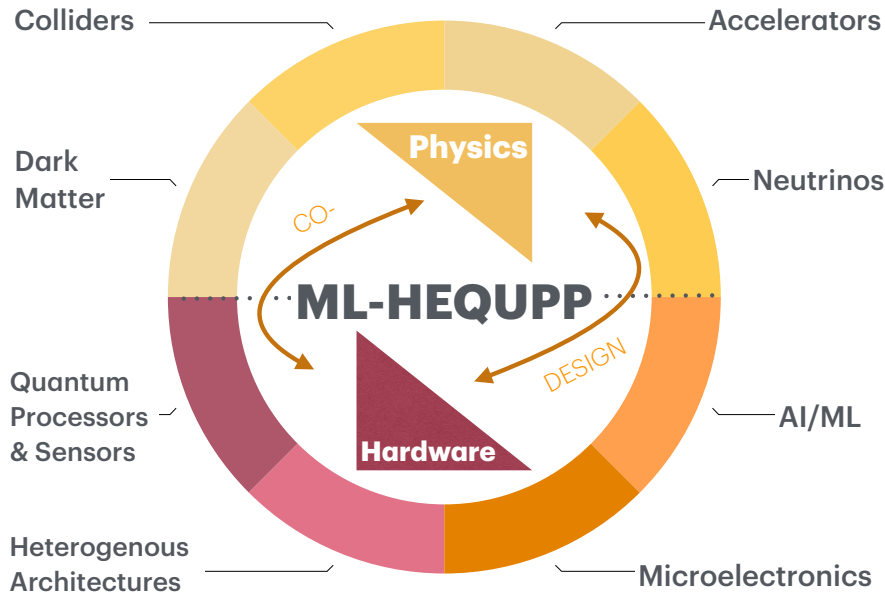


Figure 1: Diagram indicating the physics and hardware areas under the ML-HEQUPP purview.

government announcement of the Genesis mission <sup>1</sup> further underscores the timeliness of these investments by emphasizing the national importance of building secure, scalable, and energy-efficient AI/ML capabilities that can be translated from frontier research into broad economic and societal benefit.

In this spirit, the Machine Learning for Front-End (ML4FE) workshop was launched in 2025 to connect physicists and engineers interested in front-end ML developments and applications to share their latest results, brainstorm future directions, build new collaborations, pursue funding, and share infrastructure. The inaugural workshop was hosted by the University of Hawai'i at Manoa in Honolulu, HI <sup>2</sup> and was held in a hybrid format with a total of 77 registrants (approximately 25 of whom participated in person) spanning physicists and engineers across a variety of specialties. Invitations for speakers and abstract submissions were advertised broadly in related communities; namely technology collaborations, i.e. FastML [5] and the Coordinating Panel on Advanced Detectors (CPAD) <sup>3</sup>; AI interest groups within existing experiments; and future collider study efforts such as the Higgs Factory Circular Collider (HFCC) and international Future Circular Collider Detector Concepts communities. This document captures the content and discussions that took place at the workshop, where it was realized that the “front-end” indication was both ambiguous and limiting. Therefore, the white paper effort was initiated following the workshop with significant expansion to cover work and interests across the ML-HEQUPP community. While it does not match the reach of exercises like a BRN or Snowmass, it encapsulates a new and growing community while providing a means for collaboration and sharing of ideas.

This white paper is organized as follows. The workshop was divided into two core but inter-

<sup>1</sup><https://genesis.energy.gov/>

<sup>2</sup><https://indico.phys.hawaii.edu/event/2506/>

<sup>3</sup><https://cpad-dpf.org/>

related tracks, namely the core technology required for ML-HEQUPP, and the related physics applications, each covered in Sections 2 and 3 respectively. Community context, including interdisciplinary overlaps, and analysis facilities are discussed more in Section 4. Finally, the covered material is synthesized into a set of key R&D topics listed and described in Section 5.

## 2 Technology

The main challenge driving the ML-HEQUPP initiative is the dramatic increase in data rates associated with next-generation scientific facilities. There is a growing need in many experiments for flexible, high-throughput, low-latency processing solutions that can operate under the extreme bandwidth and timing constraints characteristic of modern instruments. The improvement in detector resolution and scale are leading to an increase of data volumes from gigabytes per second to hundreds of terabytes per second. The “record everything” approach that has traditionally used by many experiments has become technically and economically infeasible. In response, scientific data pipelines are now incorporating intelligent real-time filtering steps near the data generation source itself, which preserve salient scientific information while reducing data streams to manageable rates. Generally, addressing this challenge can require a distributed and heterogeneous computing ecosystem that spans detectors, front-end electronics, and offline computing infrastructure. Details of the implementation can make use of Application-specific integrated circuits (ASIC), Field Programmable Gate Arrays (FPGA), embedded processors, Graphics Processing Units (GPU), and other specialized compute platforms, depending on the constraints specific to a given application.

Several science-driven examples demonstrate the potential and benefits this distributed approach, from the edge to the data center. Attosecond streaking detectors requires MHz-rate reconstruction of ultrafast X-ray pulses at the SLAC Linac Coherent Light Source (LCLS); fusion devices like DIII-D benefit from real-time prediction of disruptive events; and high-energy physics applications at the Large Hadron Collider (LHC) rely on intelligent triggers to reduce overwhelming event rates. In these examples and more, this community emphasizes that real-time and edge/distributed machine learning is required to manage data volumes and support responsive experimental control. Furthermore, the technological approaches described here collectively support efficient, scalable, on-and-near detector intelligence to meet the physics demands of modern experiments.

### 2.1 ASICs

**Contributors: Giuseppe Di Guglielmo, Erdem Ertorer, Christian Herwig, Prashansa Mukim, Benjamin Parpillon, Marco Carminati**

ASICs are a key enabler to push machine learning into the detector front end, where extreme bandwidth and latency constraints increasingly force a shift from “record everything” toward real-time decisions at the sensor boundary. As data rates climb from GB/s to TB/s, custom silicon offers the most direct path to low-latency, low-power, and tightly integrated processing that can operate close to the signal source and reduce downstream data movement. In this regime, successful ML deployment is rarely a simple “port” of a software model; it requires co-design, where model structure, numerical precision, and hardware architecture are optimized together under stringent area and power budgets.

This section highlights three complementary ASIC approaches to edge intelligence. First, AIML65P1 demonstrates per-channel digital feature extraction with an embedded neural net-

work and a synthesis-driven, hardware-aware optimization loop. Second, SmartPix illustrates in-pixel signal processing and fully parallel ML-based filtering for tracker readout, enabling data reduction at the bunch-crossing scale. Third, analog neural networks provide an alternative compute paradigm that can eliminate or reduce A/D overhead for specific workloads by embedding multiply-accumulate operations directly in charge-domain circuits. We close by noting emerging open-source EDA and automation ecosystems that can broaden access to ASIC prototyping and accelerate iteration on ML-centric front-end designs.

### 2.1.1 Co-design of artificial neural networks for real-time feature extraction in AIML65P1 ASIC

AIML65P1 [6] is a smart readout application specific integrated circuit (ASIC), developed at BNL to address the growing data challenges in modern physics experiments. As detector technologies advance, front-end systems must process exceedingly large data volumes, making real-time data reduction and intelligent signal processing close to the signal source essential. Embedding AI/ML capabilities directly into front-end ASICs enables early feature extraction, adaptive filtering, discrimination of signal from background, and other non-linear processing steps that significantly reduce downstream bandwidth while improving physics reach.

AIML65P1 is fabricated in a 65-nm CMOS process, and integrates 23 independent channels, each containing a complete analog and digital processing chain. The chip layout and architecture is shown in Fig. 2. At the front-end, a charge-sensitive amplifier followed by a 3rd-order analog anti-aliasing filter shapes the detector signal [7]. A 12-bit hybrid analog-to-digital converter (ADC) [8] then digitizes the waveform, feeding a digital-back end that includes a programmable finite impulse response (FIR) shaping filter, waveform alignment and baseline subtraction circuitry. The digital signal processing blocks are followed by an embedded Artificial Neural Network (ANN)—a two-layer multilayer perceptron network with programmable weights and biases—that can be configured for regression (e.g., pulse amplitude and decay-time estimation) or classification (e.g., pulse shape discrimination or signal/noise separation) [9]. The ANN enables per-channel intelligent processing, effectively functioning as an edge AI engine within each readout channel.

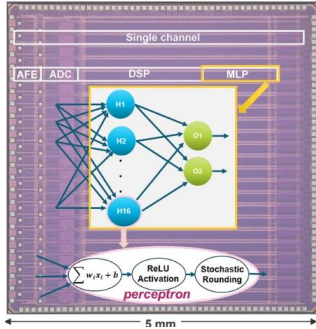


Figure 2: AIML65P1 ASIC layout and architecture

To support flexible on-chip learning and deployment, the ANN parameters were quantized to 8-bits through an optimization pipeline. The ASIC additionally implements stochastic rounding [10] in hardware, enabling in-situ learning and ensuring unbiased gradient behavior even under quantized arithmetic—a crucial requirement for effective training with low-precision weights, activations, and partial sums. Each channel contains nearly 2000 programmable bits, accessi-

ble via an I<sup>2</sup>C interface. The chip has been fabricated and is currently undergoing testing and performance characterization.

A major component of this work is the co-design strategy that guided the ANN architecture [11]. Because area and power budgets in front-end ASICs are extremely constrained, neural networks cannot be over-designed; the ML architecture must be co-optimized with the hardware implementation. The team developed an automated, hardware-aware co-design framework that uses multi-objective Bayesian optimization to explore the joint space of ANN parameters (depth, width, bit precision) and synthesis strategies. Importantly, the optimization loop incorporated actual synthesis results rather than analytical proxies, enabling accurate evaluation of area, power, and timing. Over 22,000 networks were trained and synthesized to map the Pareto frontier across accuracy, area, and latency. From this exploration, key design insights emerged: for in-pixel or in-channel implementations, two-layer networks provide the best trade-off; quantization must be carefully allocated across layers; and hardware-aware training is vital for high-precision regression tasks.

In conclusion, the AIML65P1 ASIC integrates low-noise analog front-ends, early digitization, non-linear digital signal processing, embedded machine learning, and a rigorous co-design methodology to realize next-generation AI-enabled front-end electronics. The design philosophy centers on shifting signal processing into the digital domain at the earliest feasible stage, enabling real-time intelligent data reduction, adaptive system behavior, and ultimately improved scientific discovery potential.

### 2.1.2 In-pixel integration of signal processing and machine learning based data filtering for particle tracking detectors

Pixel detectors at modern colliders generate data volumes that exceed transmission and trigger bandwidth constraints. The Level-1 Trigger (L1T) Correlator uses information from HGCal clusters to form high-level physics quantities and reduce data bandwidth. However, pixel information is not used at Level-1 due to latency and throughput limits, reducing sensitivity to displaced signatures and low-momentum ( $p_T$ ) clusters, which should be rejected by the trigger as they do not carry relevant physics information. We present a readout ASIC prototype that integrates charge processing and machine-learning data filtering directly in-pixel, enabling on-detector data reduction at the bunch-crossing scale.

**Architecture.** The ASIC, fabricated in 28 nm bulk CMOS, implements two  $32 \times 8$  superpixel matrices at  $25 \mu\text{m}$  pitch. The overall architecture is illustrated in Figure 3 and described in detail in Refs. [12, 13, 14]. Each pixel comprises a charge-sensitive preamplifier followed by a 2-bit flash ADC operating at 40 MHz. Comparator thresholds  $V_{th[0,1,2]}$  define transition levels and are adjustable off-chip. Pixel outputs are latched, encoded, and projected into 16 compressed row buses, preserving spatial information while reducing bit width by an order of magnitude. A fully parallel two-layer neural network, implemented purely in combinational logic, classifies local clusters without cycle-to-cycle latency. The network is derived from QKeras quantization and synthesized via hls4ml [15, 16] and Siemens Catapult HLS [17].

**Analog performance.** Charge is injected via programmable in-matrix capacitors to emulate realistic clusters. Repeated S-curve scans across injected charge extract both threshold dispersion and Equivalent Noise Charge (ENC). The prototype exhibits  $\text{ENC} \sim 58 \text{ e}^-$  with an average conversion gain of  $58.5 \mu\text{V}/\text{e}^-$ . These values confirm preamplifier stability and comparator resolution and align with expectations from simulation.

**On-chip ML filtering.** Cluster profiles derived from CMS simulation were injected into the pixel matrix and propagated through the digital chain. Across 104 test patterns, ASIC outputs match RTL at 99.86%, demonstrating robust inference, correct timing, and a fully functioning

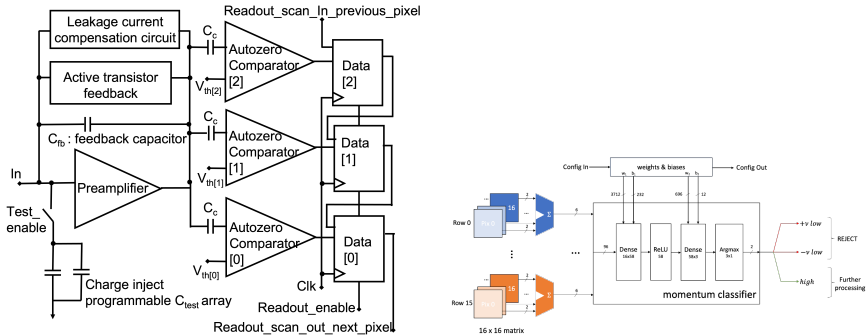


Figure 3: Overview of the SmartPix architecture: analog pixel front-end (left) and digital projection with embedded in-pixel classifier (right).

DAQ readout.

The results demonstrate that in-pixel charge processing combined with embedded machine learning can be realized in physical silicon. By performing data reduction at the earliest stage of readout, this approach offers a promising path to overcome bandwidth and latency limitations that currently restrict the use of tracker information in real-time decisions. These developments open the door to new data-driven readout strategies for future high-energy physics experiments.

While final performance studies are ongoing, this prototype already exemplifies a broader shift in detector design: intelligence is being pushed directly into the front end. By co-optimizing machine-learning models and custom ASIC architectures, pixel detectors can perform real-time feature extraction and data suppression at the point of capture, easing bandwidth and latency bottlenecks that have historically limited physics sensitivity. Equally important, the development of this chip has strengthened a new model of industry–laboratory co-design—most notably through our collaboration with Siemens EDA—which has been essential for advancing ML-centric hardware design methodologies. Together, these efforts chart a path toward scalable, data-driven readout systems for next-generation collider experiments.

### 2.1.3 Analog Neural Networks for Signal Processing Embedded in the Detector Front-End Electronics

The shift of signal processing from the digital back-end to the sensor front-end is a consolidating trend, common to several technological domains of electronics, spanning from low-power IoT (Internet of Things) to wearable devices. In the realm of radiation detectors, the main motivation for the adoption of this paradigm is the reduction of the data throughput by means of pre-processing close to the signal source, i.e. in the detector. In-sensor processing allows for reduction of the amount of raw data to be transmitted, offering significant savings in terms of signal lines, bandwidth, power, data storage and digital processing (mostly based on FPGA) requirements. Two contexts for which this shift is relevant are high-energy physics and medical imaging. Since other sections address the former, here the focus is on the latter.

The application which provides the context for the electronics described here is that of nuclear medical imaging for diagnostics, in particular of tomographic techniques based on the detection of gamma rays such as PET (Positron Emission Tomography) and SPECT (Single-Photon Emission Computed Tomography). The field of view of scanners is getting longer, targeting total-body imaging, thus increasing the number of detection modules from tens to hundreds, with thousands of channels and thus making more and more crucial streamlining the data flow by means of in-

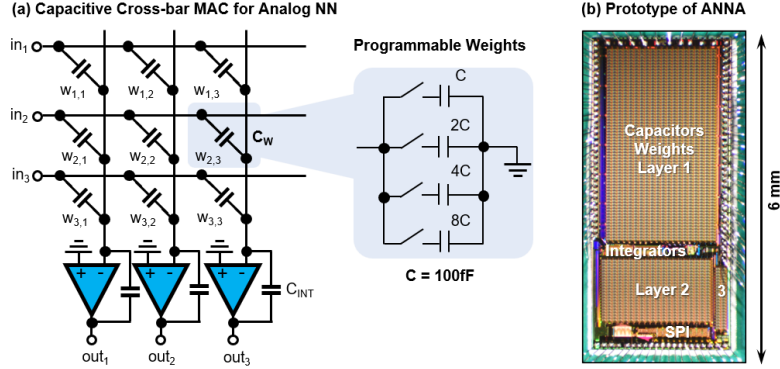


Figure 4: (a) Charge-mode implementation of MAC operation for neurons with capacitive weights and its realization (b) in a legacy  $0.35 \mu\text{m}$  technology share by SiPM front-ends.

sensor pre-processing.

Artificial neural networks (ANN) have emerged as excellent tools for image processing, suitable to address the challenges of medical imaging, at multiple levels. Considering a gamma-ray detector consisting of scintillators readout by arrays of photodetectors, usually SiPM (Silicon PhotoMultipliers), ANN are employed to estimate the scintillation position within the crystal.

The core operation of each neuron in the simplest ANN topology (a feedforward perceptron) is the weighted sum of the inputs (MAC - Multiply and Accumulate) with a bias, followed by a non-linear activation function. An analog implementation of MAC can be performed by manipulating electric charge. The input voltages are converted into charge by means of capacitors connected to the virtual ground of an integrator summing all input signals and converting the sum back into a voltage across the feedback capacitor. The weights are encoded in the values of capacitance, which, for instance, can be made programmable through a set of switched capacitors in parallel (Fig. 4). The value of weights, discretized in the first implementation in 4 bits + sign) is stored in local latches (inside the perceptron), adopting the advantageous in-memory computing paradigm. The activation function can be realized by means of the integrator saturating response (thus realizing a ReLU) or by adding non-linear stages (with sigmoidal response) in cascade. A first prototype of a fully-connected 3-layer ANN was designed [18] and fully characterized [19]. It features 64 inputs (meant to read a standard  $8 \times 8$  arrays of SiPMs), 2 hidden layers with 20 neurons each and 2 outputs, which in this case represent the  $x$  and  $y$  coordinates of the scintillation point in the crystal. The non ideal behavior of the analog components, including operational amplifiers and switches, has to be carefully assessed and embedded in the training model to achieve better accuracy [20]. This first implementation was realized in the legacy node CMOS  $0.35 \mu\text{m}$ , still used for analog front-end thanks to good noise performance. Thus, the potential for a monolithic integration of the ANN with front-end electronics for SiPM [21, 22], is demonstrated. Here the LSB of weights is  $100 \text{ fF}$ . With a  $10 \text{ MHz}$  clock timing the ASIC, the total inference time is  $4.6 \mu\text{s}$  and the power consumption is  $16.8 \text{ mW}$ , corresponding to an energy cost of  $76 \text{ nJ}$  per inference and an efficiency of  $\sim 50 \text{ GOPS/W}$ . Such an efficiency places this result an order of magnitude below what offered by FPGA-based, but the energy cost of A/D conversion of 64 signals, avoided by the ASIC, is not included in the comparison. Moreover, a new improved topology has been designed in a more scaled node ( $110 \text{ nm}$ ), with a different recursive topology and improved integrator, based on an CMOS inverter allowing lower power consumption and smoother non-linear response [23].

**Open-Source ASIC Design: Tools, Automation, and Testbed Infrastructure** Open-source Electronic Design Automation (EDA) tools eliminate commercial licensing costs (often exceeding \$1M annually per institution), democratizing ASIC development for academic collaborations. The OpenROAD project [24, 25] provides complete Register Transfer Level (RTL)-to-GDSII flows with multiple open Process Design Kits (PDKs): predictive nodes (FreePDK 45nm, ASAP 7nm) for early-stage research and production-ready nodes (SkyWater 130nm, GlobalFoundries 180nm) for fabrication. The SODA Synthesizer exemplifies this fully open approach, providing Python-to-GDSII compilation through Multi-Level Intermediate Representation (MLIR)-based frontend, Bambu High-Level Synthesis (HLS) backend, and OpenROAD physical design [26], enabling automated synthesis of arbitrary Python algorithms including data preprocessing, control logic, ML inference, and data formatting stages.

Building on these open-source tools, the End-to-end Co-design for Performance, Energy Efficiency, and Security in AI-enabled Computational Science (ENCODE) initiative addresses the next challenge: reducing chip design complexity and turnaround time [27]. ENCODE’s Intelligent Hardware Design thrust researches novel ML-driven optimization algorithms and scalable co-optimization methodologies to drastically reduce design time for advanced packaging technologies including chiplet-based systems and 3D integration. By leveraging tools like SODA and OpenROAD within automated design flows, ENCODE enables rapid exploration of design spaces that would be prohibitively time-consuming with manual approaches. The Advanced Architecture Testbed thrust establishes verification/validation methodologies and physical testbed capabilities for pre-silicon characterization and post-silicon validation. The expectation is that this will soon enable access to low-cost fabrication for prototyping new research ideas.

For HEP applications, this integrated ecosystem democratizes custom ASIC development: from detector-specific readout ASICs and ML inference accelerators to radiation-hardened designs requiring rapid design iteration and validation. Open-source flows facilitate integration of radiation-hardening techniques (Triple Modular Redundancy, error correction, specialized standard cell libraries) without proprietary tool restrictions, while automated design methodologies reduce expertise barriers and development cycles. Combined testbed access addresses the fabrication cost and complexity challenges that have historically limited academic ASIC research, enabling HEP collaborations to prototype custom designs for future detector systems considering Total Ionizing Dose (TID), Single-Event Effects (SEE), and thermal management from early design stages.

## 2.2 FPGAs

**Contributors: G Abarajithan, Javier Duarte, Abhilasha Dave, Ryan Kastner, Zhenghua Ma, Benjamin Ramhorst, Sioni Summers**

FPGA chips are the technology of choice in high energy physics (HEP) experiments for real-time trigger systems as well as situations where electronic controls need to be reconfigurable. The configurable integrated circuit allows for customized parallel operations on real-time data. They allow for more parallelism in algorithm execution compared to CPU and GPU at the expense of added complexity from the circuitry involved in implementation. They allow for more flexibility as reprogrammable devices compared to ASIC chips as the logic blocks in the silicon fabric can be dynamically “field programmed” through the interconnects. The number of logic gates have risen exponentially, from thousands in the 1980s to tens of millions today, as well as specialized compute units, such as AMD’s AI engine tiles with specific setups to optimize DSP usage. As discussed later in this document, there are new approaches that expand and create hybrid systems where FPGA mingles with new technologies, such as embedded systems.

Nevertheless, FPGAs will continue to be a staple of high energy physics. We present a few ways that are being used and some of the novel approaches that have arisen in the field.

### 2.2.1 hls4ml project

Machine learning has become ubiquitous in edge and real-time systems, creating a growing demand for efficient, low-latency hardware capable of meeting strict latency, resource, and power constraints. While FPGAs and ASICs deliver high performance and energy efficiency for such workloads, their development remains complex and requires significant expertise. `hls4ml` [16, 28] is a flexible, open-source platform that addresses these hardware development challenges by converting high-level neural networks from PyTorch, Keras, or similar frameworks into high-level synthesis (HLS) kernels suitable for deployment on FPGAs and ASICs.

`hls4ml` is structured in a modular fashion, following the design of modern compilers. The overall model conversion and compilation flow is illustrated in Figure 5. Models from supported frameworks are first translated into a unified intermediate representation (IR), which captures the computation graph and layer configurations independently of the model framework or target hardware. The IR then undergoes a series of hardware-aware optimizations, including precision adjustment, data layout transformation, and operator fusion, producing a computation graph optimized for dataflow inference on the target platform. The final hardware design is obtained by composing templated implementations of the optimized operators, which can be configured to balance between latency and resource consumption. When synthesizing the hardware, `hls4ml` abstracts the interaction with EDA tools such as Vivado and Quartus, automating synthesis, placement, and routing, allowing users to generate a deployable bitstream in a few lines of Python code.

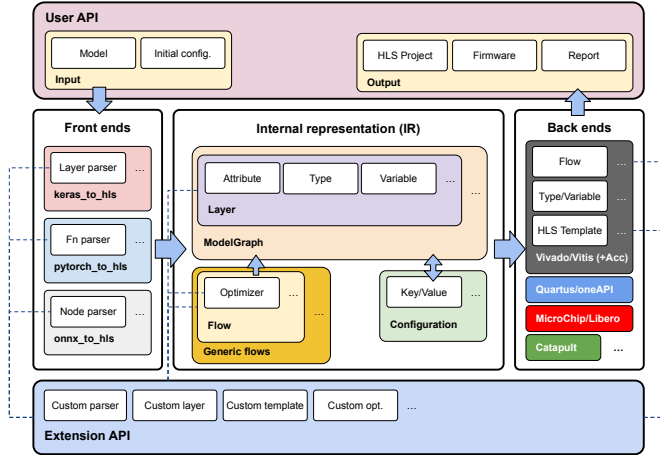


Figure 5: `hls4ml` model conversion flow; reproduced from [28].

To reduce resource utilization and inference latency, `hls4ml` emphasizes the use of quantization and low-precision arithmetic. `hls4ml` can directly parse models from popular quantization-aware training (QAT) libraries, including QKeras [29] and Brevitas. Complementary tools developed by the same community, such as heterogeneous quantization (HGQ) [30] and DSP-aware pruning [31], provide hardware-aware compression techniques that can further reduce resources when targeting FPGAs. Finally, `hls4ml` allows users to configure precision heterogeneously on a per-layer and per-variable basis, enabling fine-grained post-training quantization (PTQ) that

tailors numerical precision to the sensitivity of each operation.

`hls4ml` supports a broad set of neural network architectures, including multilayer perceptrons, convolutional networks, recurrent networks, and more recently, transformers. While most standard layers are fully supported, custom operations can be incorporated through the extension API, which allows users to provide custom HLS implementations of specific operators. `hls4ml` differentiates itself from other hardware acceleration platforms through its support for multiple frontends (i.e., Keras, PyTorch, and QONNX [32]), multiple FPGA backends (e.g., Vitis HLS and Intel oneAPI), and an ASIC backend through Siemens HLS. More recently, `hls4ml` has been extended with support for Google XLS and the Libero backend for radiation-hard FPGAs.

Targeting FPGA deployments, `hls4ml` has been used to accelerate ML in high-energy physics experiments [33, 34], spacecraft [35] and autonomous vehicles [36], quantum computing [37] and heart signal monitoring [38]. In addition, `hls4ml` has been used to generate ASIC designs for a number of on-detector frontend applications, including data compression using a neural network encoder for the CMS high-granularity calorimeter (HGCal) [39]. Similarly a “smart pixel” readout integrated circuit (ROIC) was prototyped using `hls4ml` with an implementation of a neural network to process 256 pixels to determine the momentum of the particle track [40, 41]. These frontend applications underscore the unique capabilities of `hls4ml` and the need for hardware-model codesign for the next generation of experiments.

### 2.2.2 CGRA4ML project

CGRA4ML [42] is an open-source, modular hardware/software co-design framework designed to implement deep neural networks (DNNs) for scientific edge computing applications. While existing tools like HLS4ML [43] [16] and FINN [44] excel at small, low-latency models, they struggle to scale to deeper networks due to their layer-by-layer dataflow architecture, which consumes increasing hardware resources as model depth grows. CGRA4ML addresses this by employing a lightweight and highly parameterizable Coarse-Grained Reconfigurable Array (CGRA), shown in Fig.6 that reuses processing elements (PEs) across layers, enabling deployment of larger models such as ResNet-50 and PointNet on FPGAs and ASICs.

The framework provides a holistic, full-stack infrastructure, as shown in Fig. 7. Central to this flow is a modular and extensible intermediate representation (IR) based on the concept of “bundles”. These are deterministic units of execution that encapsulate groups of DNN layers, facilitating clean hardware/software partitioning. Scientists define and train quantized models using a Python API based on QKeras, which supports sub-8-bit quantization-aware training. The frontend decomposes these models into these bundles to bridge the gap between high-level models and hardware. Compute-intensive operations, such as convolutions and matrix multiplications, are offloaded to the CGRA, while complex pointwise operations and edge cases are handled by the host CPU.

Architecturally, CGRA4ML generates synthesizable, vendor-agnostic SystemVerilog RTL. The CGRA engine (Fig.6) features a 2D array of PEs where columns can dynamically regroup at runtime to process varying convolution kernel widths and output channels. It includes a weight cache with ping-pong buffers for full throughput and a pixel shifter that exploits vertical data locality to reduce required input bandwidth. A key contribution is the automated generation of C runtime firmware that manages the unified dataflow and coordinates software-side tensor operations across diverse processors like ARM, RISC-V, and x86. For verification, the framework uses a DPI-C-enabled suite that runs the production firmware in-the-loop with the RTL simulation. This allows users to emulate real-world conditions, such as randomized memory congestion, to ensure bit-accurate parity between the software model and physical implementation.

CGRA4ML has been experimentally validated on AMD-Xilinx FPGAs and Cadence ASIC

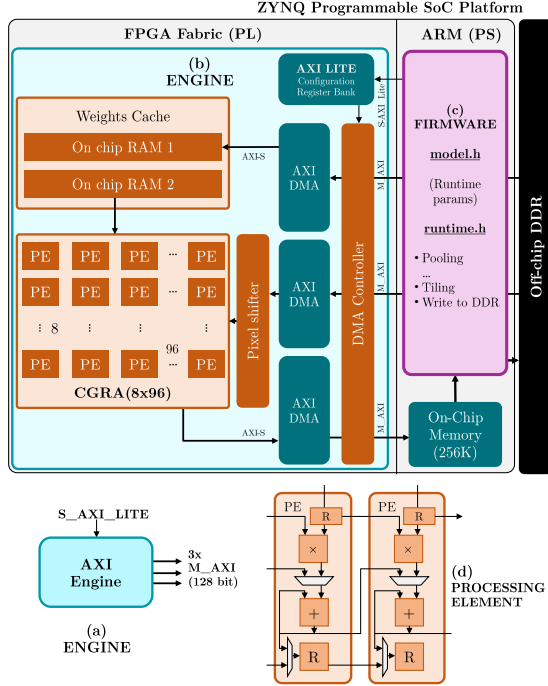


Figure 6: The CGRA4ML architecture features a CGRA engine with three 128-bit AXI Manager ports and parameterizable PEs, bit widths, and weights cache. The PEs are kept small to increase compute density. CGRA4ML offloads compute-heavy tasks to hardware while emitting ARM-based software for pixel-wise operations and edge cases.

flows. Iso-resource microbenchmarking on a Pynq-Z2 at 150 MHz (Fig. 8) shows that while HLS4ML excels at small workloads, fitting larger workloads requires an exponentially increasing reuse factor, and a  $16 \times 16$  CGRA4ML array maintains stable latency and higher throughput when extreme reuse is required to meet resource limits. Deployment is further streamlined via automated TCL scripts that handle synthesis, floorplanning, and SoC integration, facilitating a rapid transition from research prototypes to silicon realization. CGRA4ML also provides an integration with Ibex SoC [45], a popular RISC-V platform. By filling the gap between small-model dataflow tools and traditional 8-bit AI accelerators, CGRA4ML enables the scientific community to move more sophisticated processing to the extreme edge hardware.

### 2.2.3 SLAC Neural network Language (SNL)

Modern high-energy physics experiments face massive real-time data from advanced sensors, and machine learning is increasingly used at the detector edge to process, filter, and classify this information efficiently. To harness this potential, we introduce the SLAC Neural Network Library (SNL) [46, 47, 48, 49, 50], a lightweight, high-performance ML inference framework tailored for deployment on FPGAs in low-latency, high-throughput environments. SNL bridges the gap between widely used training platforms—such as Keras, TensorFlow, and PyTorch and the hardware constraints of edge devices by providing a seamless workflow from model training to FPGA inference. Critically, SNL enables dynamic reloading of neural network weights and biases without requiring re-synthesis or reconfiguration, facilitating rapid model iteration and adaptive

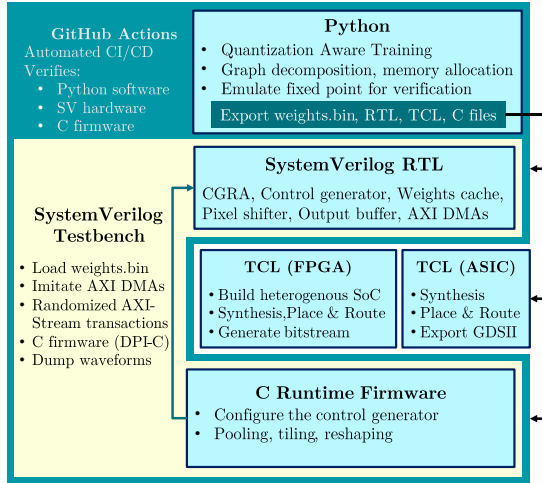


Figure 7: Python API utilizes QKeras to extract fixed-point tensors, generating binary weights, model specifications, vendor-agnostic SystemVerilog RTL, C firmware, and TCL toolflows. A DPI-C verification suite and CI/CD pipeline validate the integrated hardware/software system, emulating real-world memory congestion.

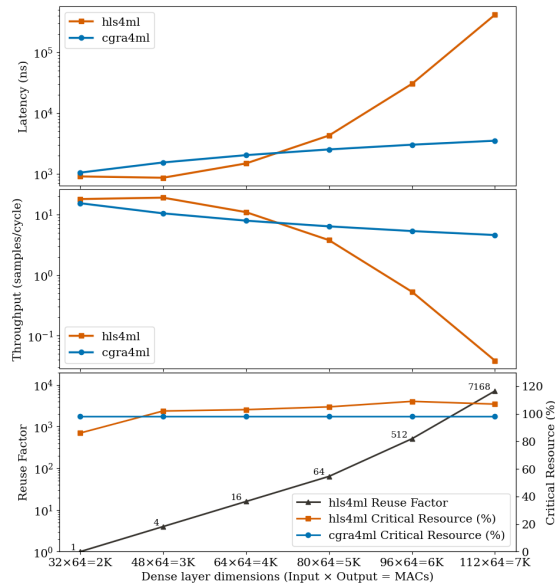
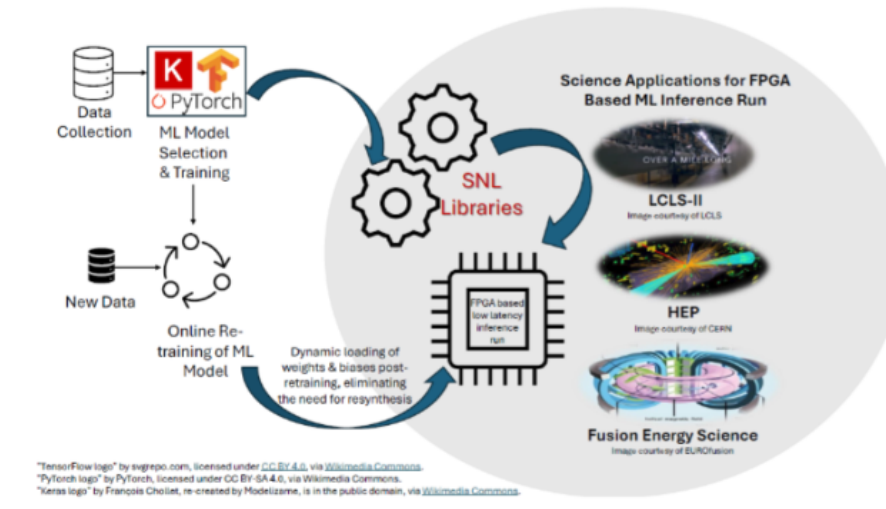


Figure 8: Iso-resource microbenchmarking on Pynq-Z2 compares a 16×16 CGRA4ML array against HLS4ML. While HLS4ML requires exponential reuse factors to fit larger workloads, causing performance to suffer, CGRA4ML performs better at high-reuse conditions by maintaining stable latency and higher throughput.



inference strategies. Developed using High-Level Synthesis (HLS) in C++, SNL provides a Keras-inspired API and supports neural networks with tens of thousands of parameters, depending on architectural complexity and available FPGA resources. With end-to-end latencies ranging from microseconds to a few milliseconds, SNL offers a pipelined, streaming dataflow architecture that balances low-latency processing with high frame-rate requirements positioning it as a key enabler for next-generation edge AI applications in scientific research and beyond.

- Provides specialized set of libraries for deploying ML inference to FPGA
- Using High-Level-Synthesis (HSL): C++ programming of FPGA
- Supports Keras like API for layer definition
- Dynamic reloading of weights and biases to avoid re-synthesis
- Supports 10s of thousands of parameters or more depending on latency requirements for the inference model
- Total end to end latency of couple of usec to couple of millisecond.
- Streaming interface between layers.
- Allow for pipeline of the data flow for a balance of latency vs frame rate
- Library approach allows for user/application specific enhancements

### **Bridging the Gap Between Software Training and Hardware Deployment: A Fundamental Challenge**

Modern high-energy and photon science instruments, such as those at LCLS-II, generate terabytes of data per second, necessitating real-time machine learning at the detector edge for intelligent data reduction and decision-making, though deploying these models on edge hardware remains challenging.

Software frameworks such as Keras, TensorFlow, and PyTorch have revolutionised model development by enabling rapid prototyping, expressive architectures, and efficient training on

GPUs, enabling highly parameterised models optimised primarily for accuracy with abundant resources. In contrast, deployment platforms such as field-programmable gate arrays (FPGAs) operate under strict constraints on logic utilisation, on-chip memory, bandwidth, latency, and energy consumption. This mismatch frequently exposes a profound disconnect between software-first model design and hardware feasibility. Simply converting a trained model into a hardware-compatible representation is rarely sufficient; instead, successful deployment requires a fundamental shift in how models are conceived, optimised, and validated.

Addressing this challenge requires a hardware-aware design philosophy in which model capacity, parameter efficiency, and inference cost are considered alongside accuracy from the earliest stages of development. Excessively large models often contain significant redundancy, and careful analysis of model capacity can reveal opportunities to enhance parameter efficiency while mitigating overfitting. Quantisation can also dramatically reduce memory footprint and computational complexity with minimal impact on accuracy. While pruning is a widely used technique for removing non-essential parameters, it is currently not supported within SNL due to the challenges associated with efficiently implementing sparse representations on FPGA hardware. In practice, comparable benefits can often be achieved through careful architectural simplification and capacity control. Additional gains can be realised through preprocessing at the data source, knowledge distillation, and focusing on inherently lightweight and resource-efficient algorithms, rather than retrofitting for deployment.

A compelling example of this co-design philosophy is provided by the LCLS-II SpeckleNN [47] application. In this use case, neural networks are employed to analyse diffraction patterns generated by molecular imaging experiments and to decide, in real time, whether individual frames contain scientifically valuable information that should be retained or vetoed. The original GPU-based SpeckleNN model achieved 94% accuracy and 98% data reduction but, with 5.5 million parameters, was too large for FPGA deployment at the detector edge. Using SNL and a hardware-aware optimization process, the model was re-engineered to 65,000 parameters, maintaining 91% accuracy while improving compression to 98.8%, and enabling FPGA deployment with microsecond latency. This example illustrates how modest sacrifices in accuracy can yield substantial gains in deployability and overall system performance. Similar efforts are underway in the domain of collider physics, where expensive transformer-based learning for classification of BSM event signatures can be replaced by lightweight MLP Mixer [51] models, offering similar performance while eliminating expensive operations.

#### 2.2.4 Decision Forests for Efficient Edge Inference

Ensembles of Decision Trees - Decision Forests - are a class of Machine Learning models that maintain a good balance of performance and efficient inference in hardware. While various flavours of Neural Network architecture excel on low-level data, Decision Forests have remained state of the art in tasks on tabular data [52, 53], only recently being superseded in performance by transformer architectures. At the same time, Decision Forests can be extremely lightweight ML models, making them suitable for constrained inference for edge applications. Decision Forests have been shown to be robust against irrelevant features, making them achieve good out-of-the-box performance, and also able to perform well in anomaly detection tasks [54]. In the domain of edge ML brought about by tools such as `hls4ml`, `CGRA4ML`, and `SNAC-PAC`, Decision Forests especially shine in extremely constrained applications. In these cases, resource usage of 100 FPGA LUTs, latency of  $\sim 10$ ns, and power consumption in the mW regime are achievable.

Tools for producing hardware synthesizable products from trained Decision Forest models include `fwXmachina` and `conifer` [55]. The `conifer` tool is designed as a source-to-source com-

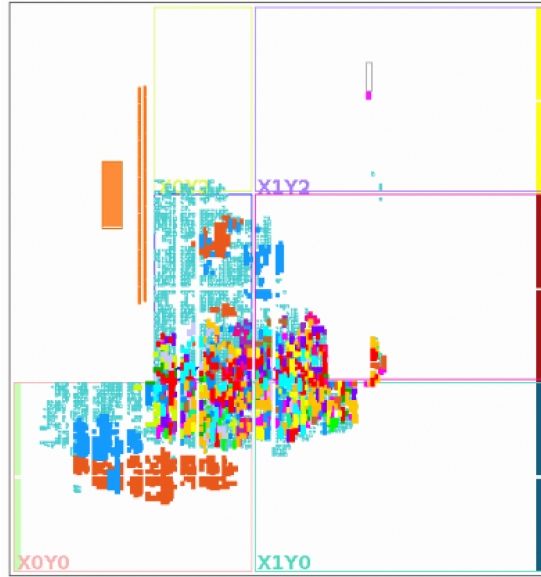


Figure 9: FPGA floorplan of a Boosted Decision Tree with 50 trees with a maximum depth of 3, implemented with `conifer` for an AMD pynq-z2 device. The small multicoloured regions of cells are each of the 50 decision trees, mapped onto independent logic cells for parallel evaluation. The large orange and blue areas are infrastructure for I/O - only provided for acceleration workflows.

piler. Converters are provided for a variety of popular DF training libraries, such as `scikit-learn`, `xgboost`, `yggdrasil` decision forests, and others. Across these libraries, support is available for classification, regression, and anomaly detection (isolation forest) tasks. From the converted model, hardware projects can be produced using implementations in Vitis HLS or VHDL. These implementations target ultra low latency by fully unrolling the DF logic and exploring all decision paths in parallel using boolean logic. The Vitis HLS implementation targets AMD/Xilinx devices, and the VHDL implementation enables support for other FPGA vendors, and even ASIC toolflows. Additional infrastructure is provided for producing out-of-the-box FPGA accelerators with AXI interfaces for high throughput, low latency BDT inference offloaded from a host CPU. Figure 9 shows an FPGA floorplan of an accelerated model on a pynq-z2 board, also highlighting the parallel logic of the Decision Forest. A third, reprogrammable, implementation is provided, termed the ‘Forest Processing Unit’. This design is implemented with Vitis HLS, but implements a generic DF processor which exposes memories that encode a specific DF model onto an interface such that DF models can be loaded and exchanged at runtime. A C++ and Python implementation are also provided for software emulation and validation.

The `fwXmachina` framework is an open-source toolchain for translating boosted decision tree (BDT) models into ultra-low-latency FPGA implementations suitable for real-time inference in high-energy physics environments such as hardware trigger systems [56]. Originally developed to support nanosecond-scale classification tasks—achieving  $O(10 \text{ ns})$  latency with minimal FPGA resource usage by restructuring BDT logic and exploiting a parallel decision paths architecture, `fwXmachina` has since been extended to support deep boosted trees for regression [57] and interpretable decision-tree-based autoencoders for anomaly detection [58] in trigger systems. Figure 10 shows the parallel decision path structure used for the FPGA implementation, where all decision paths through each Decision Tree are evaluated in parallel. The framework

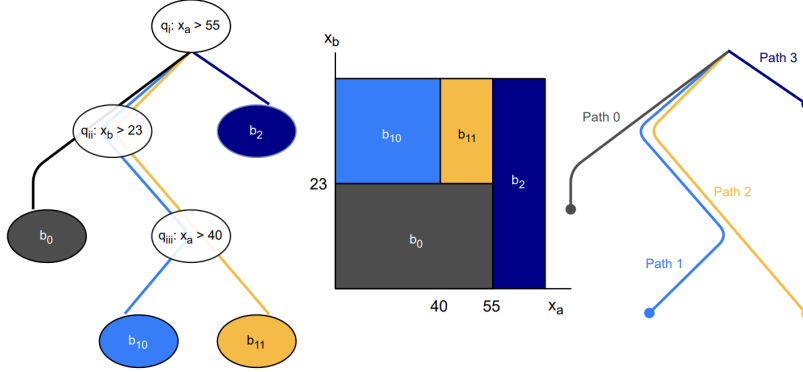


Figure 10: Visualisation of the mapping of Decision Tree structure onto decision paths in `fwXmachina` [57]. Left: the structure of the Decision Tree; centre: the visualisation of the splits in feature space; right: the decision paths of the tree, which are evaluated in parallel in the FPGA implementation.

integrates with standard ML training workflows, optimizing bit-precision per input and BDT structure for both physics performance and hardware efficiency, then synthesizing the design via HLS into firmware that meets stringent timing constraints typical of Level-1 triggers at collider experiments. Benchmarks on physics tasks—from vector boson fusion classification to missing transverse momentum estimation and exotic decay anomaly detection—demonstrate competitive physics performance with latency and resource footprints tailored for stringent embedded contexts, providing a complementary tool to other edge ML compilers in the particle physics ecosystem.

Applications of Decision Forests in trigger and data acquisition systems at modern collider experiments go back to early LHC data taking, where the LHCb experiment high level trigger made extensive use of so-called “bonsai” Boosted Decision Trees, highlighting their robustness and fast inference [59]. In hardware triggering, BDTs were used in the CMS muon trigger system, using a custom external low latency look-up table module that enumerated the BDT over address space of the features [60]. This model was able to reduce the trigger background rate by a factor three without compromising the signal efficiency.

More recent applications have deployed DFs directly in FPGA logic, as supported by `conifer` and `fwXmachina`. The ATLAS experiment has used a BDT during LHC Run 3 to select hadronically decaying  $\tau$  leptons using information from the calorimeter [61]. This algorithm is more resource efficient than the previous heuristic algorithm and provides a valuable platform to study the real-world deployment of ML in detector data taking.

Both the ATLAS and CMS experiments plan extensive use of ML in their upgraded hardware trigger systems for the High Luminosity LHC (HL-LHC). In the HL-LHC data taking conditions of a significantly increased number of simultaneous proton-proton collisions (pileup), ML will provide a powerful handle to maintain signal efficiency without overwhelming detector readout and data acquisition. The CMS experiment plan to use BDTs to reject fake tracks that are reconstructed from false coincidences of tracker hits in its Level 1 Track Finder development [62]. The BDT algorithm is more performant than basic cuts, while being sufficiently resource, latency, and throughput efficient to fit within the tight system constraints. A BDT will also be used in the reconstruction of electrons in the Level 1 Trigger, where a calorimeter cluster and charged particle track are linked [63]. After a first loose linking of pairs of calorimeter clusters with tracks, based on kinematic properties, a BDT ultimately identifies the most likely

pairings originating from electrons, suppressing background and maintaining high efficiency. In this application 10 instances of a small BDT are required in the densely packed FPGA in order to fit resource, latency, and throughput constraints.

Sizeable use of ML is also envisaged at the ATLAS experiment for its HL-LHC upgrade. Several event-selection level tasks have been developed for its Global Event Processor, including classifying events of Higgs Bosons produced by Vector Boson Fusion (a priority for HL-LHC data taking) and regressing the Missing Transverse Energy using BDTs.

The task of Anomaly Detection has also become prominent in online data section, with Neural Network anomaly detectors in use in data taking at both CMS and ATLAS during Run 3. DF-based anomaly detection algorithms are also under study, seeking to combine the robust and hardware efficient inference they offer with the signal agnostic target of anomaly detection. Methods include quantile regression using BDTs [64], tree-based autoencoders [58], and isolation forest [65], proving that anomaly detection with latencies of tens of nanoseconds is achievable.

Having become well established in software and now hardware triggering, use of DFs closer to sensor readout is also emerging as a viable approach to on-detector intelligence. At the Belle II muon CDC system, ML in FPGAs is being explored as a means to reduce the high rate of noise resulting in fake tracks being reconstructed in the Level 1 Trigger system [66]. Even with a very small model, BDTs emerged as the most performant model at rejecting noise hits. In this case extreme resource efficiency is required as one FPGA processes measurements from tens of detector channels simultaneously, requiring correspondingly many instances of the ML model operating in parallel. A single Decision Tree was deployed onto an extremely resource constrained eFPGA - with only 448 LUTs - as part of a pixel readout chip with on-chip data selection rejecting hits from particles with low transverse momentum [67]. Using a hardware-aware co-design methodology, the eFPGA resource requirement for a task of on-chip classification between neutron/gamma incidences has been explored [68]. Both Neural Networks and BDT models were used to explore the trade-off between classification performance, hardware cost, and throughput. BDTs were found to be resource efficient and capable of low latency and high throughput inference [68].

In summary, Decision Forests are robust, efficient ML models highly suited to edge inference in the resource constrained, low power, low latency, and high throughput regimes. This makes these simple ML models especially relevant for in-hardware inference, such as in hardware trigger systems and in frontend readout chips. The capability to efficiently reject background signals at high throughput will ensure future experiments can readout their desired signal data while maintaining reasonable data rates in data acquisition.

## 2.3 Quantum Algorithms, Processors, and Networks

**Contributors: Sagar Addepalli, Lorenzo Borella, Talal Ahmed Chowdhury, Alberto Coppi, Benedikt Maier, Mark Neubauer, Cristián Peña, Ema Puljak, Daniel Tapia Takaki**

### 2.3.1 Overview of Current Quantum Processor Technologies

Quantum processors are physical systems engineered to implement controllable quantum degrees of freedom—qubits—together with high-fidelity operations, measurement, and connectivity. Over the past decade, multiple hardware platforms have matured from laboratory prototypes into programmable devices accessible via cloud interfaces. Each platform reflects a distinct trade-off between coherence, gate speed, scalability, fabrication complexity, and integration with classical control hardware. No single technology has yet emerged as dominant, and it is increasingly clear that different quantum processor modalities may coexist, each optimized for particular application domains and scaling strategies [69].

**Superconducting Quantum Processors** Superconducting qubits currently represent the most mature and widely deployed quantum processor technology. These systems are based on lithographically fabricated superconducting circuits incorporating Josephson junctions, which provide the nonlinearity required to define discrete quantum states [70]. Qubits are typically operated at millikelvin temperatures in dilution refrigerators and manipulated using microwave pulses. The principal advantages of superconducting processors include fast gate times (tens of nanoseconds), compatibility with established microfabrication techniques, and a robust industrial ecosystem. Major efforts by IBM and Google have demonstrated programmable devices with over 100 physical qubits and steadily improving two-qubit gate fidelities, including landmark demonstrations of quantum computational advantage on noisy devices [71], along with several studies [72, 73, 74] showcasing quantum utility with more than a hundred physical qubits. Recent work has emphasized tunable couplers, suppression of crosstalk, and surface-code [75] error correction experiments that demonstrate increasing logical qubit lifetimes with code distance. Machine-learning-facilitated readout of superconducting qubits is another area of intensive research [37]. Despite all this progress, superconducting qubits remain sensitive to materials defects, electromagnetic noise, and fabrication variability. Scaling beyond a few thousand qubits poses challenges in cryogenic wiring density, control electronics, and thermal management, motivating research into three-dimensional integration, cryogenic CMOS control, and modular chiplet architectures [70].

**Trapped-Ion Quantum Processors** Trapped-ion quantum processors encode qubits in the internal electronic states of individual atomic ions confined using electromagnetic fields in ultra-high vacuum. Quantum gates are implemented through laser- or microwave-driven interactions mediated by collective motional modes of the ions [76, 77]. This platform offers exceptionally long coherence times—often seconds or longer—and among the highest demonstrated gate fidelities across all qubit technologies [77]. In small to medium-scale systems, trapped ions provide effectively all-to-all qubit connectivity, simplifying circuit compilation and error-correction protocols. The primary challenge for trapped-ion processors is scalability. As system size grows, motional mode spectra become increasingly complex and laser control overhead scales unfavorably. Current research directions include modular architectures based on segmented traps and photonic interconnects between ion modules, which aim to combine high fidelity with scalable system design [77].

**Neutral Atom Quantum Processors** Neutral atom quantum processors use optically trapped atoms arranged in programmable arrays as qubits. Optical tweezers or optical lattices provide precise spatial control, while strong Rydberg-state interactions enable fast, entangling two-qubit gates [78]. Neutral atom platforms have demonstrated rapid progress in scalability, with experimental systems controlling hundreds to thousands of atomic qubits in two-dimensional arrays [79]. Because neutral atoms are intrinsically identical, these systems benefit from high qubit uniformity, and the absence of net charge reduces sensitivity to electric-field noise. Key challenges include maintaining high gate fidelities across large arrays, stabilizing complex optical control systems, and achieving fast, low-error readout. Nevertheless, the favorable scaling properties of neutral atom architectures make them strong candidates for near-term demonstrations of error-corrected logical qubits [79].

**Photonic Quantum Processors** Photonic quantum processors encode quantum information in properties of light such as polarization, temporal modes, or spatial paths. These systems can operate at or near room temperature and are naturally compatible with quantum communication networks [80]. Photonic platforms offer extremely low decoherence and intrinsic suitability for

long-distance quantum information transfer. However, deterministic two-qubit gates are difficult to realize, and many architectures rely on probabilistic entanglement combined with measurement and feedforward, leading to substantial resource overhead. Integrated photonic circuits have enabled increasingly large interferometric networks, but scalability to fault-tolerant, general-purpose quantum computation remains an open challenge [80].

**Semiconductor Spin Qubits** Spin-based quantum processors use the spin states of electrons or nuclei confined in semiconductor nanostructures—such as silicon quantum dots or donor atoms—as qubits. These systems are attractive due to their compatibility with advanced CMOS fabrication and their extremely small physical footprint [81]. Spin qubits have demonstrated long coherence times and high single-qubit fidelities, but two-qubit gate fidelities and device reproducibility remain active areas of research. Atomic-scale variability and the need for precise electrostatic control present significant engineering challenges. Nonetheless, the prospect of leveraging mature semiconductor manufacturing infrastructure continues to motivate substantial investment in this platform [81].

**Topological Quantum Processors** Topological quantum computing seeks to encode qubits in non-local degrees of freedom that are intrinsically protected from certain error mechanisms. Proposed implementations rely on exotic quasiparticles, such as Majorana zero modes, which can emerge in engineered superconducting–semiconducting heterostructures [82]. In principle, topological qubits could dramatically reduce the overhead required for quantum error correction by providing built-in fault tolerance. In practice, experimental evidence for scalable, robust topological qubits remains limited, and the platform is still in an exploratory phase. Nevertheless, continued research reflects the potentially transformative impact of hardware-level error protection [82].

**Outlook** All existing quantum processor technologies remain within the noisy intermediate-scale quantum (NISQ) regime, where error correction is costly and computational advantage is limited to specialized tasks [69]. Across platforms, the central challenge is the realization of scalable, fault-tolerant logical qubits with acceptable physical-qubit overhead. Progress is increasingly driven by system-level considerations—including control electronics, packaging, cryogenics, and software–hardware co-design—rather than qubit performance alone. Rather than converging on a single hardware solution, the field is likely to evolve toward a heterogeneous quantum computing ecosystem in which different processor technologies serve complementary roles in computation, communication, and sensing.

### 2.3.2 Quantum Algorithms

**Circuits and qubits** Most near-term quantum algorithms are formulated in the quantum circuit model, where computation is performed by applying sequences of parameterized quantum gates to an initial register of qubits, followed by measurement. In this framework, algorithms are typically expressed as variational quantum circuits (VQCs), which combine fixed entangling gate patterns with tunable single- and multi-qubit rotations. The expressivity of a circuit is controlled by its depth, connectivity, and gate set. This circuit-based paradigm is largely hardware-agnostic and maps naturally onto most leading quantum processor technologies, making it the dominant abstraction for quantum computing in the NISQ era.

Different physical realizations of qubits give rise to distinct circuit primitives and computational trade-offs. Discrete-variable qubit systems, such as superconducting circuits, trapped ions,

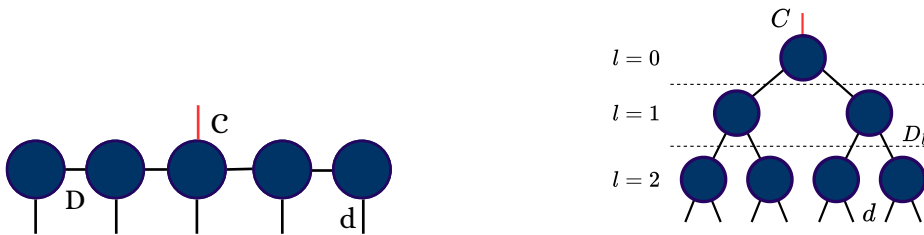
neutral atoms, and semiconductor spins, implement gates that directly correspond to unitary operations on two-level systems [70, 77, 79, 81]. In contrast, photonic and bosonic architectures often operate in higher-dimensional Hilbert spaces, where information is encoded in continuous degrees of freedom such as photon number, quadratures, or temporal modes [80, 83]. These bosonic systems enable compact representations and naturally support operations like squeezing and displacement, but require careful control of loss, noise, and non-Gaussian resources. From an algorithmic perspective, many circuit constructions can be translated between qubit and bosonic encodings, albeit with different resource requirements and error sensitivities.

The long-term viability of circuit-based quantum algorithms hinges on fault tolerance and error correction. While large-scale surface-code implementations remain out of reach, recent experiments have demonstrated small logical qubits and early forms of error suppression [84]. As quantum hardware matures, circuit-based quantum models are expected to evolve alongside advances in compilation, control, and hardware–software co-design, forming a foundational layer for quantum-enhanced AI applications in particle physics.

**Quantum annealing** In contrast to the gate-based circuit model, quantum annealing implements computation through the controlled adiabatic evolution of a many-qubit system governed by a time-dependent Hamiltonian. The system is initialized in the ground state of a simple transverse-field Hamiltonian and is slowly evolved toward a problem Hamiltonian whose ground state encodes the solution to a combinatorial optimization problem, typically expressed in Ising or quadratic unconstrained binary optimization (QUBO) form [85, 86]. Quantum annealers natively realize this continuous-time dynamics using fixed qubit connectivity and analog control of couplings, rather than discrete quantum gates. While quantum annealing is not universal for quantum computation and cannot directly implement general quantum circuits, it occupies a complementary niche to circuit-based processors, offering a physically scalable approach to solving structured optimization problems. In high-energy physics and related domains, quantum annealing and quantum-inspired annealing algorithms have been explored for applications such as track reconstruction [87], clustering [88], and pattern recognition [89].

**Tensor Networks** Tensor Network (TN) models provide an algorithmically novel and hardware-efficient alternative to conventional deep learning architectures [90, 91, 92] for real-time classification tasks operating under extreme latency constraints. In front-end processing systems, decisions must often be taken within microsecond or sub-microsecond timescales, while memory, logic resources, and power consumption are tightly constrained. In this regime, standard deep neural networks—despite strong classification performance—frequently struggle to satisfy strict timing and resource requirements.

Originally developed in the context of quantum many-body physics, TNs offer a structured framework for representing high-dimensional functions through factorizations into low-rank tensors. Architectures such as Matrix Product States (MPS) [93, 94] (see Fig. 11a) and Tree Tensor Networks (TTN)[95] (see Fig. 11b) can be adapted as supervised learning models operating directly on input features mapped to a higher-dimensional feature space [96, 97, 98, 99]. Their key algorithmic novelty lies not merely in parameter reduction, but in the explicit use of network topology and bond dimension as tunable quantities that directly govern model expressivity, computational complexity, and hardware cost. Unlike dense neural networks, inference in TN models corresponds to a sequence of deterministic tensor contractions whose computational cost scales polynomially with bond dimension and linearly with the input dimension, enabling predictable and controllable execution.



(a) *Matrix Product State* (MPS) structure designed for a classification task with five tensors connected via bond indices of dimension  $D$ , where each tensor has a physical (input) dimension  $d$ . The central tensor has an additional output leg corresponding to the class index  $C$ .

(b) *Tree Tensor Network* (TTN) designed for a classification task, approximating an 8-order tensor with three layers  $l$ , bond dimension  $D_l$  for each layer, and an output index  $C$  corresponding to the number of classes.

Figure 11: Tensor network architectures used for classification: (left) MPS and (right) TTN.

From a hardware perspective, this structured computation maps naturally onto FPGA and other reconfigurable architectures. The contraction patterns inherent to MPS and TTN models lend themselves to efficient pipelining and parallelization, while fixed-point arithmetic and aggressive quantization can be employed with minimal degradation in performance. As a result, TN-based inference can achieve low latency and reduced memory bandwidth requirements, making such models well suited for deployment in real-time, resource-constrained environments [101, 102, 96] (see Fig.12).

As a practical application of tensor networks (TNs) in low-latency, resource-constrained hardware settings, one prominent example is the trigger system of CMS and ATLAS detectors at the Large Hadron Collider at CERN [103]. The first level of the trigger system, the Level-1 Trigger (L1T), is an FPGA-based system that requires fixed latency, resource-efficient inference, and strict power constraints. While deep neural networks have demonstrated strong performance in this regime, they often lack intrinsic interpretability and structured control over correlations. These limitations can be overcome using TNs. In addition to offering competitive accuracy (Fig. 13), analyzing the pairwise correlations of the model’s inputs via quantum mutual information (QMI) provides insight into the correlations within the model itself. QMI analysis enables reduction in effective long-range correlations across a tensor chain or tree, simply by permuting the input features, thereby lowering the parameter count and arithmetic complexity with minimal performance loss [96]. Further directions include development of TN-specific compression strategies that exploit gauge freedom, coverage of a wide range of trigger-level tasks including anomaly detection and particle identification and the establishment of standardized workflows (model  $\leftrightarrow$  interpretation  $\rightarrow$  quantization  $\rightarrow$  firmware) for integrating TNs into the broader HEP front-end machine learning ecosystem.

**Quantum embeddings** A central bottleneck in applying quantum computing techniques to particle physics problems is the non-trivial task of mapping high-dimensional classical data from the experiments into the smaller and highly constrained state space of current quantum system. Unlike classical models, quantum hardware natively operates on amplitudes and phases of qubits, making data loading itself a potentially dominant cost and source of information loss. As a result, many existing approaches rely on hybrid quantum–classical pipelines, where classical neural networks are first used to preprocess, compress [106, 107], or learn task-relevant representations

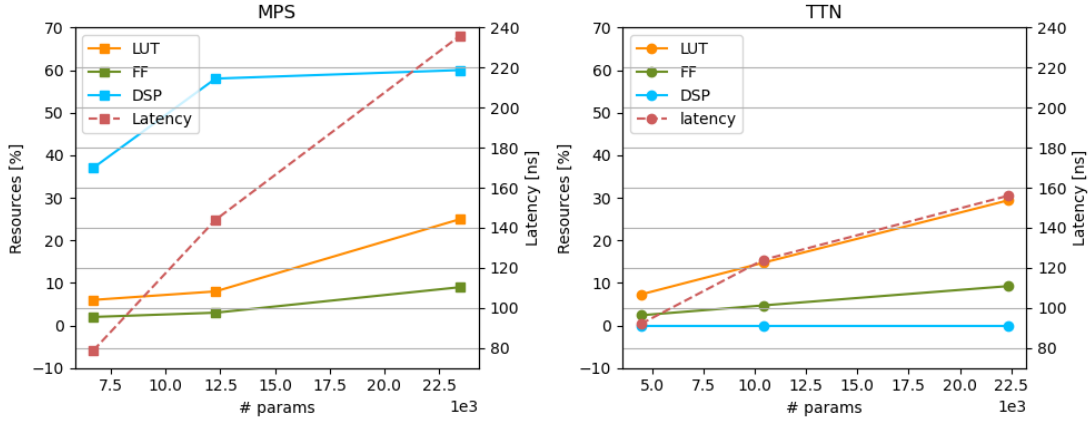


Figure 12: FPGA resource utilization and inference latency for quantized MPS (left) and TTN (right) models as a function of the number of parameters. Shown are the percentages of Look-Up Tables (LUTs), Flip-Flops (FFs), and Digital Signal Processors (DSPs) used on an XCVU13P FPGA, along with the corresponding inference latency (right y-axis). While MPS implementations exhibit high DSP utilization and rapidly increasing latency with model size, TTN implementations avoid DSP usage entirely and show more favorable scaling in both resource consumption and latency. Models were trained using the dataset from Ref. [100] and synthesized as reported in Ref. [96], following HLS and VHDL firmware respectively for MPS and TTN.

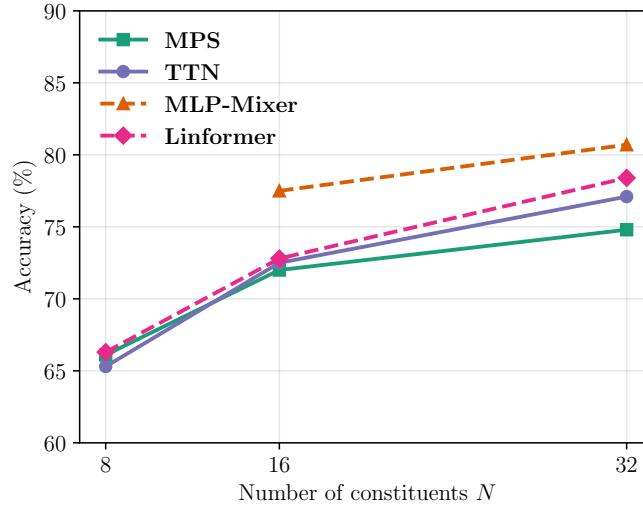


Figure 13: Accuracy of MPS and TTN models reported in [96] compared for different number of parameters guided by increased input size and dimension between neighboring tensors. Models are both trained and evaluated using the dataset from Ref. [100] designed for jet tagging (multi-class classification) task. State-of-the-art classical ML models for fast inference on FPGA are shown as dotted lines for comparison [104, 105].

of the data [108], which are then encoded into quantum states via angle, amplitude, or basis encodings. While this strategy makes near-term implementations feasible, it also shifts much of the representational burden back to classical models, making it challenging to identify where genuine quantum advantage can emerge. Recently, an embedding scheme that uses the raw experimental data—without prior compression—has been proposed that establishes a correspondence between a reconstructed particle and a single qubit [109]. Designing quantum embeddings that preserve structure, correlations, and symmetries of classical data—while remaining efficient, expressive, and compatible with noisy intermediate-scale quantum devices—remains an open and active area of research and a key determinant of the practical impact of quantum-based data processing approaches.

**Quantum Machine Learning** Quantum machine learning (QML) models are typically trained by optimizing the parameters of a variational quantum circuit using hybrid quantum–classical optimization loops [110], closely mirroring backpropagation in classical deep learning. In this paradigm, a parameterized quantum circuit prepares a quantum state, measurements define a loss function, and a classical optimizer updates the circuit parameters to minimize this loss [111]. Gradients can be computed either via automatic differentiation (autograd) frameworks, which treat the quantum circuit as a differentiable computational graph and propagate derivatives through expectation values, or via explicitly quantum methods such as the parameter-shift rule [112, 113], which evaluates gradients by executing the circuit at shifted parameter values on quantum hardware. These gradients are then used in classical optimization schemes (e.g. gradient descent, Adam), or, in more formal settings, in quantum gradient descent, where gradient information is estimated directly from quantum measurements. While this training loop enables principled optimization of quantum models, it also introduces challenges absent in classical backpropagation, including shot noise from finite measurements, barren plateaus in the loss landscape [114], and the high cost of repeated circuit evaluations, making efficient gradient estimation and optimizer design central research questions in QML.

### 2.3.3 Quantum Networking, Distributed Quantum Computing and Sensing

The recent vision and push towards a quantum internet has transitioned from a theoretical ambition to a concrete engineering reality through the Advanced Quantum Networks for Scientific Discovery (AQNET) project. Led by Fermilab in collaboration with Argonne National Laboratory, Caltech, and Northwestern University, and UIUC, AQNET represents the “second generation” of quantum networking. While its predecessor, IEQNET, successfully demonstrated that quantum information could coexist with classical data on existing fiber-optic cables, AQNET is exploring a more complex mission: achieving metropolitan-scale scalability while integrating distributed quantum computing and multi-node sensing arrays. For HEP, this project is not merely about communication; it is about building the quantum fabric that will allow geographically separated quantum resources – whether they be processors or sensors – to function as a single, coherent instrument.

A primary technical bottleneck in quantum networking is the high rate of signal loss in fiber optics, which causes entangled photon pairs to “decohere” or disappear over long distances. In late 2025, AQNET researchers achieved a milestone by successfully integrating a high-rate entanglement source, with an order of magnitude improvement in information density. By using highly dense encoding mechanism enabled by state-of-the-art superconducting nanowire single photon detectors (SNSPDs), the team demonstrated a dramatic increase in the rate of entanglement distribution. This breakthrough is critical towards the goal of building quantum repeaters, which act as “amplifiers” for quantum signals. Without this technology, quantum networks would be

limited to a few dozen kilometers; with it, the vision of a transcontinental quantum internet becomes feasible.

Equally vital is the project’s success in picosecond-level synchronization. To perform an “entanglement swap” – the process that allows two nodes to connect through an intermediate station—clocks at both ends must be synchronized with extreme precision. AQNET has achieved a world-record synchronization of under 3 picoseconds across 50 km of fiber. This level of timing accuracy ensures that photons arriving from different sources can be measured in the exact same temporal window, a requirement for any scalable quantum architecture.

Beyond computing, AQNET is revolutionizing the field of distributed quantum sensing. By entangling sensors at distant locations, the network can function as a single, ultra-high-resolution detector. This has immediate implications for the DOE’s Fundamental Physics mission:

- **Dark Matter Detection:** Entangled sensors can distinguish between local noise and the global “wind” of dark matter particles passing through the Earth. AQNET is creating the necessary conditions to allow distributed axion searches such as the proposed BREAD experiment.
- **Gravitational Wave Detection:** emerging theories suggest that detecting photons (e.g with SNSPDs) at synchronized geographically distant locations can detect gravitational waves in frequencies currently out of reach for LIGO.

## 2.4 Novel Paradigms

Particle physics experiments at future colliders and upgrades to existing facilities face unprecedented computational challenges driven by exponentially increasing data rates, event complexity, and granularity requirements. The Electron-Ion Collider (EIC), Future Circular Collider (FCC), High-Luminosity LHC (HL-LHC), and proposed muon collider designs will generate particle interaction rates exceeding tens of terahertz with sensor channel counts in the billions. Conventional computing architectures—even those leveraging state-of-the-art commercial processors, FPGAs, and GPUs—approach fundamental limits in power efficiency, latency, and bandwidth required for real-time event selection and data reduction at detector front-ends.

This section explores emerging computational paradigms that promise order-of-magnitude improvements in energy efficiency, latency, and integration density by fundamentally rethinking how computation, memory, and communication interact. These novel approaches span the full technology spectrum from reconfigurable logic embedded directly within custom silicon (eFPGAs), to optical interconnects for energy-efficient high-bandwidth data transmission (photonics), to computation performed in the analog domain exploiting physics rather than digital logic (analog compute), to heterogeneous integration of specialized chiplets optimized in different process nodes (System-in-Package), and democratized access through open-source hardware design toolchains eliminating commercial licensing barriers.

Each paradigm addresses specific bottlenecks in the HEP computing pipeline: eFPGAs enable algorithm evolution after detector deployment while maintaining ASIC-level power efficiency; analog compute performs inference and signal processing with drastically reduced energy consumption; chiplet-based integration combines optimal technologies for sensing, processing, and communication within compact packages suitable for detector constraints; and open-source compilation infrastructure democratizes custom accelerator development for the broader HEP community without proprietary tool dependencies. Collectively, these technologies represent the pathway toward sustainable computing for future HEP experiments where detector instrumentation must process, filter, and compress petabytes of data per second at the sensor interface

under extreme constraints of power budget (milliwatts per channel), material budget (radiation lengths), radiation tolerance (megarads), and latency (nanoseconds).

The subsections that follow detail specific implementations, recent prototypes demonstrated for HEP applications, and critical research directions required to mature these technologies for large-scale detector deployment in the 2030s and beyond.

### 2.4.1 Embedded FPGAs

**Contributors:** Carl Grace, Jyothisraj Johnson, Larry Ruckman

Advances in High Energy Physics (HEP) experiments increasingly require instrumentation capable of real-time and low-latency processing under extreme constraints. As future collider concepts such as the Electron-Ion Collider (EIC), Future Circular Collider (FCC), and the proposed muon collider progress toward higher granularity and unprecedented data rates, front-end electronics must balance power efficiency, material budget, radiation hardness, and design flexibility. Traditional Application Specific Integrated Circuits (ASICs) satisfy many of these demands but are fixed in functionality once fabricated. Commercial Field-Programmable Gate Arrays (FPGAs) provide reconfigurability but generally exhibit higher power consumption, lower radiation tolerance, and limited suitability for cryogenic operation. Embedded Field Programmable Gate Arrays (eFPGAs) integrate reconfigurable logic directly within ASICs, enabling a promising combination of flexibility and efficiency. By supporting FPGA-like programmability inside a custom chip, eFPGAs allow in-field updates to algorithms, firmware patches, and evolving Machine Learning (ML) based data processing without redesigning the underlying ASIC. This architecture enables real-time feature extraction, intelligent triggering, and data reduction at the sensor interface. A conceptual illustration of an eFPGA integrated inside a larger ASIC is shown in Figure 14.

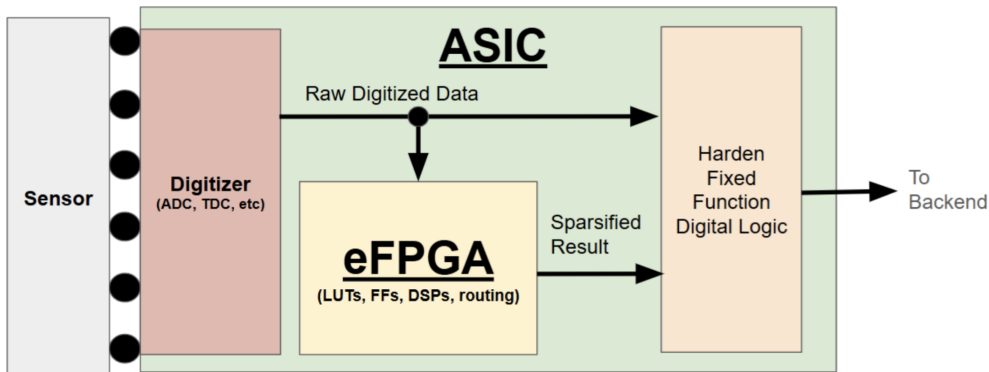


Figure 14: Conceptual illustration of an embedded FPGA integrated within an ASIC.

**eFPGAs for Intelligent Front-End Electronics in High Energy Physics** At the ML4FE Workshop, we presented an introduction to eFPGA technology and discussed its increasing relevance for HEP instrumentation. Open source eFPGA design frameworks such as FABulous [115] and OpenFPGA [116] have matured due to the expiration of key FPGA patents and the growth of community-driven toolchains. These platforms support customizable and royalty free logic

fabrics, making it easier for research institutions to prototype reconfigurable front-end systems tailored for specific detector environments.

SLAC National Accelerator Laboratory has recently demonstrated two eFPGA prototypes fabricated in 130 nm and 28 nm CMOS ASICs [67]. These devices validate the feasibility of incorporating small eFPGA fabrics with approximately 500 lookup-table (LUT) equivalent logic elements within HEP ASICs. One initial physics application is a smart pixel proof of concept in which a Boosted Decision Tree (BDT) classifier was deployed on an eFPGA to identify high transverse momentum (pT) tracks directly from pixel level sensor data. The demonstration achieved full agreement with the quantized software model while emphasizing the need for increased logic density and improved power optimization.

Looking forward, eFPGAs create new opportunities for intelligent detectors, front-end co-processors, and mixed-signal architectures that combine digital logic with emerging analog compute techniques. Their reconfigurability supports evolving Artificial Intelligence (AI) and ML workflows, adaptive calibration, and real-time anomaly detection. Ongoing efforts aim to advance open source design tools, evaluate radiation and cryogenic performance, and scale architectures for next generation, low latency, and upgradeable front end systems.

**Reconfigurable Pulse-Shape Discrimination Algorithm Implementations using eFPGAs** Emerging neutron imaging applications, such as single-volume scatter cameras (SVSCs) [117] require high-channel count readout ASICs with low power dissipation to enable mobile application. Neutrons can be imaged using organic scintillators that provide a Pulse-Shape Discrimination (PSD) capability. With PSD, the scintillator’s pulse response for gamma rays and neutrons are slightly different, and this difference can be used to discriminate between gamma rays and neutrons. This is critical in mobile applications where the gamma rate may be two orders-of-magnitude larger than the neutron rate. The separation of the calculated PSD for the two scintillators shown in Figure 15 allows classification of incident radiation as gamma or neutron. Traditional PSD signal processing techniques, based on high-speed digitization and digital post processing of the data are highly effective, but they dissipate too much power to be practical in a mobile application [118].

Machine learning (ML) algorithms such as boosted decision trees (BDTs) and neural networks (NNs) hold great promise in reducing the energy needed to perform PSD with practical scintillators and radiation environments. Typically, neutron imaging modalities require different triggering, filtering, and PSD settings. Emerging applications such as SVSCs can significantly benefit from ASIC technology. However, providing sufficient tunability to meet the needs of various scintillators and imaging systems is impractical. eFPGA technology allows a readout ASIC to be reconfigured after fabrication, allowing a single ASIC to support various imaging systems. This reconfigurability is critical when applying ML to PSD applications. This is because the input features and NN or BDT parameters can vary greatly across scintillators and energies. While weights in an ASIC-based NN can be adjusted via training after fabrication, the hyperparameters (e.g. number of hidden layers, fixed-point accuracy, optimization algorithms, etc) are often fixed. In an eFPGA, however, this hyperparameters can be readily adjusted via reconfiguring the eFPGA core.

Applying eFPGA technology to neutron imaging systems allows a single readout ASIC to be more flexible and applicable to a wider range of imaging modalities, energies, and scintillator types [68]. Recently developments in open-source eFPGA development frameworks, such as FABulous [115] have made the inclusion of eFPGAs on radiation detection ASICs developed by small teams in academic or the National Lab complex feasible for the first time. A prototype eFPGA fabricated in a low-cost CMOS process and capable of implementing a reduced-complexity ML model for PSD is shown in Figure 16. eFPGA technology holds significant potential to simplify

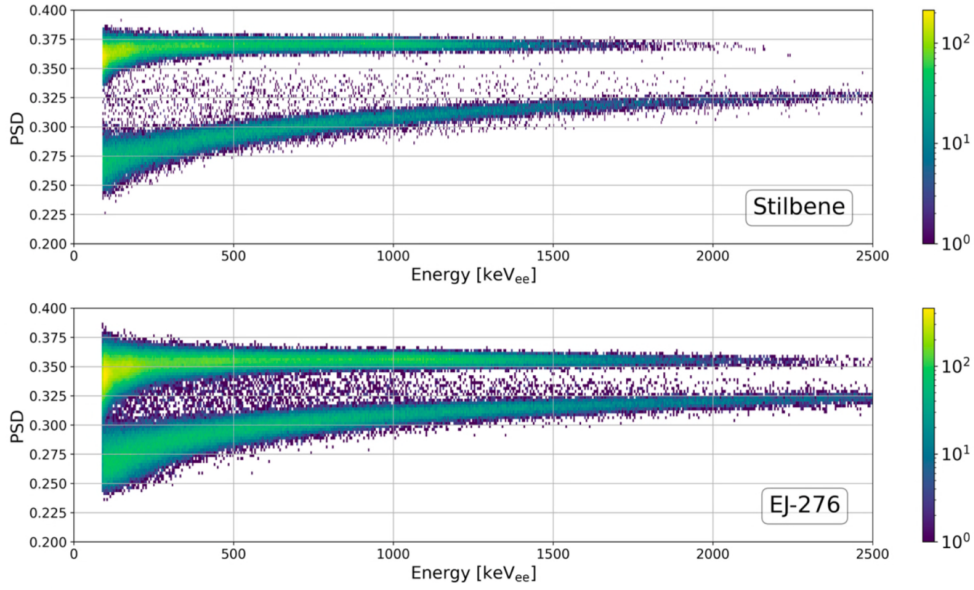


Figure 15: PSD performance for two organic scintillators. In each trace, the PSD measurement shows two concentrations: the top for gammas and the bottom for neutrons.

readout electronics for neutron imaging and other radiation detection modalities by allowing application-specific tailoring and ability to implement reduced-complexity ML models on-chip, reducing the data rate and lowering power.

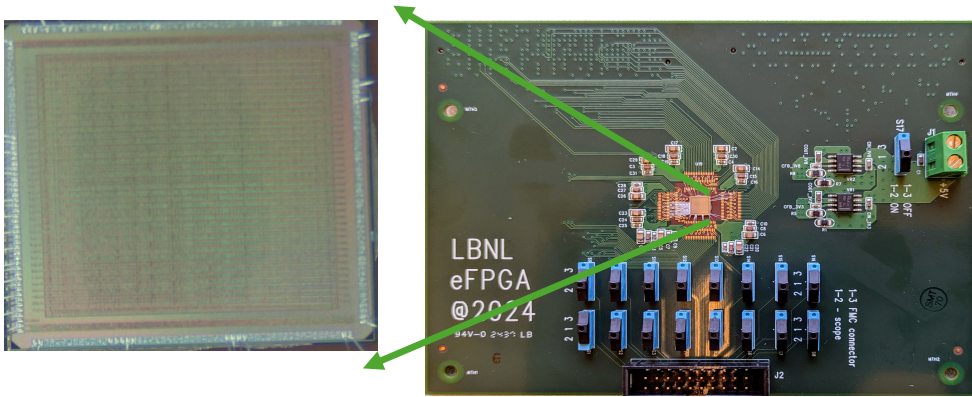


Figure 16: Prototype eFPGA developed at LBNL. The right shows the eFPGA attached to a test board and the zoomed image on the left shows the eFPGA die.

**Implementation Vision** For the most area and power efficient solutions, ML models can be mapped to RTL code and implemented using the usual custom digital ASIC design flow. Our goal is to use embedded FPGAs (eFPGAs) in such ASICs, rather than a custom digital implementation for the ML models in order to maintain configurability of the algorithm, architecture details and weights/biases.

When it comes to eFPGA targets for ML model deployment, resource constraints inevitably require sparse model deployments. One straightforward application that we are initially considering for ML algorithms on an eFPGA is neutron/gamma classification for neutron imaging systems. Ideally, we want to be able to identify if an event is a single or multiple scatter event, pileup, accidental coincidence or dark count/noise and be able to classify a neutron from gamma for single or multiple scatter event sequences. This is mostly done in “offline” processing of recorded events in many current detector systems but eFPGAs can potentially be used for this application instead. We can train ML algorithms to use features of the input pulses to perform particle identification between neutron, gamma or pileup/other events and deploy the model on an eFPGA fabric. The output classification of each inference per channel/pixel per event can determine whether that channel’s hit is considered valid and contributes to a global event reconstruction (i.e. will the info be sent off chip), but the output can also serve as an input feature to a more complicated secondary stage ML model in a master (commercial) FPGA. This stage can use multiple channel info (across chips if needed) to, in theory, make a determination of constituents in a pileup event (nn, gg, ng, gn) and also reconstruct the time of flight (TOF) in identified multiple scatter events from using position (and particle classification) information of all channels hit within a delta-T window (i.e. 10s of ns). For low power and real-time applications, this kind of event filtering will be immensely useful compared to “offline” processing, which consumes considerably more power due to having to record and save all waveform events above some global triggering requirement and then performing event filtering on a PC/laptop. In addition, by performing active real-time vetoing, we can potentially reduce deadtime of the system (especially in high-rate gamma background applications). We can more efficiently target triggering on neutron events to provide source reconstruction to a useful position resolution. More complicated models with multiple stages can be the target for a combined eFPGA + commercial FPGA deployed system architecture.

The key limitation for an eFPGA ML model deployment are the available input features; these are much harder to change so a lot of effort will have to go into studying and selecting an optimal set to use. Depending on the level of configurability built into other parts of the chip design (i.e. integration windows), inputs can be adjustable to a degree.

#### 2.4.2 Analog Compute

**Contributors:** Luca Macchiarulo, Boris Murmann, Antonino Tumeo

**DeCoDe at PNNL** While current HEP applications employ primarily digital processing, emerging analog computing paradigms warrant consideration for future detector systems. Recent workshops sponsored by DOE-SC, Advanced Scientific Computing Research (ASCR) Program Office on analog computing have identified key challenges for integration into scientific applications:

- **Hybrid Partitioning:** System-level co-design must quantify Analog-to-Digital Converter (ADC) and Digital-to-Analog Converter (DAC) conversion overhead when partitioning algorithms between analog and digital domains. Interface costs (area, power, latency) may dominate gains from analog acceleration for fine-grained partitioning.
- **Noise Characterization:** Analog accelerators require noise models accounting for HEP detector conditions—radiation-induced parameter drift, temperature variations, supply voltage fluctuations. Non-stationary noise models reflecting time-varying detector conditions differ from static laboratory characterization.

- **Parameter Variability:** Device mismatch and process variation impact analog circuit precision. Strategies include device averaging (using larger arrays to statistically reduce variation), algorithmic redundancy (error-correcting codes, ensemble methods), and run-time calibration (periodic recalibration against digital reference implementations).
- **Radiation Effects:** Total Ionizing Dose (TID) and Single-Event Effects (SEE) cause threshold voltage shifts, leakage current increases, and transient upsets in analog circuits. Co-design tools must incorporate radiation-aware device models for detector proximity applications.
- **Scalability:** Analog circuit performance degrades with scaling due to wire parasitics, increased crosstalk, and reduced device matching. System architectures must account for these physical limitations when projecting performance to future technology nodes.

PNNL’s DeCoDe project support for heterogeneous co-design provides infrastructure for exploring these analog-digital integration challenges as the technology matures for HEP applications

**Mixed-Signal Interfaces and Compute Fabrics for tinyML Systems** As machine learning (ML) algorithms are marching closer to physical sensors, the design of analog and digital subsystems is becoming more intertwined. This paper provides a short summary of related recent research on “tiny” ML systems by the Murmann Mixed-Signal Group at UH Mānoa (formerly at Stanford University).

**Analog/Mixed-Signal Preprocessing.** Signal acquisition and processing pipelines in integrated circuits have been heavily influenced by the needs of communication systems, which use “human- designed” signals (e.g., QAM-16) to convey a relatively large amount of information per processed sample. On the contrary, in AI inference for sensors, the amount of information conveyed per sample is very small. For instance, Nyquist-sampled speech signals produce a data stream of hundreds of kbit/sec, while only yielding 39 bits/sec of relevant information. This mismatch between the physical bandwidth and information rate motivates many opportunities for analog pre-processing and data reduction prior to sampling and digitization [119]. A specific example catered toward an ML sound classification system is shown in Figure 17 [120]. Here, the input signal is pre-processed by an N-path filter bank before low-rate digitization with reduced bit-precision. The filter bank is composed of only passive components and consumes merely 800 nW. The circuit’s unwanted harmonic mixing products are absorbed by the machine learning model during a one-time training (independent of manufacturing environmental variations, due to the stability of switched capacitor circuits). Another example is the object detection imager described in Ref. [121]. It computes logarithmic gradients in the analog domain to enable data reduction and compression of the succeeding convolutional neural network (CNN) [122].

**Efficient Hardware for Neural Network Inference.** Once a sensor signal is properly conditioned and pre-processed, ML inference for sensors typically relies on deep neural networks like CNNs, or (more recently) transformer-like models. The main challenge here is to minimize data movement across the system’s memory hierarchy [123]. One approach for amortizing memory accesses has been to create compute arrays that can “unroll” the filter kernels to amortize memory access over many multiply- add operations performed in parallel. One way to achieve this is through analog arrays using capacitive or resistive crossbar approaches. While the block specifications of such compute macros are often impressive [124] (measured in TOPS/W), their benefit at the system level tends to be less pronounced due to their limited bitwidths and resulting penalty on the required network size. As a compromise, we explored a fully digital implementation with custom-designed compute cores and efficient, closely interspersed custom memory banks. A snapshot of this prototype is shown in Figure 2 [125]. Its 8-bit architecture

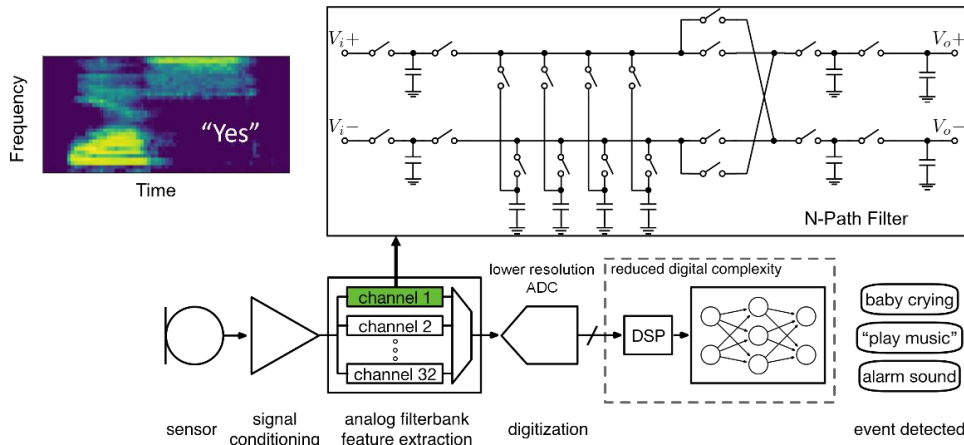


Figure 17: Analog preprocessing using N-path filters in a sound classification system [119].

achieves state-of-the-art inference energy across a range of tinyML tasks. Its custom latch arrays (CLAs) achieve a read energy of only 15 fJ/Byte. The architecture is engineered such that these efficient local memories are hit most frequently, while access energy to system-level memory is reduced by up to 9.5x over conventional architectures.

**Chiplet-Based Heterogeneous Integration** System-in-Package (SiP) technology enables seamless integration of multiple chiplets— analog accelerators, digital processors, memory, specialized Intellectual Property (IP) blocks— within a single package, creating modular heterogeneous systems optimized for energy efficiency [126]. Recent advances in open chiplet ecosystems and standards combined with open-source co-design tools make this approach increasingly accessible. The Department of Energy (DOE), Office of Science (DOE-SC), Microelectronics Science Research Center (MSRC) project Democratization of Co-design for Energy-Efficient Heterogeneous Computing (DeCoDe) integrates MLIR-based compiler infrastructure, architectural simulation, and thermal analysis to support co-design of heterogeneous SiPs [126]. For HEP applications, chiplet-based approaches could enable integration of analog sensor interfaces with digital ML accelerators and high-speed serializers, each fabricated in optimal process nodes and technologies, while managing power/thermal constraints through advanced packaging (2.5D interposers, 3D stacking).

**Nalu Scientific HPSoC** Traditionally time of arrival gets estimated using TDC (time-to-digital-conversion) on a pulse-shaped signal derived from the sensor. Such a solution is simple and amenable to good integration, but it relies on single point measurement, which makes it prone to many sources of error, such as: Noise on the threshold voltage and on signal, Variable signal amplitude (time walk), Jitter on reference clock, Measurement jitter on TDC logic (variable delay in internal logic), all of which degrade the performance. On the other hand, with a full waveform sampling, the entire shape of the signal can be used to average out the effect of most of these noise sources (e.g. DC or slow frequency noise using pre-pulse baseline estimation, high frequency noise via multi-sample interpolation or convolution). Even if a full waveform recording is available, the large variability and interdependence of inter-channel and intra-channel events can make it hard to pre-design an estimator that is adapted to all foreseeable situations (e.g. channel crosstalk, event pileup, channel-dependent parameter variation, etc.). In such cases, a

Machine learning approach (inference at the edge) is the most promising and adaptable estimation methodology. However, this requires a joint design of the readout mechanism, and possibly the incorporation in the ROIC of the mechanism to pre-distill relevant information to perform a first-layer data reduction while at the same time maintaining flexibility to handle diverse signal combinations.

As an example of a possible readout solution that could empower ML-based experiments, Figure 18 below shows the architecture of the HPSoC series of ROICs designed by Nalu Scientific. The architecture is based on the following ideas:

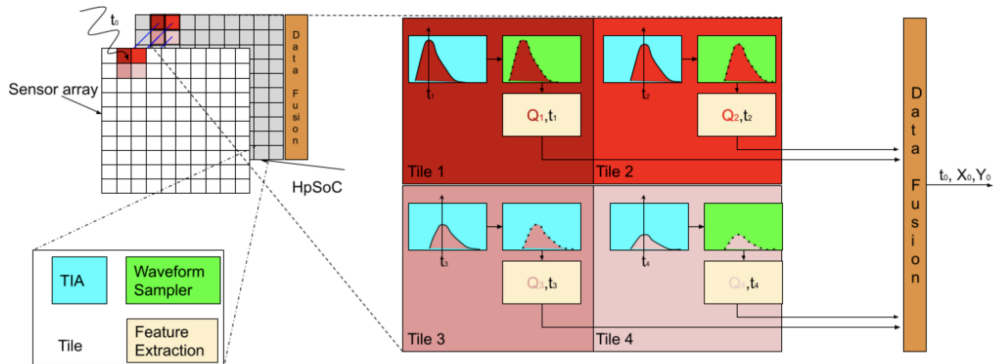


Figure 18

- Dense sensor array readout
- Modular, independent (“tiles”), per pixel
- On chip signal amplification (TIA+gain)
- Continuous waveform sampling and triggered digitization - with internal buffering of past triggers to avoid deadtime.
- On the fly timing and amplitude (charge) extraction
- “Data fusion” and export.

The output of any of these components could be the target for the application of a more or less sophisticated exploration of ML extraction, operating directly on the raw samples, the individual extracted  $Q$  and  $T_s$ , or the output of the fusion logic. The implementation of the latter as an inference engine is a good candidate for first experimental evaluation of the methodology and is being considered as a good demonstrator in a follow-up study.

Nalu Scientific is developing several application-specific integrated circuits (ASICs) and related technologies, partially funded by various US SBIR grants and JLAB programs.

### 2.4.3 Open Source Tools for Hardware-Software Co-Design

Contributors: Antonino Tumeo

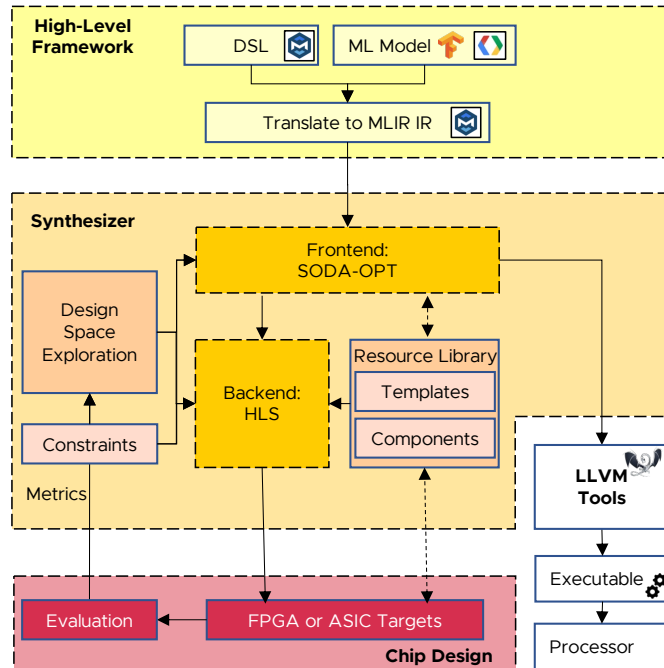


Figure 19: SODA open-source toolchain architecture enabling Python-to-GDSII compilation without commercial EDA tools. The flow integrates Python ML frameworks (TensorFlow, PyTorch) through MLIR-based intermediate representation, SODA-OPT hardware-software partitioning, Panda-Bambu high-level synthesis, and OpenROAD physical design. The complete open-source flow supports multiple Process Design Kits (PDKs) and enables custom ASIC development accessible to academic institutions without commercial licensing barriers.

The HEP community has benefited from open-source tools that democratize hardware acceleration. Complementary efforts in computing research provide capabilities for automated hardware generation from arbitrary Python algorithms, domain-specific compilation, and system-level co-design.

**MLIR-Based Compilation Infrastructure** PNNL’s open-source compilation framework leverages MLIR (Multi-Level Intermediate Representation) [127] to provide unified infrastructure spanning high-level algorithm descriptions through heterogeneous hardware generation. The COMET compiler [128, 129] targets domain-specific languages for tensor algebra, supporting computational chemistry (NWChem) and graph analytics with optimizations for CPUs, GPUs, and dataflow accelerators. The SODA Synthesizer [26] interfaces with Python frameworks (TensorFlow, PyTorch), performs hardware-software partitioning and hardware-oriented optimizations through its SODA-OPT frontend [130], then generates custom accelerators via Panda-Bambu open-source HLS [131]. For end-to-end flows, SODA connects to OpenROAD [132] for physical design, enabling complete Python→MLIR→Bambu→OpenROAD→GDSII compilation without commercial tools. Recent extensions support custom instruction sets for pattern-specific accelerators and integration with OpenCGRA for CGRA mapping [133].

Figure 19 illustrates the complete open-source toolchain architecture. SODA provides general-purpose compiler infrastructure for arbitrary Python algorithms—including ML frameworks

(TensorFlow, PyTorch), scientific computing kernels, data preprocessing, control logic, and complete algorithm pipelines. SODA supports flexible optimization targets (low latency, high throughput, or balanced trade-offs) and multiple backends: FPGAs and ASICs with access to commercial Process Development Kits (PDKs) or multiple open PDKs (FreePDK 45nm, ASAP 7nm, SkyWater 130nm, GlobalFoundries 180nm). This enables end-to-end detector readout pipeline synthesis from high-level Python specifications. Reported results include 364 GFLOPS/W energy efficiency on CNN operators and dramatically reduced turnaround time for hardware prototyping compared to manual HDL development [26].

These MLIR-based tools provide: (1) broad scope from ML models to arbitrary scientific algorithms including data preprocessing, feature extraction, control logic, and data formatting, (2) unified compiler infrastructure enabling cross-optimization between different hardware targets (CPU, GPU, FPGA, CGRA, ASIC), (3) direct ASIC synthesis paths with flexible optimization targets (latency, throughput, energy efficiency), (4) integration with architectural simulation for design space exploration. The modular MLIR architecture allows domain experts to extend the framework with custom dialects for specialized operations, enabling HEP-specific extensions for detector algorithms, trigger logic, or data compression without rebuilding entire toolchains.

**Spatial Computing and Reconfigurable Architectures** OpenCGRA [133] provides the first open-source unified framework for Coarse-Grained Reconfigurable Arrays (CGRAs), offering multi-level modeling (Functional Level, Cycle Level, RTL) using PyMTL with Low-Level Virtual Machine (LLVM)-based compiler integration. For HEP applications with structured computation patterns—convolutions in calorimeter processing, nearest-neighbor searches in tracking, streaming data reduction—CGRAs offer efficiency between Field-Programmable Gate Arrays (FPGAs) fine-grained flexibility and ASICs’ fixed functionality. The Dynamic Rebalancing of Pipelined Streaming (DRIPS) extension [134] adds partial dynamic reconfiguration, demonstrating  $1.46\times$  throughput improvements for workloads with data-dependent execution times—directly applicable to variable HEP event characteristics, pileup conditions, and adaptive triggering scenarios requiring runtime algorithm adjustment.

**Hybrid Analog-Digital Considerations:** The DeCoDe framework extends MLIR-based compilation to support novel computing paradigms including analog accelerators. While current HEP applications remain primarily digital, the co-design methodology for integrating analog components (handling precision constraints, interface costs, noise-tolerant algorithm formulations) may inform future mixed-signal detector systems as analog computing matures.

**Key Message:** Open-source compilation frameworks provide the international HEP community with accessible infrastructure for general-purpose hardware development from Python algorithms: (1) broad algorithmic scope from ML to complete detector pipelines, (2) flexible optimization targets (latency and/or throughput), (3) unified MLIR-based optimization across multiple targets (CPU, GPU, FPGA, CGRA, ASIC), (4) fully open synthesis flows including ASIC paths, (5) extensible architectures supporting custom domain-specific extensions. These capabilities democratize custom accelerator development for academic collaborations worldwide.

#### 2.4.4 Heterogeneous Pipelines

**Contributors:** Julia Gonski, Ryan Herbst

Heterogeneous data pipelines are processing frameworks that interconnect a wide range of computing technologies, such as FPGAs, embedded processors, GPUs, IPU, Groq devices, and custom ASICs, to efficiently manage and analyze the enormous data flows generated by modern scientific instruments. A core principle in designing these systems is the mapping of technologies

onto front-end and back-end processing categories. Front-end technologies, often deployed directly on or near the sensors (e.g., FPGAs, ASICs, eFPGAs, SoCs), handle immediate high-speed data capture, localized processing, and initial feature extraction. Back-end technologies (GPUs, CPUs, etc.) manage more complex analysis that is not time or resource-limited. Defining these roles with an eye towards optimization for a particular instrument’s conditions and environment ensures each device is used where its strengths best match the physics-driven specifications. Figure 20 shows an example mapping of hardware to data task for LCLS.

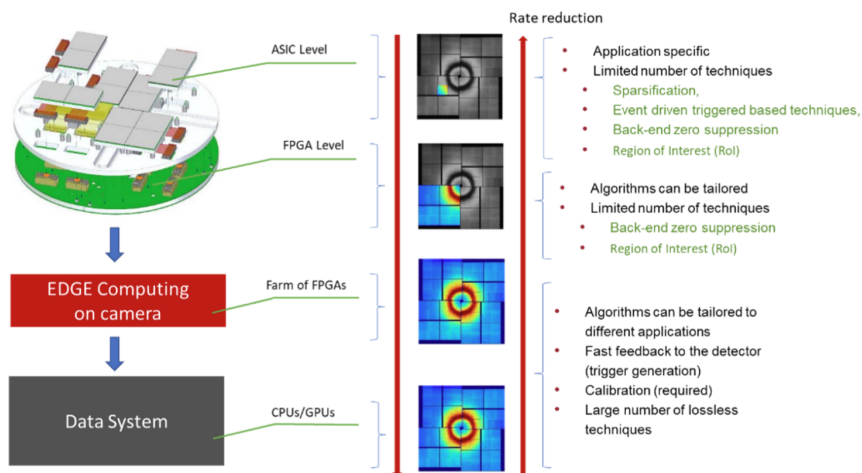


Figure 20: Distributed data processing from the detector to the back-end in the case of the LCLS-2 facility at SLAC.

Optimizing these heterogeneous pipelines involves careful design not just of processing stages, but also of the high-performance transmission and linking mechanisms that relay data from the detectors through the pipeline. Efficient, low-latency communication, utilizing high-speed links and advanced networking protocols, is vital for ensuring that key scientific features extracted by front-end devices arrive at the back end without bottlenecks, maintaining data integrity and enabling real-time insights.

A practical example of heterogeneous optimization in practice is the SLAC Streaming Artificial Intelligence (S3AI) testbed (Figure 21). It serves as a comprehensive integration platform that connects sensors, heterogeneous accelerators, mid-scale HPC resources, S3DF systems, and IRI orchestration frameworks. The testbed enables realistic assessment of streaming pipelines, cross-hardware interactions, security considerations, and algorithm deployment under live data conditions. Ample opportunity exists for industrial benchmarking and collaboration by introducing modern commercial computing hardware in a plug-and-play manner. S3AI thus functions as a valuable proving ground for validating the full edge-to-exascale workflow envisioned in ML-HEQUPP.

## 2.5 Analysis Facilities

**Contributors: Yuan-Tang Chou, Giordon Stark**

Analysis Facilities (AFs) serve as critical infrastructure connecting the development of machine learning models with their deployment on front-end hardware systems. The vision of AI-native high-energy physics—embedding AI end-to-end across the entire experimental lifecycle—

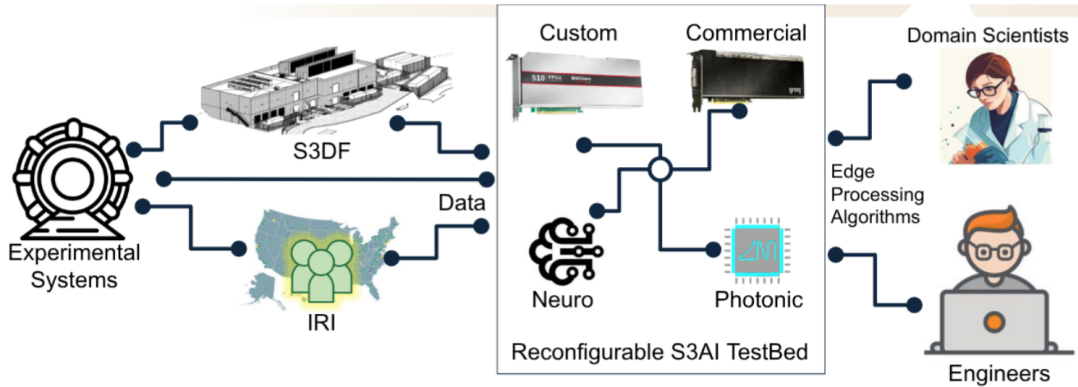


Figure 21: S3AI enabling development of heterogeneous streaming workflows.

cle, from design and optimization through simulation, data processing, and discovery—requires a computational infrastructure that bridges the gap between model development and hardware deployment. AFs provide the computational resources, data access, and collaborative environments necessary to develop and validate the ML algorithms that ultimately run on detector front-ends. For example, the SmartPixels project (Section 3.1.1) was fully supported by the Fermilab and Purdue AFs, and the analog compute work (Section 2.4.2) by the BNL and UChicago AFs — both leveraging community resources available to the respective teams.

The HSF Analysis Facilities White Paper [135] documents the R&D status and future directions for these facilities, noting that in the HL-LHC era (beginning 2029), analysts may need to process up to an order of magnitude more data than currently. The whitepaper emphasizes requirements for fast “time-to-insight” through interactive access, the ability to scale out to distributed resources, and integration with the broader WLCG infrastructure. In the context of this whitepaper, AFs play a dual role: they enable the computationally intensive training of ML models destined for resource-constrained front-end hardware, and they provide platforms for validating that deployed models perform correctly at scale.

### 2.5.1 Training Infrastructure for Edge Deployment

Machine learning models destined for front-end deployment face unique constraints: submicrosecond latency requirements, limited memory, fixed-point arithmetic, and radiation tolerance—that differ fundamentally from models running in offline analysis. However, the development cycle for these models necessarily begins in traditional computing environments before translation to hardware implementations. This is particularly true as the field moves toward physics foundation models that can be fine-tuned for specific front-end tasks, and as novel architectures such as learnable logic networks (Section 2.4) require computationally expensive training despite their efficient inference.

Analysis Facilities provide several essential capabilities for this development cycle:

1. **GPU Access for Model Training:** Training neural networks for front-end applications, including those requiring quantization-aware training for FPGA deployment, demands significant GPU resources. The AF whitepaper notes that AFs “may not have sufficient GPUs” for training large machine learning models, highlighting the need for AFs to either provide adequate GPU resources or integrate with external GPU-rich resources, such as

HPC centers. For applications highlighted in this whitepaper, this includes training foundation models that can be fine-tuned for specific detector configurations, as well as the computationally intensive training required for novel multiplication-free architectures.

2. **Interactive Development Environments:** The R&D phase of front-end ML development requires rapid iteration—testing different architectures, quantization schemes, and pruning strategies. AFs supporting Jupyter-based interfaces with scale-out capabilities (such as Dask integration) enable physicists to interactively explore the trade-off space between model accuracy, latency, and resource utilization.
3. **Access to Representative Data:** Training front-end ML models requires access to realistic detector data or high-fidelity simulations. AFs integrated with experiment data management systems and caching infrastructure ensure developers can access the large datasets needed for training without managing complex data logistics. As trigger-less architectures emerge, the volume of data available for training front-end models will increase substantially.

### 2.5.2 Model Optimization Workflows

The path from a trained floating-point model to a deployable fixed-point implementation involves multiple optimization stages that benefit from AF infrastructure:

- **Quantization Studies:** Systematic exploration of bit-width configurations (e.g., using QKeras) to find optimal precision-performance trade-offs
- **Pruning and Sparsification:** Identifying and removing redundant network connections while maintaining physics performance
- **Architecture Search:** Automated exploration of network topologies subject to hardware constraints
- **Hardware-Aware Training:** Iterative refinement incorporating feedback from synthesis tools like `hls4ml`

These workflows are computationally demanding and benefit from the batch-mode capabilities that AFs provide for transitioning from interactive development to large-scale parameter sweeps.

### 2.5.3 Analysis Facility Landscape

Several prototype and production AFs currently support HEP analysis workflows with varying degrees of ML infrastructure. The US ATLAS Analysis Facilities provide a concrete example of the capabilities that exist today and illustrate both what is working and what gaps remain for edge hardware development.

#### **Example: US ATLAS Analysis Facilities**

The US ATLAS collaboration operates Analysis Facilities at BNL, SLAC, and UChicago that are available to collaboration members. These facilities provide GPU resources, ML software environments, data caching, and batch computing capabilities representative of what the broader HEP community requires for front-end ML development.

1. **GPU Resources:** Modern AFs increasingly provide access to high-end GPUs essential for ML training. For example, the UChicago facility includes nodes with NVIDIA A100

(40GB), V100 (16GB), and consumer-grade GPUs (RTX 2080 Ti, GTX 1080 Ti), as well as recent additions of H200 nodes (141GB HBM3 memory). This range of hardware supports everything from interactive prototyping to large-scale training runs. JupyterLab interfaces allow users to request GPU resources interactively, with MIG (Multi-Instance GPU) support enabling efficient sharing of high-end accelerators.

2. Batch Computing: AFs integrate with batch systems (HTCondor, SLURM) that allow scaling from interactive development to large parameter sweeps. This is essential for hardware development workflows that require systematic exploration of quantization configurations, architecture search, and hyperparameter optimization.
3. Containerized Environments: Standardized ML containers (available via CVMFS and container registries) provide reproducible environments with common ML frameworks (TensorFlow, PyTorch, scikit-learn) and HEP-specific tools. This standardization enables workflows to move between facilities and ensures reproducibility.

### Inference-as-a-Service

NVIDIA Triton Inference Server [136] deployments at several facilities enable transparent CPU & GPU access for inference workloads without requiring users to manage compute scheduling directly. This architecture allows model serving at scale with automatic batching and load balancing, supports multiple ML frameworks and model formats, enables validation of trained models against large datasets before hardware deployment, and provides a model for how front-end inference could be validated at scale. For edge hardware development, inference-as-a-service (IaaS) provides a testbed for validating model performance characteristics before committing to hardware synthesis.

A related community effort within Fast Machine Learning is focused on making it easier to deploy IaaS capabilities across both HPC centers and Tier-3/analysis facilities for HEP and multi-messenger astronomy applications. In particular, SuperSONIC (Services for Optimized Network Inference on Coprocessors) [137] (Figure 22) provides a server infrastructure designed for deployment at Kubernetes clusters equipped with GPUs. Experiments using SuperSONIC include the ATLAS and CMS experiments at the LHC and IceCube at the South Pole.

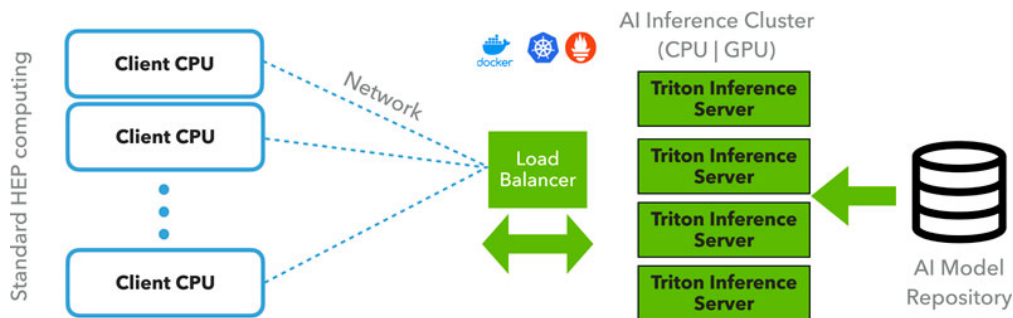


Figure 22: SuperSONIC: shared server infrastructure for HEP and MMA experiments.

#### 2.5.4 Data Access Infrastructure

AFs integrate with distributed data management through caching proxies (XCache) that enable transparent access to remote data while caching locally for faster repeated access—essential when iterating on ML training with the same datasets. Global namespace support allows users

to reference data by logical name rather than physical location, simplifying workflows that span multiple facilities.

### **FPGA Development Tooling Integration**

A critical capability for edge hardware development is the integration of FPGA synthesis and development tools within AF infrastructure. Some facilities have begun deploying Xilinx/AMD development tools (Vitis, XRT) alongside standard analysis software, enabling researchers to perform the complete model-to-firmware workflow within a single environment.

Such integration requires substantial storage resources—FPGA development suites can require 150+ GB of disk space per installation, plus additional space for synthesis outputs. The computational requirements for synthesis can also be significant. However, this investment enables:

- **Synthesis-in-the-loop development:** Researchers can iterate between model training and hardware synthesis without transferring files between systems
- **Co-design workflows:** Tools like `hls4ml` [138] and open-source frameworks can be integrated with vendor synthesis tools, enabling automated translation from trained models to deployable firmware
- **Validation against hardware constraints:** Synthesis feedback (resource utilization, timing closure, latency estimates) can inform model architecture decisions early in the development cycle

The next frontier is integrating actual FPGA hardware into AF clusters, enabling researchers to validate firmware on physical devices as part of their development workflow.

### **2.5.5 Bridging Analysis Facilities and Front-End Deployment**

A critical gap exists between models developed in AF environments and their deployment on front-end hardware. The hardware community requires infrastructure that spans this gap, enabling the kind of differentiable, end-to-end optimization that is increasingly recognized as essential for maximizing physics performance. The typical workflow involves:

1. **Interactive Development:** Physicists use JupyterLab environments at AFs to prototype ML models using standard frameworks, with access to GPUs for rapid iteration.
2. **Scale-Out Training:** Once a promising architecture is identified, training scales to batch resources for hyperparameter optimization and full-dataset training. Distributed computing frameworks (Dask, Ray) enable seamless scaling from interactive notebooks to cluster-scale computation.
3. **Quantization and Optimization:** Models are converted to fixed-point representations using tools like QKeras, with systematic studies of bit-width configurations to find optimal precision-performance trade-offs. For novel architectures like learnable logic networks, this phase involves the computationally expensive differentiable relaxation training.
4. **Hardware Translation:** Optimized models are translated to hardware implementations via `hls4ml`, FINN, or similar tools, generating firmware for FPGAs or specifications for ASICs. With FPGA development tools integrated into AFs, this step can occur within the same environment as training.

5. **Validation at Scale:** AFs provide the compute resources to validate that hardware implementations produce results consistent with the original floating-point models across representative datasets.

### **Infrastructure Requirements for Co-Design**

Enabling true co-design between ML model development and hardware implementation requires infrastructure that goes beyond traditional analysis facilities:

1. **Integrated Synthesis Environments:** FPGA development tools must be accessible within AF environments. This requires substantial storage allocation (150+ GB for toolchains) and may require specific OS environments. License server access must be managed across distributed users.
2. **Hardware-in-the-Loop Development:** The natural extension of software-based synthesis is access to physical FPGA hardware for validation. AFs could integrate FPGA accelerator cards that researchers can target for testing, enabling validation of timing, resource utilization, and actual inference performance before deployment to detector systems.
3. **Heterogeneous Computing Support:** Future detector systems will employ heterogeneous architectures combining different processor types. AFs should support similar heterogeneity—x86 and ARM CPUs, various GPU architectures, FPGAs—enabling researchers to develop and test on representative hardware.
4. **Automated Workflows:** As the field moves toward agentic systems that can orchestrate complex workflows, the infrastructure must support automated pipelines that traverse the full development cycle. This includes integration with version control, experiment tracking, and continuous integration systems that can validate deployability at each stage.

### **Distributed Computing for ML Workflows**

Distributed computing frameworks like Dask provide a bridge between interactive development and large-scale computation. Users can develop code interactively in Jupyter notebooks, scale computations to hundreds of workers via integration with batch systems (SLURM, HTCondor), monitor execution through dashboards. This capability is particularly relevant for front-end ML development, where systematic parameter sweeps (quantization studies, architecture search, hyperparameter tuning) require significant computational resources. The same infrastructure supports the computationally expensive training required for novel architectures like learnable logic networks, where training costs are high but inference is exceptionally efficient.

### **Validation and Monitoring**

AFs also play a crucial role in validating deployed front-end ML systems:

- **Scale Testing:** Processing large data samples through both AF-based software implementations and hardware emulations to verify consistency
- **Performance Monitoring:** Comparing online (front-end) and offline (AF-based) inference results to detect degradation
- **Retraining Workflows:** When detector conditions change, AFs provide the infrastructure to rapidly retrain and validate updated models

### 2.5.6 Recommendations for Optimal Analysis Facilities

To maximize the effectiveness of AFs for front-end ML development, stakeholders need to consider the following:

1. GPU and Accelerator Resource Planning: Ensure sufficient allocation of modern GPUs (A100, H100/H200 class) or establish pathways to HPC resources for training workloads that exceed AF capacity. Plan for integration of FPGA accelerator cards for hardware-in-the-loop development.
2. FPGA Tool Integration: Expand the deployment of FPGA development environments across AFs. This requires dedicated storage allocation (150+ GB per toolchain version), license management infrastructure, and potentially containerized environments to manage OS dependencies.
3. Inference-as-a-Service: Deploy and standardize inference server infrastructure (e.g., Triton [136]) across facilities to enable scalable model validation and provide a testbed for front-end inference patterns.
4. Heterogeneous Computing Testbeds: Develop AF resources that mirror the heterogeneous architectures being deployed in detector systems. This includes not only GPUs but also FPGAs, and potentially ARM-based systems for testing the portability of ML inference code.
5. Workflow Automation: Ensure AF infrastructure supports automated pipelines that span training, synthesis, and validation. This includes robust APIs, containerized execution environments, and integration with experiment tracking tools.
6. Cross-Experiment Collaboration: Leverage multi-experiment facilities to share front-end ML techniques and tools across collaborations. A common infrastructure for model development, synthesis, and validation benefits the entire community.
7. Benchmarking and Validation Infrastructure: Establish standardized benchmarks that include front-end ML components, measuring both physics performance and hardware deployment metrics (latency, resource utilization, power consumption).
8. Training and Documentation: Develop tutorials specifically targeting front-end ML development workflows. Existing HEP training materials provide starting points, but specific guidance on the training-to-synthesis workflow is needed.

### 2.5.7 Future Directions: Quantum Computing Integration

Looking further ahead, Analysis Facilities may need to provide access to quantum computing resources as these technologies mature for HEP applications. DOE’s QuantISED program and initiatives like the HEP.QPR project at Berkeley Lab are already exploring quantum algorithms for pattern recognition in tracking applications. While current quantum hardware remains limited in scale, the infrastructure developed for heterogeneous classical computing—including job scheduling across diverse accelerators, containerized environments, and inference-as-a-service architectures—provides a foundation for eventual quantum-classical hybrid workflows.

Several national laboratories and cloud providers now offer access to quantum processors, and Analysis Facilities could serve as gateways to these resources for HEP researchers. Key requirements include: integration with existing batch and workflow systems; standardized interfaces for submitting quantum circuits; and hybrid execution environments that combine classical

pre/post-processing with quantum computation. The codesign principles emphasized throughout this whitepaper—tight integration of algorithms with hardware constraints—will be equally critical for realizing practical quantum advantage in HEP applications.

## 3 Physics Applications

The past decade has seen a rapid expansion in the capabilities of AI/ML, resulting in a broad array of potential applications in high energy physics. While the impact of new AI/ML methods has been felt across the field, the constraints imposed by front-ends and data acquisition systems limit the possibilities for model deployment in these critical areas. These constraints vary across experiments, but encompass restrictions imposed by low latency inference requirements, radiation tolerance needs, and minimal resource availability, among others. Successfully enabling AI/ML solutions in these regimes is challenging, but can greatly enhance the physics performance of experiments. These enhancements are not confined only to planned or current experiments, or only to collider experiments or neutrino experiments, but cover a broad range of experiments and physics goals. In some cases modern AI/ML offers the possibility for improving the performance of standard tasks such as particle identification, while elsewhere they could potentially enable completely new techniques that have previously been impossible, such as smart data compression. While some challenges for these application are the same as those faced in the broader use of AI/ML in physics, there are also some challenges that are unique. In this section, we detail potential applications that could benefit from advances in HEQUPP ML. While these applications are grouped according to the relevant physics and type of detector technology, we stress that principles such as the need for codesign, effective general tools, and preservation/validation of models and solutions are shared across applications [139]. We believe that solutions for these shared problems represent ideal targets for future work, with specialization for the given application possible.

### 3.1 Collider Physics

**Contributors:** Nural Akchurin, Saptaparna Bhattacharya, James Brau, Martin Breidenbach, Antonio Chahine, Mariarosaria D’Alfonso, Giuseppe Di Guglielmo, Karri DiPetrillo, Erdem Yigit Ertorer, Jan Eysermans, Yongbin Feng, Emmett Forrestel, Dolores Garcia, Julián García Pardiñas, Lino Gerlach, Julia Gonski, Loukas Gouskos, Katya Govorkova, Lindsey Gray, Timon Heim, Abraham Holtermann, Gian Michele Innocenti, Jelena Lalic, Tommy Lam, Vladimir Lončar, Yun-Tsung Lai, Haoyun Liu, Christopher Madrid, Victoria Nguyen, Simone Pagan Griso, Benedikt Maier, Isobel Ojalvo, Christoph Paus, Dylan Rankin, Sebastian Schmitt, Eluned Anne Smith, Kaito Sugizaki, Yash Vora, Andy White, Keisuke Yoshihara

#### 3.1.1 Applications to Vertex Detectors

**High Luminosity LHC** At the HL-LHC, on-device ML for vertex detectors is being extensively studied by the Smartpixels collaboration [140, 141, 142, 143] from the standpoint of implementation as a full detector system. The sensor technology being targeted here is the same as for the Phase 2 upgrade, but with a smaller sensor pitch of  $12.5 \times 50 \mu\text{m}^2$ , using a 28 nm technology node for the ASIC. The vertex detector is the last remaining subsystem of the CMS and ATLAS detectors that is not part of the Level-1 trigger systems of those detectors. Using ML in the front-end to compress data either to a latent space or useful physical cluster features provides the means to stream pixel data at the HL-LHC collision rate, providing the data necessary for heavy flavor tagging and detailed tracking, and thereby enabling the Level-One triggers of these experiments to significantly improve background rejection for events with displaced vertices across a range of  $c\tau$  values relevant to  $\tau$ -leptons, b-hadrons, a variety of beyond-standard-model long lived-particle scenarios, and narrow mass gap SUSY with soft-particle based signatures.

The Smartpixels team, within CMS, is developing a program to study the feasibility of implementation and deployment of such a detector within the next ten years aiming for roughly half-way through HL-LHC. Of particular note is that if such an upgrade were to be realized, there would be a corresponding upgrade of the CMS Level-One trigger system as well as the pixel backend system to handle the increased data rate and new telecom technologies required to execute such a system. This notably increases the complexity of delivering such a detector, but the improvements could also be staged for improved feasibility. The group is also developing a detailed physics case of the HL-LHC to support such an aggressive addendum to the CMS Phase 2 program that stands to improve the physics legacy of the HL-LHC.

Thinking to further future colliders, this sort of technology could be extended to entire tracking systems. ML-based processing elements that link hits, and then tracks segments, together could be integrated into support structures and detector bulkheads embedding a extremely low latency track trigger into future tracking detectors. Moreover, a calibration strategy even only reading out the tracks is possible through statistical sampling of regions-of-interest around found tracks. Managing the material budget and cooling of such a detector will be challenging, but the resulting simultaneous reduction of data rate while preserving a robust calibration strategy yields an instrument capable of scaling through orders of magnitude in luminosity at hadron and muon colliders. Demonstrations in the coming years of such highly integrated technologies has the potential to set a new direction in detector design.

**Electron-Ion Collider** The Electron-Ion Collider (EIC), the future U.S. Nuclear Physics flagship facility at Brookhaven National Laboratory (BNL), will collide high-energy polarized electrons with protons and nuclei at center-of-mass energies of roughly 20–140 GeV, enabling precision studies of quarks and gluons in protons and nuclei in both momentum and coordinate space [144]. The EIC will address fundamental questions in nuclear physics, including the origin of the nucleon mass, the nucleon spin, and the behavior of nuclear matter in regimes of high gluon density.

Achieving outstanding spatial resolution for the reconstruction of charged hadrons over the widest possible pseudorapidity range, down to low transverse momentum ( $p_T < 1 \text{ GeV}/c$ ), is one of the key experimental challenges. The capability to reconstruct and tag charm- and beauty-hadron decays, which are essential elements of the EIC physics program, requires identification of decay vertices displaced by a few tens of micrometers from the primary interaction point. This goal can be achieved by maximizing single-hit spatial resolution by employing highly segmented sensors (small pixel sizes), and minimizing the overall amount of matter that a particle traverses, since a high *material budget* increases multiple Coulomb scattering and leads to poorer impact-parameter resolution. Monolithic Active Pixel Sensors (MAPS) have been identified as the ideal technological choice to equip the future vertexing and tracking experiments at the EIC [145]. State-of-the-art MAPS integrate the sensitive pixel structure and full CMOS readout on the same silicon die, building on commercial technology. Compared to conventional “hybrid” pixel detectors [146, 147, 148] widely used in the community, in which a separate sensor and a readout ASIC are integrated via bump bonding, MAPS achieve reduced material budget, elimination of interconnects, reduced assembly complexity, and smaller pixel sizes.

Despite the unquestionable experimental advantages, the existing MAPS technology poses challenges associated with the specific conditions of electron-ion collisions and the stringent experimental constraints posed by the EIC physics program. Because it was designed for the extreme hit densities in ultra-relativistic lead-lead (PbPb) collisions at the LHC, MOSAIX employs eight high-speed links (5.12–10.24 Gb/s) to cope with a massive aggregate output bandwidth per sensor segment of  $\mathcal{O}(30) \text{ Gb/s}$  [149, 145]. Since the rate of truly hadronic PbPb collisions at the LHC is relatively low (about 50 kHz), the sensor was designed to operate with a relatively long

integration time of  $2 \mu\text{s}$ <sup>4</sup>. Finally, MOSAIX was designed for a small-sized tracking detector (ITS3) composed of only three small layers ( $R < 4 \text{ cm}$ ) with no forward disks, providing ample space for the large amount of services and cabling needed to power the sensors, and to route the data flow out of the experimental area. In electron–proton and electron–ion collisions at the EIC, the typical event multiplicity is about two orders of magnitude smaller than one hadronic lead–lead collision at the LHC. On the other hand, the typical interaction rate of deep-inelastic scattering (DIS) events considered in the ePIC design is about 500 kHz, which calls for shorter integration times for the vertexing and tracking detectors. The need for differential measurements as a function of both transverse momentum and pseudorapidity forces the experimental collaborations to build a much larger, nearly hermetic detector with forward disks, and substantially strengthens the constraints on minimizing the material budget introduced by cabling, services, and cooling systems, especially at forward pseudorapidities.

By substantially reducing the data flow at the source and optimizing the data-aggregation process at the sensor periphery, and potentially at the matrix level, on-chip AI addresses the principal experimental limitations of MAPS in electron–ion collisions, namely the need to minimize the material budget of tracking detectors, reduce the reliance on services, and shorten the integration time associated with signal collection and processing. Ongoing activities focus on the design, optimization, and physical implementation of an AI-enabled chip capable of performing local on-chip reconstruction and adaptive data reduction and compression. Recently, a fully scripted end-to-end automated flow has been developed for neural-network training, quantization, and ASIC synthesis, enabling the first realistic estimates of power consumption, area, and latency. Supporting this project would make it possible to define the experimental boundaries for the use of AI devices, benchmark both algorithmic performance and hardware constraints of the corresponding implementations, and thereby inform a more global optimization of future data-compression strategies. Developing such techniques within the design of a real-life MAPS sensor, such as MOSAIX, has unique experimental value, as it enables a direct comparison between traditional on-chip data compression strategies adopted in the most advanced MAPS sensors and the potential benefits of AI-based approaches.

Supporting this R&D program and expanding its scope to a global on-chip data reduction strategy for future upgrades of the ePIC experiment and for additional EIC detectors, such as the so-called Detector 2, would substantially enhance the reach of the EIC physics program. Moreover, the expertise gained from developing on-chip solutions for MAPS detectors at the EIC could have significant impact across a wide range of future experiments, including the FCC, which plan to rely on MAPS sensors. This effort would further leverage and extend the unique experience developed within the nuclear physics community in the design and application of MAPS technology.

**FCC-ee** Monolithic Active Pixel Sensors (MAPS) are a leading candidate technology for future collider vertex detectors due to their fine granularity, low material budget, and cost effectiveness. At the FCC-ee, a MAPS-based Inner Vertex Detector with  $20 \times 20 \mu\text{m}$  pixels is foreseen in major detector concepts such as IDEA [150] and CLD. Initial projections predict an occupancy in the inner layers that is at the upper end of estimated readout capabilities, primarily driven by low- $p_T$   $e^+e^-$  pairs from beam-induced background (BIB) processes. This necessitates the exploration of a lightweight trigger system that reduces rates without compromising the stringent physics goals. Alternatively, if BIB can be mitigated during readout, an innermost pixel layer that is closer to the interaction point could be afforded.

To that end, we propose a feasibility study for sensors that are not only passive data providers

---

<sup>4</sup>Integration time is defined as the time interval during which a pixel is active and integrates charge.

but incorporate intelligence directly on-chip and can be used for data compression and/or filtering directly at the sensor level. Inspired by the concept of SmartPixels currently being studied for the HL-LHC [140, 141], we propose the idea of intelligent MAPS, “iMAPS”. By embedding AI-based processing capabilities directly into MAPS architectures, track parameter estimation could be achieved in-situ, enabling local BIB suppression. Our study will start with obtaining a detailed electromagnetic field map of the sensor, implementing it in a TCAD framework, and carrying out full device-level simulations to evaluate charge transport, collection dynamics, and the feasibility of embedding lightweight AI primitives into the pixel architecture.

**Muon collider** A muon collider represents a fantastic opportunity to explore the 10 TeV scale in a compact and power efficient machine. However, beam-induced background (BIB) due to muon decays near the interaction region pose a significant challenge for the experiment [151]. Tungsten nozzles placed in the forward region of the detector convert high energy muon decay products into a shower of  $\mathcal{O}(10^8)$  low energy neutrons, photons, and electrons that leak into the detector each bunch crossing. BIB tends to produce hits which are out of time with respect to particles produced in collisions and generally do not point back to the interaction region.

The combination of extreme data rates and complex spatiotemporal structure of hits strongly motivates on-chip AI for real-time filtering at the front-end of the detector [152]. Hit rates in the innermost layers of the vertex detector are expected to reach  $\mathcal{O}(10\text{--}100)$  hits/mm<sup>2</sup>, calling for  $25 \times 25 \mu\text{m}^2$  silicon pixels with 30 ps temporal resolution. With an anticipated event rate of 30 kHz, data rates between 20 and 70 Gb/s per front-end are expected. Without on-detector data reduction, conventional trigger and DAQ architectures cannot buffer or transmit the resulting data within latency and bandwidth constraints.

Possible handles for reducing data volume include hit timing and pixel cluster shape. Selections based on hit timing alone, while possible with offline reconstruction and calibrations, cannot be implemented with sufficient precision online. Pixel cluster shapes, which are sensitive to the trajectory of the incident particle shape, must be incorporated. Particles produced in collisions tend to produce clusters with shapes and sizes consistent with the expected incident angle, smaller in the central region where particles are perpendicular to the sensor, and longer in the forward region where particles traverse at larger angles. In contrast, the majority of BIB pixel hits are caused by low energy 10 MeV electrons looping parallel to the beamline. BIB clusters tend to be longer than signal regardless of their position in the detector [153, 154].

Several promising efforts to demonstrate data reduction based on pixel cluster shapes are ongoing. Simple selections on pixel cluster size have been demonstrated to reject approximately 20–30% of pixel clusters from BIB with  $< 5\%$  signal cluster loss, depending on the pixel detector layer. Because larger clusters are preferentially rejected, this strategy results in an overall bandwidth reduction of up to 50%. Preliminary studies using a digital neural network for cluster classification further enhance background rejection with moderate signal efficiency loss. These studies exploit features such as the cluster charge profile or charge image, using lower-level simulation inputs, and are inspired by the *smartpixels* concept [40, 141, 155]. Sensor-level optimizations are also being explored; for example, increased sensor thickness may improve signal–background separation [156]. Together, these efforts motivate continued development of detailed simulations and hardware–algorithm co-design tools to fully exploit data reduction capabilities at the front end.

### 3.1.2 Applications to Tracking Detectors

**Cluster Counting in Drift Chambers** Drift chambers are a proven detector technology capable of precision tracking over large volumes with minimal material budget. In these detectors,

an incident charged particle ionizes atoms in a gaseous volume, and the freed electrons are attracted to a central wire by an electric field where they are measured. Traditional particle identification in a drift chamber relies on a measurement of the total energy deposited per unit length ( $dE/dx$ ), but it has long been known that this method suffers from a long tail in the energy distribution as a result of the secondary electrons freed as the initial primary ionized electrons drift towards the collection wire. A measurement of the number of primary electrons collected per unit length ( $dN/dx$ ) instead of  $dE/dx$  can provide a significantly more accurate particle identification.

A crucial component of  $dN/dx$ , or “cluster counting”, would be the ability to resolve individual electron arrival times and amplitudes on each wire with fine detail, which traditionally requires high-bandwidth digitization and large off-detector bandwidth. For high-rate environments such as future Higgs factories or Z-pole runs where sampling rates and triggers would generate data streams approaching terabits per second. The development of ML algorithms capable of analyzing the raw waveforms in real time and extracting  $dN/dx$  directly on the front end would alleviate major bottlenecks in both data volume and bandwidth. Preliminary studies with simulated data have already shown promising capabilities to both distinguish primary and secondary electrons as well as fit within resource/latency constraints, as shown in Figure 23 [157]. Future work is expected to explore the potential of more advanced AI/ML techniques and their ability to meet the front-end needs of particle identification in future experiments with drift chambers.

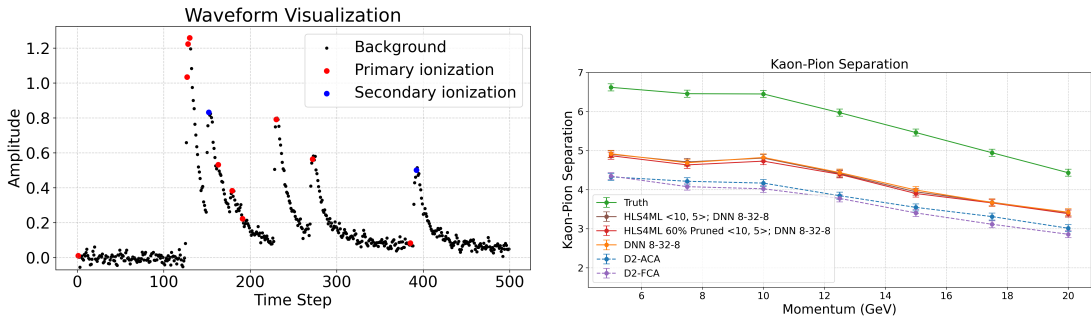


Figure 23: Example drift chamber simulated waveform used to develop ML methods (left), and corresponding PID performance in terms of pion-kaon separation across particle momenta (right).

### 3.1.3 Applications to Calorimetry

**CMS HGCal Readout** At the HL-LHC, to cope with the increasing radiation in the forward region and with the larger number of particles from pile-up, the CMS Collaboration will install a new High-Granularity Calorimeter (HGCal) in the endcaps of the detector. It represents one of the most data-intensive calorimeters ever built, estimated to produce raw rates of  $\sim 5$  Pb/s (per endcap), comparable to the global internet traffic rate [158]. To handle this unprecedented data volume, the front-end electronics must perform substantial on-detector data reduction and feature extraction before transmission off-detector.

Data from the HGCal will be used in the CMS Level-1 Trigger (L1T). Together with the information on tracks, available for the first time at the HL-LHC, the high granularity will facilitate the usage of particle-flow [159] in L1T, increasing the ability to deal with particles from pile-up.

As the first stage of HGICAL’s trigger system, the goal of the **Endcap Concentrator Trigger (ECON-T)** chip is to reduce data volume before transmission off-detector. It is an on-detector radiation-tolerant digital ASIC which receives information on trigger cells (TCs), an aggregation of raw signals from multiple detector cells, computed at an earlier stage of the on-detector data processing. The ECON-T compresses and transmits TC information off-detector under stringent latency ( $<250$  ns) and power ( $<2.5$  mW/channel) constraints. To do that, the ECON-T runs different rule-based data reduction algorithms. It also supports a hardware implementation of a neural-network (NN) encoder for data compression [160].

ECON-T is the first radiation-tolerant, digital ASIC to provide ML inference directly at the detector edge for particle physics applications. The NN encoder itself operates with latency less than 50 ns and power dissipation less than 50 mW, which corresponds to 1.2 nJ per inference.

Integrating ML into such a device requires careful co-optimization between algorithmic design and ASIC implementation, balancing physics performance against area, power, and timing requirements. Quantization, fixed-point arithmetic, and model pruning are essential to meeting these constraints while maintaining low-latency operation.

Ongoing R&D efforts explore the use of a **Conditional Autoencoder (CAE)**[161] architecture within the ECON-T ASIC. The CAE extends previous autoencoder-based compression strategies [162] by conditioning the latent representation on sensor-specific metadata—such as sensor type and geometric location in the detector—and by training models for varying bandwidth constraints. This approach aims to achieve a physics-aware compression that adapts to the heterogeneous detector configuration while respecting the tight throughput requirements of the trigger system. Although results are forthcoming, this work demonstrates a broader paradigm shift toward intelligent, on-detector processing, where co-designed ML algorithms and custom ASIC architectures jointly enable real-time data reduction for next-generation particle-physics experiments.

**EIC LFHCal** The Longitudinally segmented forward Hadron Calorimeter (LFHCal) is designed as a plastic scintillator-steel sandwich calorimeter, which is transversely segmented into  $5\times 5$  cm<sup>2</sup> tiles and each tile is coupled to a silicon photomultiplier. The aggregate of the signals from all the photomultipliers are routed out of the detector and digitized by external readout electronics based on the H2GCROC3, a front-end readout ASIC, developed for the CMS HGICAL project.

There are three construction units of the following type. There are 8M modules  $10\times 20\times 140$  cm<sup>3</sup>, 4M modules  $10\times 10\times 140$  cm<sup>3</sup>. Insert modules which will be installed in the two halves surrounding the beam pipe. The 8M and 4M modules consist of tungsten and 61 layers of steel interleaved with scintillator material with a transverse tower size of  $5\times 5$  cm<sup>2</sup>. Multiple consecutive tiles are summed to 7 longitudinal segments per tower. The insert modules will consist of 10 layers of tungsten and 54 layers of steel interleaved with scintillator. Hexagonal tiles of 8 cm<sup>2</sup> are going to be installed, each of which will be read-out individually. The high granularity of the detector will aid in distinguishing particle shower maxima close to the beam pipe. The read-out of the detector needs to be designed to cope with its high granularity. There are 60,928 read-out channels corresponding to the 8M and 4M modules, while there are 23400 read-out channels for the insert modules.

The LFHCal uses the HGCROC for its read-out. This ASIC was developed by the OMEGA group for the CMS HGICAL project. There are several advantages associated with this ASIC, such as its high dynamic range and low power consumption (2W per chip). There are 78 channels per ASIC and the time of arrival is 25 ps. The HGCROC was chosen due to its strong synergy with ALICE FoCal readout R&D. The test boards are designed and produced and bear interfaces compatible with commercial digitizers.

**Hadron calorimeters** Calorimeters are one of the critical elements of collider-based experiments, essential for the precise measurement of physics observables, such as jets, photons, and missing transverse momentum, which directly impact our understanding of the Standard Model and the discovery potential of new physics.

In recent decades, calorimeter granularity has increased substantially to capture fine shower structures, enhancing both measurement precision and physics potential. However, this improvement has generated a massive increase in data volume, exacerbated by the rapid multiplication of particles during shower cascades. Given readout bandwidth limitations, it is critical to deploy online algorithms that process detector information “immediately”, preserving physics-relevant data within tight latency constraints. Machine learning offers a robust solution to this bandwidth and latency bottleneck, capable of extracting hidden correlations and making rapid decisions under the harsh resource constraints of the detector front-end.

The integration of dual-readout techniques [163, 164] with high-granularity designs represents a new frontier in calorimetry. Concurrently, rapid advancements in photodetector technology, specifically silicon photomultipliers, and readout electronics have significantly enhanced timing precision. Such developments enable the reconstruction of longitudinal shower profiles through timing information, effectively providing depth segmentation in detectors lacking physical layers. When combined with modern machine learning algorithms, such as Convolutional Neural Networks (CNNs) and Graph Neural Networks (GNNs), these hardware improvements promise to significantly enhance energy measurement performance from simulation studies [165], as illustrated in Figure 24. To experimentally validate this synergy between high-granularity dual-readout calorimetry, precision timing, and ML-driven on-chip and offline reconstruction, a prototype “HG-DREAM” has been developed, with a campaign of beam tests currently underway to assess its performance.

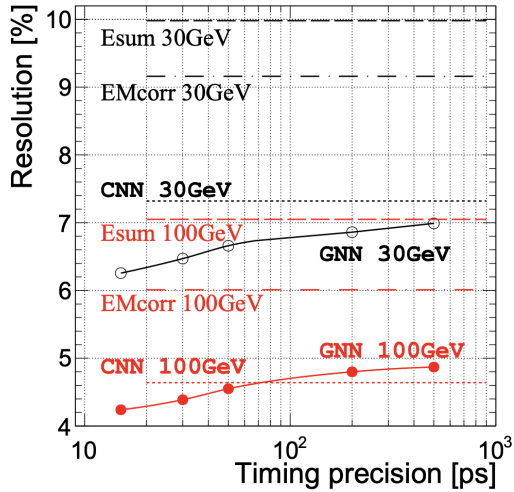


Figure 24: Energy measurement resolution comparing classical hadron calorimeter with energy sum (“Esum”), dual-readout (“EMCorr”), and using machine learning algorithms (“CNN” and “GNN”), for pions at 30 GeV (black) and 100 GeV (red). The figure is taken from [165].

Realizing high-precision timing in real experiments demands efficient processing of signal waveforms. Initial studies demonstrate that spectral deconvolution effectively extracts photon arrival times from raw pulses, enabling the reconstruction of the shower’s longitudinal development (energy vs longitudinal depth). One example is shown in Figure 25. A critical next step is

to investigate the pruning and simplification of these algorithms, adapting them in real-time execution within the strict power and bandwidth constraints of front-end readout systems, ensuring that the reduction in complexity does not compromise the performance of downstream energy reconstruction or high-level physics observables such as jet energy scale and mass resolution. This optimization is a prerequisite for the fabrication of prototype chips, which will allow for rigorous performance testing. The final objective is the integration of the calorimeter together with validated chips and algorithms into future experiments for enhanced data quality.

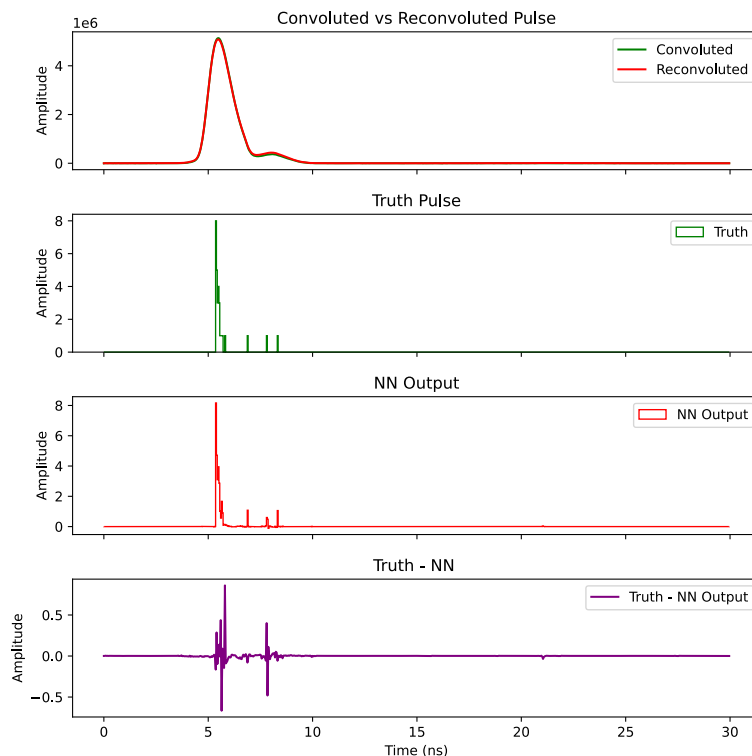


Figure 25: LSTM-based deconvolution of calorimeter pulse shapes. The reconstructed photon time profile (third panel) is compared against the ground truth pulse (second panel), demonstrating good agreement (fourth panel).

**5D calorimetry** Most physics analyses use some form of AI/ML to identify physics objects such as jets and electrons and/or for whole event classification. However, such an approach has generally been taken a long time after the detector was designed and constructed. It is therefore relevant to question whether a proposed design of a future calorimeter is optimal for the application of AI/ML techniques and, if such techniques are also to be used onboard the detector, what are the potential benefits of an integrated online/offline AI/ML approach. The first area to consider is what aspects of calorimeter design would benefit the use of AI/ML for object and/or whole event topological recognition. These aspects include the level of granularity, inclusion of timing and tracking layers, inter-layer communication, and traditional ECal/HCal separation or a more integrated design. There are tradeoffs in terms of complexity versus efficiency for online or offline ML algorithms, increased information and reduced mis-associations (e.g. in PFAs)

versus increased power requirements and cooling/material needs, complexity of design versus calibration and systematic errors determination, and size of data structures and propagation through online/offline systems.

Next is consideration of aspects of an integrated online/offline AI/ML calorimeter system. How ambitious can we be given limitations of present front-end systems versus realistic projections of future capabilities for when systems would actually be needed? Could we envision, for instance, a reduced online PFA version, with input from tracking and calorimetry? What could be gained from a ML/topological pattern trigger system versus a traditional trigger menu approach? Should the results of online ML algorithms be captured as seeds for offline ML? Should we view the DAQ as an organizing stage for input to offline AI/ML algorithms?

Then there are the more operational aspects of an integrated AI/ML system such as monitoring, calibration, fault detection, and data quality assurance. ML can be used for flagging dead/intermittent/noisy channels, deciding when a recalibration is needed (using a DB history), tracking and reporting data quality and making symmetry checks (e.g. phi, forward/backward), suggesting/deciding when certain tasks are needed such as charge injection to FE electronics or laser pulsing for SiPMs. Reliance on ML for these tasks will need very careful design and verification due to the potentially irrecoverable nature of decisions or actions.

In summary, an integrated AI/ML approach to calorimeter design, implementation and operation raises a large number of challenging questions and will require many studies to understand the issues and define the most promising R&D directions.

**Pixelated calorimetry** Monolithic active pixel sensors used in future sampling electromagnetic calorimeters at collider experiments can provide excellent detection and measurement of gamma and electron initiated showers, as well as the energy deposited by hadrons passing through and eventually completing their energy deposition in the hadron calorimeter [166]. This will enable excellent input to the particle flow analysis built from the use of both tracking and calorimetry. There are possible improvements to performance and data collection from application of machine learning techniques.

The hits in the pixels of the electromagnetic calorimeter will be sparse, as illustrated in the figure. This shows two simulations of 10 GeV gamma showers with 25 um x 100 um pixel sensors sampled every 0.7 radiation lengths. Layer 10 hits show a typical transverse distribution after about 7 radiation lengths, and layer 18 after about 12 radiation lengths. The vacancies are obvious, motivating readout optimized for sparse data. With an example design (SiD for the linear collider [167]) the calorimeter contains about  $5 \times 10^8$  pixels, while typically less than 106 will be active during any beam crossing event. For future electron-positron colliders the event rate is generally moderate enough (with the possible exception of the *teraZ* factory) that on-detector sparsification and organization can simplify and optimize the operation. The individual layer process is generally straight-forward, although multiple threshold applications might be of benefit and need machine learning approaches. Matching of layers would require more sophisticated analysis where machine learning might have an additional impact, with the obvious place for such processing in data collection/compression nodes that collect from the full calorimeter. While the pixels are generally isolated, as the figure shows, cluster formation based on machine learning approaches during readout could benefit on-line analysis. It should be noted that electron-positron linear colliders are expected to be trigger-less.

One critical aspect that needs understanding is any significant increased power required by sensors with readout involving machine learning, and designs for handling any such thermal load without harming performance.

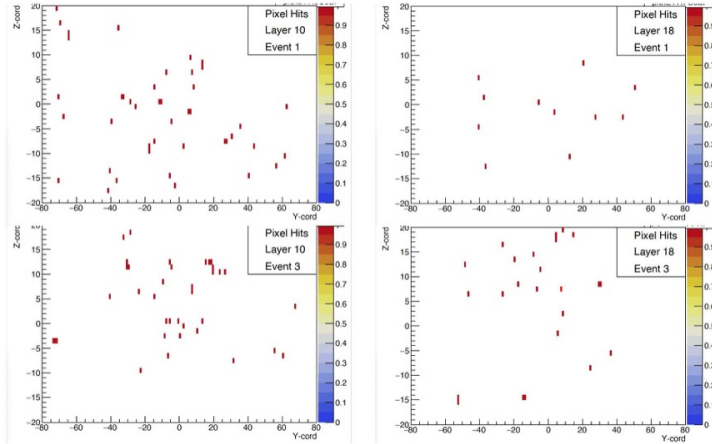


Figure 26: Transverse distribution of hits for 25  $\mu\text{m}$  ( $y$ )  $\times$  100  $\mu\text{m}$  ( $z$ ) pixels around the axis of 10 GeV gamma showers for two events in the SiD ECAL. Plots on left show distribution in layer 10 and plots on right in layer 18 (first layer is layer 0). The plots show the hits for 16  $\text{mm}^2$  around the core of the shower.

**LHCb ECAL Upgrade II** The LHCb Upgrade II [168], foreseen to operate after the long-shutdown 4 of the Large Hadron Collider (LHC), will produce data rates of about 200 Tb/s, necessitating major upgrades of the detector including the front-end (FE) electronics. One example where improvements of the performance are needed is the electromagnetic calorimeter, the so-called PicoCal. The readout is based on photo-multiplier tubes (PMTs), which produce a voltage signal proportional to the number of scintillation photons that are produced in the active detector material. It is estimated that, in order to cope with the data-rates between the on-detector FE and backend electronics, only two numbers with a similar bit size of around 10-bits can be used to describe the measured pulse-shape in each channel per bunch crossing. This dictates that a highly efficient compression algorithm running on the on-detector FE boards is needed in order to persist the pulse-shape information. With the pulse shape information, pile-up can be mitigated more efficiently and the energy resolution can be improved.

As the on-detector electronics are subject to the high-radiation environment of the LHC, we choose the PolarFire field programmable gate arrays (FPGAs) to implement our compression algorithm. The PolarFire FPGAs use a flash-based architecture which inherently makes them less susceptible to single event upsets (SEUs). In order to allow for a broader adoption of machine learning on those FPGAs by the community, we have extended the `hls4ml` [169, 170] framework to also include support for the PolarFire FPGAs.

The compression algorithm is based on an autoencoder architecture, using a latent space comprising two 10-bit floating point numbers where four bits encode the integer base. This representation is chosen using a quantization-aware training procedure [171, 172, 173] employing a search over latent-space configurations with different bit-representations. By comparing the mean squared error (MSE), as illustrated in Figure 27, we show that our choice offers the best performance compatible with the constraints imposed by the data-rates. The training is

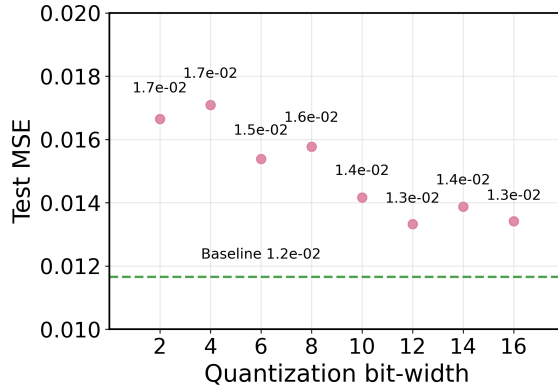


Figure 27: Impact of the quantisation on the autoencoders reconstruction performance measured using the mean squared error (MSE). The baseline corresponds to the unquantised training performance.

performed using a dedicated Monte Carlo simulation of the LHCb PicoCal prototype [168], producing realistic signal responses under the expected conditions. In addition to greatly reducing the data-rate, the compression algorithm also improves the timing-resolution. For this purpose we use a constant fraction discrimination (CFD) algorithm [174] to determine the time-stamp of a simulated pulse and compare it with the true arrival time. As shown in Figure 28, the resolution of the measured time stamp is approximately two times better for the compressed pulses compared to the original pulses. This is because the compressed pulses are smoothed and background contributions are suppressed. In the future the loss function may be changed to include physical benchmarks, such as the energy resolution of reconstructed particles instead of MSE. This would allow to optimally package the information in the latent space for the reconstruction algorithms.

With the newly introduced support of PolarFire FPGAs in `hls4ml`, which will be publicly available from version `v1.3.0` onwards, we synthesise our model and show that the utilisation of the hardware resources is minimal. The algorithm achieves a maximum frequency of 234 MHz, well above the target of 160 MHz. Using an inference latency of 25 ns corresponding to four clock-cycles at 160 MHz and an initiation-interval of four, the implementation only utilises 3.1 % of the lookup tables and 0.3 % of the dedicated math blocks. This is well within the bunch crossing rate of 40 MHz at the LHC.

### 3.1.4 Applications to Triggers

**AXOL1TL: Anomaly Extraction Online L1 Trigger Lightweight** The Anomaly Extraction Online L1 Trigger Lightweight (AXOL1TL) is a model-agnostic anomaly detection trigger at CMS that identifies rare, non-Standard Model events by analyzing high-level objects at the Global Trigger (GT). Traditionally, triggers rely on fixed object definitions and thresholds, which can overlook complex, unforeseen signatures. AXOL1TL addresses this by processing the 3-vector information  $(p_T, \eta, \phi)$  of the 10 highest-energy jets, 4 muons, 4 electrons/photons, and missing transverse energy (MET). By flagging unusual events directly from data, AXOL1TL complements conventional approaches and increases sensitivity to unknown physics.

AXOL1TL employs a Variational Autoencoder (VAE) architecture trained unsupervised on Zero Bias collision data to learn the underlying probability density of typical background events.

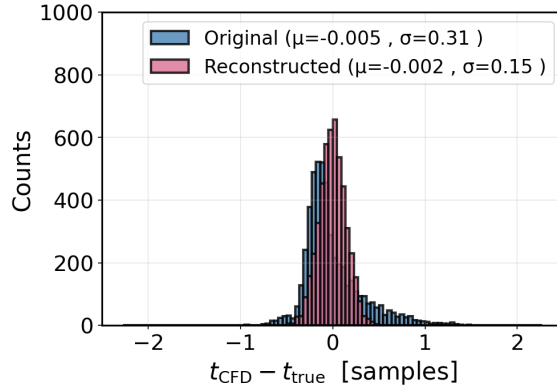


Figure 28: Residual distribution between the CFD reconstructed timestamps of the original and compressed pulses. The time axis is given in the discrete sampling units of the application specific integrated circuit discretising the signal from the PMTs.

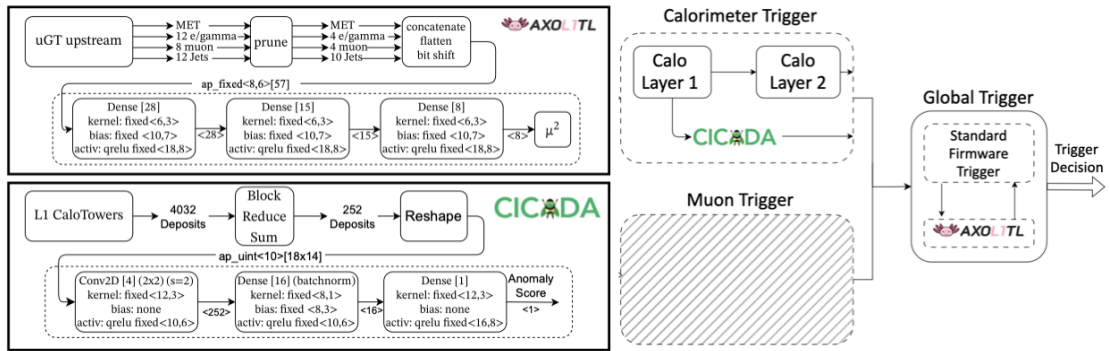


Figure 29: The left shows the architecture and quantization schemes of the deployed AXOL1TL (top) and CICADA (bottom) models. The right shows an overview of the CMS L1 trigger system and where AXOL1TL and CICADA sit in the data processing chain.

To meet a strict latency requirement of 50 ns (2 FPGA clock cycles), only the encoder portion is deployed during real-time inference. The algorithm was first deployed in 2024 and has recorded significant datasets, including  $54.7 \text{ fb}^{-1}$  for its core seeds. Analysis of this recorded data shows that while there is some overlap with conventional L1 triggers, AXOL1TL also demonstrates sensitivity to unique events that would otherwise be missed. Performance evaluations using simulated signals reveal that AXOL1TL is particularly sensitive to novel events containing well-clustered, SM-like decay products. First physics analyses based on the 2024 recorded data are currently in development.

**CICADA: Calorimeter Image Convolutional Anomaly Detection Algorithm** The Calorimeter Image Convolutional Anomaly Detection Algorithm (CICADA) is a signal-agnostic trigger for CMS designed to identify anomalies using low-level, unclustered calorimeter information. Unlike object-based triggers, CICADA processes raw energy deposits from the Calorimeter Trigger Layer-1, providing sensitivity to unusual energy topologies that might not be reconstructed as standard jets or leptons. The algorithm is implemented as a Convolutional Autoen-

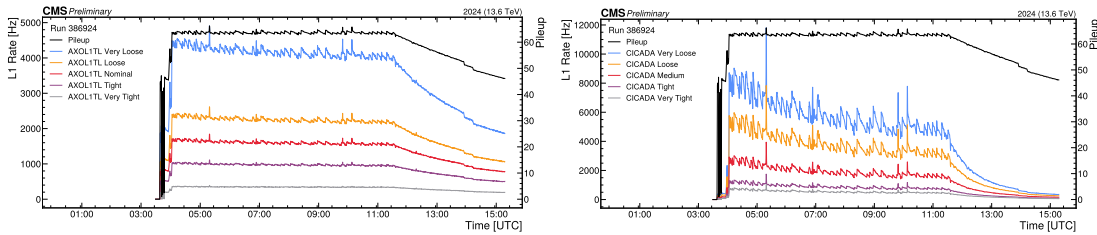


Figure 30: Trigger rate of various AXOL1TL (left) and CICADA seeds during late 2024.

coder that captures spatial correlations across the detector’s  $\eta - \phi$  cylindrical surface.

To ensure efficiency within the L1 hardware, CICADA uses a ”Teacher-Student” training approach where a complex Teacher model’s knowledge is distilled into a quantized Student model optimized for FPGAs. The Student model achieves an inference latency of 81.25 ns (13 clock cycles). Deployed in 2024, CICADA has successfully recorded data and operates with a pure rate budget of approximately 150 Hz for its Medium seed. Initial analysis of recorded data indicates that CICADA triggers on unique events not captured by standard L1 algorithms. While AXOL1TL focuses on clustered objects, CICADA excels at identifying high-multiplicity, low-energy signatures, such as soft unclustered energy patterns (SUEP).

**GELATO: A Generic Event-Level Anomalous Trigger Option for ATLAS in LHC Run 3** Trigger systems require an a priori definition of ”interesting” events, which can exclude unexpected new physics. The Generic Event-Level Anomalous Trigger Option (GELATO) effort is a model-agnostic anomaly detection trigger for ATLAS that identifies rare events without assuming specific signal models. By flagging unusual events directly from data, such triggers complement conventional approaches and increase sensitivity to unknown physics. GELATO was deployed in 2025 and is the first such trigger for ATLAS, with similar efforts underway in CMS [175].

GELATO is a two-level AD algorithm and consists of GELATO L1 and GELATO HLT (Figure 31). Both are autoencoder-based architectures that train over four vectors of leading particles in the event, with the distinction that the L1 model employs a VAE with a generative adversarial network (GAN) to refine the latent space during training without adding resources in the constrained scenario of inference at trigger-level. GELATO L1 runs on 40 MHz input data and targets an output unique rate of 500 Hz, while GELATO HLT runs only over GELATO L1 events and targets 20 Hz output rate. As shown in , GELATO L1 and HLT both adopt an autoencoder architecture In GELATO, each MSE is calculated by ignoring input zero values, which is referred to as ”masked MSE”.

The GELATO L1 and HLT models are trained on the 2024 enhanced bias dataset [176], which provides an unbiased event sample with weighted low-rate tails, and closely matches the detector conditions expected for 2025. The performance of the GELATO L1 and HLT pipeline are estimated using an EB test set and simulated samples of a variety of signatures such as dark photon models, heavy neutral leptons, and BSM Higgs. GELATO achieves signal efficiency gains of 5–70% at L1 and 3–30% at HLT, demonstrating sensitivity across a broad range of signatures.

The implementation of GELATO into the ATLAS trigger system is conducted using various tools. The GELATO L1 algorithm is converted to high-level synthesis (HLS) using `hls4m1` [15], a package for machine learning inference in FPGAs. It is then synthesized with AMD Vitis. The GELATO HLT model is converted to ONNX format for implementation into Athena, the ATLAS software framework used for collision-event processing, including the HLT system. The GELATO

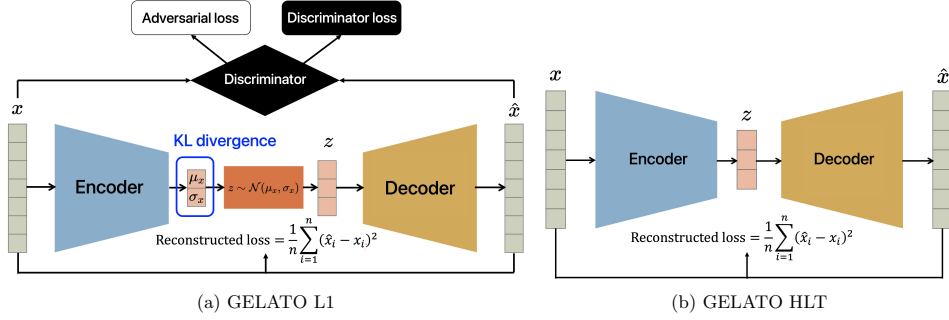


Figure 31: Model architectures for GELATO L1 and HLT.

trigger pipeline is constructed by combining GELATO L1 and HLT algorithms with dedicated object preselections and seeding algorithms, which have been tuned to meet the required latency of  $O(100 \text{ ms})$ .

As of August 2025, gradual commissioning steps are in progress for safe deployment of GELATO. As a first step during early LHC ramp-up period in April to early May of 2025, the GELATO L1 rate at the ATLAS Central Trigger system was monitored for stability checks as shown in Figure 32, however, it was not actually enabled for trigger decisions. It has been confirmed that the total trigger rate of GELATO L1 is as expected and is also consistent with the LHC luminosity and rates of other primary triggers. Following the rate stability checks, in the first runs with stable beams, GELATO L1 was enabled with a prescaled rate of about 1 Hz. In 2026 it is planned to enable the whole GELATO pipeline with full capacity at target unique trigger rates of 500 Hz and 20 Hz for L1 and HLT, respectively. Studies are in progress to deepen the understanding of the triggered events and ultimately use them to search for new BSM physics.

**NomAD: Nanosecond Anomaly Detector at ATLAS in LHC Run 3** NomAD is an anomaly detector that distills a fully trained variational autoencoder (VAE) using decision trees for implementation on FPGA. The distillation is accomplished by regressing the latent space parameters with the software package and framework FWXMACHINA, discussed in earlier in this document. The training and distilling process is shown in Figure 33. In the three-step process, the left-most panel shows the neural network training of the VAE as the “mind.” The middle panel shows the regressed decision tree as the “body.” The right-most panel shows the deployed VHDL model on the FPGA.

Implementation is accomplished using muons as input objects, targeting new physics scenarios involving multimuon final states. The correlation plot between the VAE anomaly score and the regressed BDT is shown in the left plot of Figure 34. Increased acceptance of, for example, final states from  $B_s$  decays, are shown on the right plot of the same figure. Commissioning of this trigger is on-going as of this document.

We note that while this particular model targeted multimuon final states for deployment, the approach is general and can be applied to a wider scope of final states and physics scenarios.

### 3.1.5 SuperKEKB/Belle II

The SuperKEKB/Belle II experiment aims to perform precision measurements of CP violation in the  $B$ -meson sector and to search for physics beyond the Standard Model using unprecedented

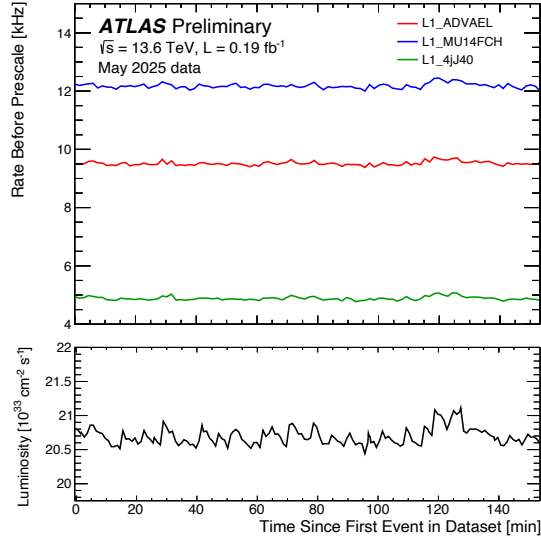


Figure 32: The trigger rate of the GELATO L1 monitored at the ATLAS Central Trigger in May 2025. The GELATO L1 rate is shown in red, along with the single muon trigger rate in blue and four-jet trigger in green shown as reference. The GELATO L1 rate is consistent with the reference trigger rates and the LHC instantaneous luminosity shown in the bottom panel.

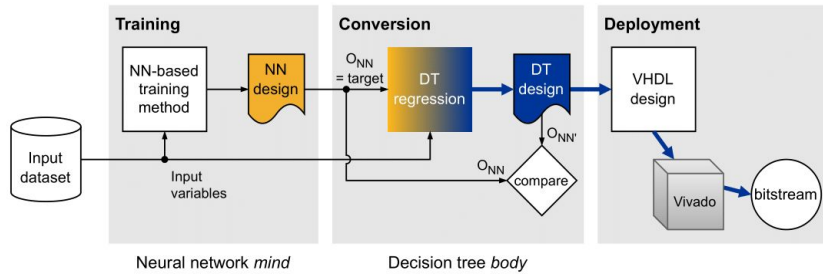


Figure 33: Distilling process of the variational autoencoder for NomAD at ATLAS.

dataset of  $50 \text{ ab}^{-1}$ . Achieving the design luminosity requires the nano-beam scheme, but current accelerator operations encounter sudden beam-loss (SBL) events that can damage detector components or accelerator hardware. Fast beam-abort capability is therefore essential. In this context, AI/ML-based anomaly detection and real-time diagnostics are becoming increasingly important elements of the machine protection strategy.

- BOR (Bunch Oscillation Recorder):** The BOR system provides bunch-by-bunch measurements of horizontal and vertical beam motion using Beam Position Monitors (BPMs) together with RFSoc-based or other embedded readout systems. By capturing oscillation patterns at nanosecond timescales, BOR enables diagnostics of injection noise, beam-beam interactions, and the precursors of SBL events. Integration of AI/ML models can significantly enhance BOR's capability: real-time pattern recognition can identify subtle instabilities earlier than traditional "loss detection"-based methods. Such early warning open the possibility for preemptive beam-abort decisions, preventing damage to the accelerator

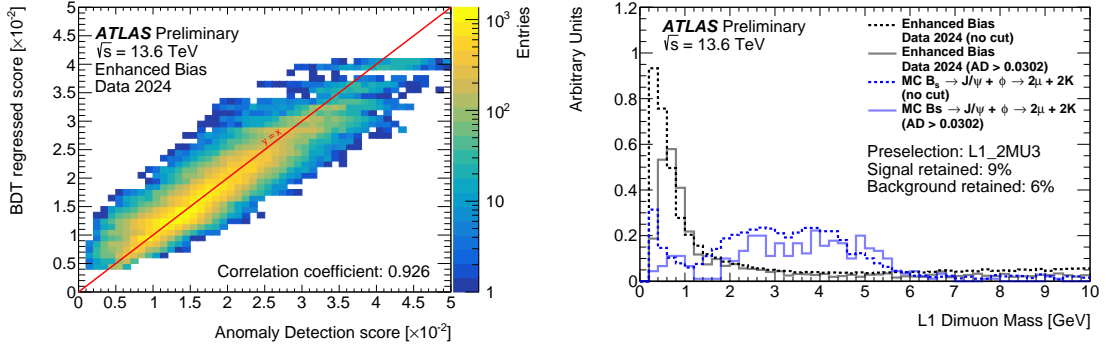


Figure 34: Results for NomAD at ATLAS. (Left) Correlation of the VAE anomaly score and the regressed BDT score. (Right) Dimuon distributions of data and MC with and without NomAD.

and improving the overall stability of the machine operation.

- **XRM (X-ray Beam Size Monitor):** The XRM system measures the vertical beam profile on a bunch-by-bunch basis using synchrotron X-rays, a coded-aperture imaging system, and a fast silicon sensor. This enables rapid beam-size diagnostics and supports a transition from reactive, "loss-based" schemes to predictive monitoring. Deploying hardware-aware ML inference on RFSoc or similar embedded platforms can identify early signatures of SBL events, and support low-latency abort or mitigation decisions.

At the same time, Belle II also offers opportunities to incorporate AI/ML into detector sub-systems, where low-latency inference can enhance timing performance and reduce data volume at the earliest stages of readout.

The data-acquisition system employs a dedicated hardware Level-1 trigger to select physics events. The trigger system comprises  $\mathcal{O}(100)$  FPGA devices that perform real-time processing of detector information within a strict latency of roughly  $5\mu\text{s}$ , set by the available buffer depth in the front-end systems. These FPGAs, including Xilinx Virtex UltraScale devices during current operations, enable reconstruction of full-detector signatures such as charged-particle tracking from the drift chamber, calorimeter clustering, and event-topology identification. ML-based algorithm design for FPGA inference has already become an important tool in this environment.

By contrast, the front-end electronics (FEE) receive ADC waveforms and timing information from smaller subsets of detector channels and are typically built around more resource-limited FPGAs (e.g., Xilinx Virtex-5, Spartan-6). Consequently, the scope and implementation strategy for ML applications at the front-end differ from those in the Level-1 trigger. Front-end ML must operate under tighter constraints in latency, logic resources, and power, motivating the development of highly optimized and hardware-aware inference models.

- **CDC (Central Drift Chamber):** The CDC is the primary tracking detector used for both offline reconstruction and the real-time Level-1 trigger. We developed an ML-based noise-reduction method using ADC waveform processing. To avoid introducing additional latency or dead time in the trigger path, a channel-by-channel parallel implementation is essential. Given the limited resources of the Virtex-5 FPGA used in the current CDC front-end boards, each ML module must be extremely compact. For this reason, a boosted decision tree (BDT) model was chosen over neural-network approaches due to its much

higher resource efficiency. The resulting implementation adds only two clock cycles of latency and occupies approximately 5% of the Virtex-5 resources. An upgraded CDC front-end, incorporating a new ASIC and a Kintex-7 FPGA, is currently under development and is expected to support more sophisticated ML models to further mitigate cross-talk noise and enhance tracking performance.

- **TOP (Time-of-Propagation Detector):** The TOP detector provides charged-hadron identification in the barrel region, particularly for  $\pi/K$  separation. AI/ML-based waveform feature extraction is currently being explored on the back-end readout PCs, where GPU-accelerated systems can support low-latency inference. The planned electronics upgrade over the next 7 years aims to migrate these feature-extraction algorithms directly onto the front-end FPGAs. This would enable real-time event selection, reduce data volume, and improve the robustness of the identification performance under high-luminosity conditions.
- **ECL (Electromagnetic Calorimeter):** The ECL is preparing a major upgrade of its front-end electronics, replacing the Spartan-3-based shaper DSP boards with a modern platform equipped with significantly larger FPGAs (e.g., Virtex UltraScale+). This transition opens the opportunity to incorporate AI/ML algorithms directly into the front-end. Hardware-aware ML models could enable real-time waveform analysis for improved  $e/\pi$  separation, double-pulse and pile-up suppression that are increasingly important under higher background conditions.
- **KLM ( $K_L$  and Muon System):** The KLM consists of RPCs in the barrel and scintillator modules in the endcap, providing essential muon and  $K_L^0$  identification. The current Level-1 trigger is based largely on hit counting, offering limited rejection of cosmic-ray and beam-induced backgrounds. A neural-network-based trigger that uses muon-track candidates and basic track-parameter information would significantly improve muon identification while reducing fake triggers. In the endcap, ML-based inference of photoelectron counts from the waveforms would improve timing resolution and strengthen muon and  $K_L^0$  identification under high-background conditions.
- **Dispaced Vertex Trigger (DVT):** The search for long-lived particles is a key part of the physics program at Belle II, focusing on neutral particles that decay into charged pairs from vertices displaced from the interaction point. The existing Level-1 track trigger is tuned for prompt tracks and would likely reject these displaced-vertex events, motivating a dedicated Displaced Vertex Trigger (DVT) [177]. Implemented on FPGA boards within Belle II's pipelined, deadtime-free 5  $\mu$ s Level-1 latency, the DVT runs in parallel with current triggers and selects events where two oppositely charged tracks form a common displaced vertex. It performs track finding using multiple Hough transforms over a grid of assumed track origins, then uses neural networks to identify the correct vertex via shape analysis of Hough clusters. A Hough-map-based preselection reduces the number of origin hypotheses and significantly cuts FPGA resource usage.

## 3.2 Dark Matter

**Christian Boutan, Tom Braine, Ryan Coffee, Chance Desmet, Stephen Jones, Amy Roberts, Belina von Krosigk**

### 3.2.1 Hardware AI/ML at the Dark Matter Frontier

As dark matter detectors become more sensitive, they no longer capture only potential dark matter events but also neutrinos from natural sources such as the Sun. This neutrino background,

often referred to as the “neutrino fog,” is shown in Figure 35. The figure indicates that imminent experiments should soon attain the sensitivity necessary to detect solar neutrinos [178]. Neutrino signals, which cannot be eliminated or masked, resemble the rare dark matter interactions, presenting an irreducible background that constrains the detection capabilities of dark matter detectors.

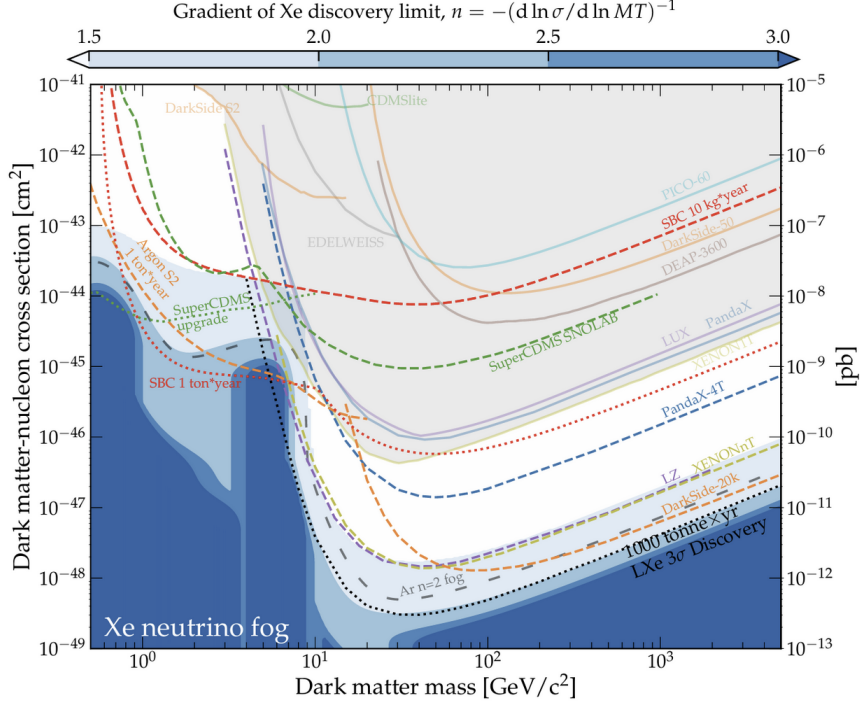


Figure 35: Experiments are sensitive to solar neutrinos (i.e., the “neutrino fog”), making neutrinos an irreducible background [178]. Maintaining dark matter sensitivity will increasingly rely on directional detectors and annual modulation analyses.

This challenge raises the importance of annual modulation searches. Because the Earth orbits the Sun, the relative velocity of Earth through the galactic dark matter halo changes throughout the year, producing a predictable annual modulation in the expected dark matter signal [179]. Solar neutrinos also modulate annually, but, as shown in Figure 36, their modulation is nearly out of phase with the dark matter signal predicted by the standard halo model [180, 181]. This phase difference provides one of the few ways to disentangle dark matter interactions from the otherwise indistinguishable neutrino background. Annual modulation studies are essential for sustaining discovery potential as experiments approach the neutrino fog.

Dark matter experiments are also sensitive to environmental factors. Annual modulation searches, with a one-year period, are fundamentally dependent on the long-term stability of the detectors. If the detector performance fluctuates, the modulation signal may become obscured or misjudged. Additionally, an increase in noise levels establishes a higher threshold for the entire year’s data, thereby reducing the modulation search’s sensitivity. Real-time data analysis with rapid signal-integrity monitoring can give experiment operators the ability to detect anomalies within minutes rather than months or years later. This awareness enables active, real-time correction of systematic errors and ensures the stability required for annual modulation studies.

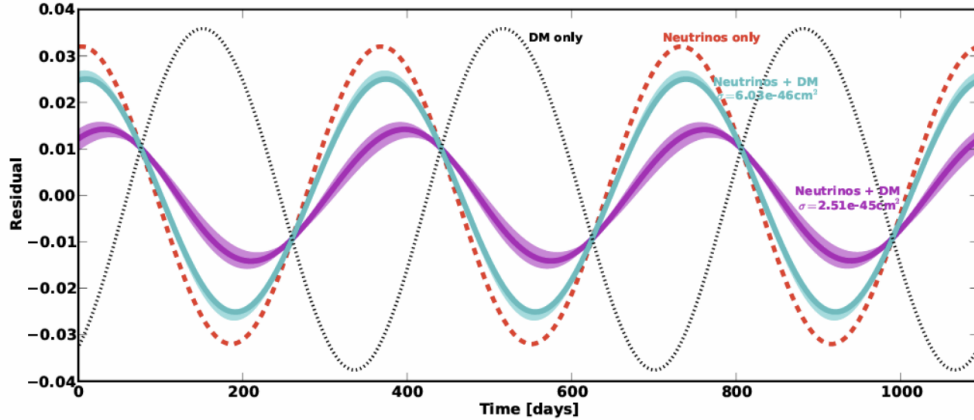


Figure 36: From [180]. The annual modulation of solar neutrinos has almost the opposite phase of the annual modulation of dark matter in the standard halo model. However, to be sensitive to even a 3% amplitude will require up to 10 years of stable data from a 50-ton Xenon detector [181] - and this assumes a perfectly stable experiment.

By contrast, conventional analyses in dark matter experiments often take months to years to complete, which precludes timely corrective action.

Given the upcoming neutrino background, efforts to address experiment stability are increasingly critical. Lightweight AI models on edge devices have the potential to report analysis-level data-quality indicators (such as noise spectra, pulse-shape trends, and energy spectra) within minutes, operating within the power and space constraints of underground detector environments. Enabling real-time monitoring of dark matter experiments is critical to maintaining the stability experiments need as they approach the neutrino floor and annual modulation experiments become increasingly important.

For dark matter searches that focus on low mass candidates, noise reduction is an ever-present concern because the noise floor directly limits the sensitivity to small dark matter signals. Dark matter experiments are already using (non-ML) FPGA processing to lower the signal trigger threshold while minimizing noise triggers [182] and are exploring ML-based approaches on FPGA [183]. Variational autoencoders [184, 185] are another method that may lower trigger thresholds, and may be less susceptible to distorting the signal by de-weighting noise frequencies. In both cases, having the ability to update the signal filtering prior to the trigger may offer improved stability. Also of interest are low-power electronics that can act as a full data acquisition system, producing digitized pulses or even final physics estimators. In many dark matter detection experiments, the need to pull signals out to room temperature to read the signals adds significant noise; using low-power AI/ML hardware at the 77 K temperature stage would avoid unnecessary Johnson and pickup noise.

### 3.2.2 Exploring AI/ML tools for axion dark matter detection

The nature of dark matter is one of the most perplexing questions in physics today. The axion, a compelling dark matter candidate, if discovered, could simultaneously solve the Strong CP Problem of QCD and account for dark matter. The "axion haloscope" is a detection technique, designed to convert  $\mu\text{eV}$  axions into detectable microwave photons in a tunable, high-Q, resonant cavity permeated by a strong static magnetic field. These detectors, used by collaborations

like the Axion Dark Matter eXperiment (ADMX), HAYSTAC, CAPP, and ORGAN, are ideal for 0.5–10 GHz photons. However, higher frequency haloscope-like detectors will face significant challenges. Traditional haloscopes lose sensitivity, due to decreased detector volume and increase in quantum noise at higher frequencies, making axion detection near-impossible without novel noise mitigation and signal boosting techniques. Proposed solutions, such as multi-cavity and quantum sensing approaches, will increase detector complexity; a complexity only tractable with advanced automated controls. New AI/ML techniques for in-situ RF response characterization and quantum device control would ease operations in an environment that will change with respect to temperature and magnetic field over time, sometimes voiding standard sensor calibrations. We present example potential uses of AI/ML for future axion discovery applications.

**ML for cold RF characterization** In anticipation of a future scenario where the periodic ensemble characterization of a scaled-up multiplexed system is eating into axion search data collection, we seek opportunities to glean more information from fewer measurements. Inspired by the way environmental changes such as magnetic field and temperature change the RF responses of devices, we performed a series of measurements designed to tease out the feasibility of using Vector Network Analyzer (VNA) RF scattering parameter (S-parameter) responses as dual-purpose measurements. We performed three experiments investigating the viability of using neural networks (NN) for mapping S-parameters to device environment [186]:

1. Learning an RF "fingerprint": Two identical circuits with near-identical RF circulators were assembled. A set of switches toggled a VNA to collect S-parameters on either device. This data was fed to a NN along with a label of which circuit was being measured for supervised learning.
2. Predicting a magnetic field from an RF fingerprint: A toy model of an axion search, involving a cavity, an antenna, and a circulator was assembled. A permanent magnet's proximity to the circulator could be adjusted. S-parameters through the toy model were captured for different magnet positions, and magnet position was provided to the NN as a label (Fig 37, left).
3. Predicting a temperature from an RF fingerprint: A circulator was mounted for S-parameter measurements on the mixing chamber plate of a dilution refrigerator; temperature information, collected from all fridge stages acted as labels to the NN (Fig 37, right).

Each case supported the hypothesis that S-parameters hide features of physical phenomena occurring in an RF network that may be recognized by existing NN techniques to aid in in situ characterization. Figure 37 shows this predictive power. We are optimistic that currently unused wide band measurements may diagnose equipment anomalies and physical conditions. We hope this work inspires more complex applications of machine learning in the axion detection field.

### 3.3 Neutrino Physics

#### 3.3.1 Applications in LArTPCs and DUNE

Liquid Argon Time Projection Chambers (LArTPCs) combine fine-resolution spatial and calorimetric measurements of ionization deposits across multiple sensing views to produce 3D images of particle interactions. Combined with timing and calorimetric information from photon detectors, they enable low-threshold particle ID and reconstruction in a new generation of detectors—like the Deep Underground Neutrino Experiment (DUNE)—that are capturing neutrino interactions

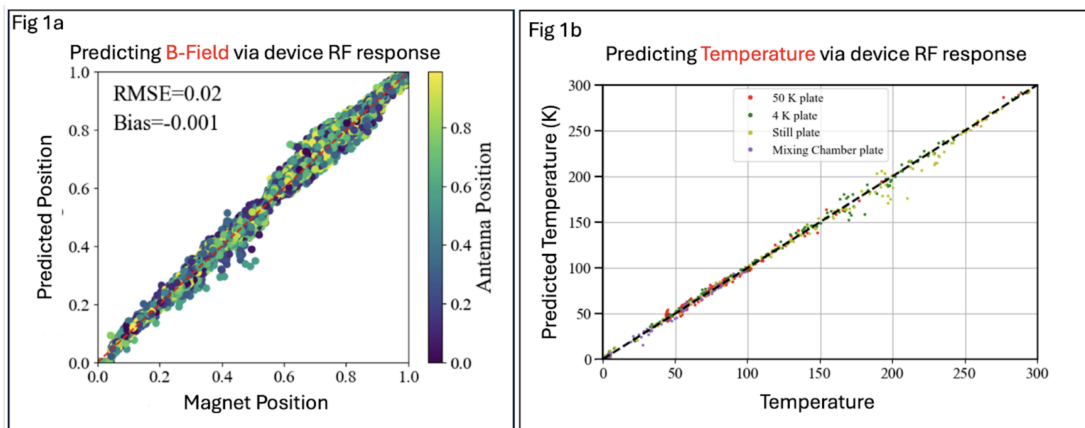


Figure 37: Two examples demonstrating that a NN can learn an RF fingerprint and then predict device environment, whether it be magnetic field strength (left) or temperature (right).

from a variety of sources across a broad energy range.

The high-resolution and large-dynamic range imaging capability of large LArTPCs comes at the cost of massive data volumes. A single 10-kton DUNE far detector module will generate over 10 Tb/s from its front-end electronics, with individual recorded events exceeding 7 GB. Detector monitoring and data selection systems must handle large data streams to both ensure efficient detector operation and reduce the volume of data to fit within offline data processing and storage resources. Real-time TPC data processing has been demonstrated in both firmware [187] and fast parallelized software [188, 189]. Fast parallelized software processing will be used in DUNE [190] to process the stream of TPC data through a hierarchical set of algorithms that identify regions of interest on each TPC channel, cluster them into localized activities, and form final trigger candidates to inform data selection. DUNE’s data selection system is designed and expected to efficiently record interactions depositing more than 100 MeV of visible energy, identify single interactions down to 10 MeV, and capture galactic supernova neutrino bursts.

The image-like nature of LArTPC raw data, the success of AI/ML methods in offline reconstruction and analysis, and stringent resource constraints on space, power, and cooling in detector environments like DUNE’s motivate exploration of AI/ML closer to the detector, both in heterogeneous computing and “at the edge” in readout electronics. Improvements in anomaly detection, data forecasting, and decision agents could significantly improve the performance of LArTPCs with better monitoring and more stable and efficient operation. Data reduction through intelligent compression, filtering, and selection could benefit from AI/ML techniques to enhance the physics reach of current and future LArTPCs. We highlight some specific examples of thrusts under active research and development in the following subsection (from 3.3.2 to 3.3.7).

### 3.3.2 Low-Latency Machine-Learning-Based Supernova Burst Pointing in DUNE

**Contributors:** Kate Scholberg, Michael H.L. S. Wang, Amanda Weinstein, Georgia Karagiorgi

The next nearby core collapse of a massive star will yield unprecedented physics and astrophysics

information from gravitational wave, photon and neutrino messengers. The intense, few-tens-of-second, few-tens-of-MeV all-flavor core-collapse supernova neutrino burst is expected to precede the electromagnetic observables by some time. The interval could be tens of minutes, to hours, to days [191], depending on the nature of the progenitor star. The prompt neutrino burst means that the neutrino observation can provide an early warning to astronomers [192] of an impending supernova.<sup>5</sup>

Directional information from the neutrino burst is clearly of immense value for subsequent early-time observation of the supernova or potential localization of a vanished star. Anisotropic neutrino interactions provide the best prospect for neutrino-based pointing. DUNE’s tracking of neutrino-electron elastic scattering (eES) events has been shown to enable several-degree pointing [193], assuming sufficient “channel-tagging” (interaction classification) to separate eES from the dominant quasi-isotropic  $\nu_e$  charged-current ( $\nu_e$ CC) events. However, to be useful to the astronomical community, such reconstruction must happen with low latency—ideally within several minutes.

Because the baseline expectation for DUNE is that full reconstruction will require at least several hours in order to transfer data to Fermilab for processing, we are pursuing a faster “in-situ compute” approach [194, 195]. In this approach, the full raw dataset can be reduced (background rejection, region-of-interest selection and denoising steps) on buffered data from DUNE DAQ readout units, making use of FPGA or GPU co-processors, and then sent over the network to a single processor for directional reconstruction of the SN burst data. Recent proof-of-concept studies have demonstrated overall acceleration of reconstruction with machine-learning algorithms [194, 195, 196]. Further opportunities for low-latency pointing improvement will address channel-tagging (critical for high-quality pointing) as well as potential use of  $\nu_e$ CC event final-state pattern distributions [193]. Full implementation of low-latency pointing will need to address power and cooling challenges.

### 3.3.3 Capturing Neutrinos and New Physics at ProtoDUNE with a Machine Learning Online Trigger Algorithm

**Contributor:** Ciaran Mark Hasnip

#### Searching for Neutrinos and New Physics at ProtoDUNE

The massive LArTPCs of DUNE will measure the properties of neutrinos with unprecedented precision [197]. Currently, two full-scale prototypes of the DUNE far detectors are at CERN, which are called ProtoDUNE-HD and ProtoDUNE-VD [198]. Recent studies indicate that the ProtoDUNE detectors have the potential to detect neutrinos and beyond-standard model (BSM) particles from one of the targets in CERN’s north area that is exposed to the 400 GeV Super Proton Synchrotron (SPS) beam [199]. As a proof of concept, initial studies have focused on observing neutrino interactions in ProtoDUNE [200]. A challenge in surface detectors like ProtoDUNE is the selection of interesting signals coming from BSM and neutrino interactions whilst rejecting the overwhelming cosmic-ray background. This has motivated the development of an exclusive trigger algorithm within the context of the DUNE data acquisition system (DAQ).

#### Machine Learning Online Trigger Algorithm for ProtoDUNE

A new online trigger algorithm was developed for ProtoDUNE-HD and ProtoDUNE-VD in order

---

<sup>5</sup>Note that there may be no bright supernova for the case of a black hole formation.

to maximize the potential sample size in a future ProtoDUNE neutrino and BSM program. The ProtoDUNE DAQ runs a hierarchical series of algorithms in real time that determine whether to record an event. At the lowest level, Trigger Primitives (TPs) are generated, which represent a cluster of charge on an individual detector channel. The TPs from a plane of ProtoDUNE detector channels are then processed by the following algorithm:

1. Check whether the sum of the charge of the TPs in a 0.3 ms window of time crosses a minimum threshold of 200,000 ADC units.
2. Generate a coarse pixelated time versus channel number image of the TPs in the 0.3 ms window, where the amplitude of each pixel is the total charge of the TPs in the pixel.
3. Pass the image to an XGBoost machine learning (ML) model, which calculates the probability that the image is a neutrino. If the probability crosses a threshold, trigger ProtoDUNE.

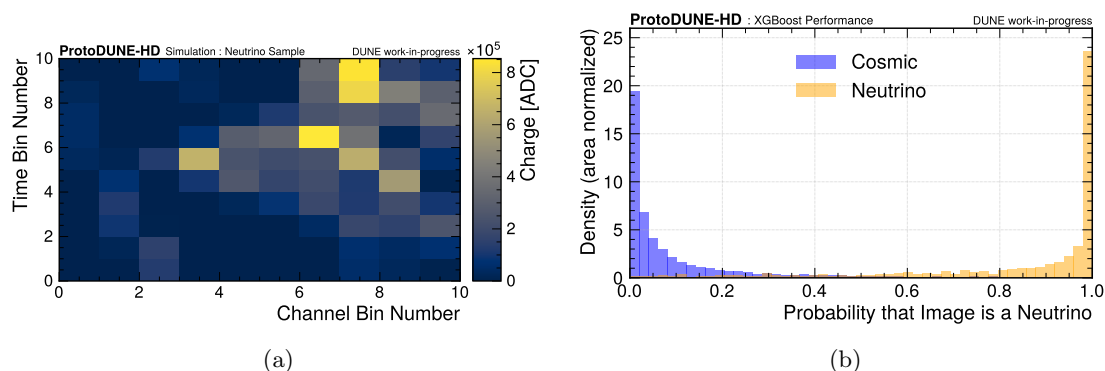


Figure 38: Figure 38a shows an example of a neutrino image used to train the XGBoost model. The XGBoost model is trained on cosmic and neutrino images that pass a minimum total charge threshold of 200,000 ADC and its performance is shown in Figure 38b.

This trigger algorithm therefore relies on an XGBoost model to classify images as either neutrino or cosmic-like [201]. To train this model, tens of thousands of cosmic and neutrino ProtoDUNE-HD images were simulated using LArSoft [202]. Figure 38a shows an example of a simulated neutrino image used for training and testing the model. Each pixel of the image is a feature of the XGBoost model in addition to the total charge across all the pixels. Therefore, for a ten-by-ten pixel image there are 101 features in the XGBoost model. Figure 38b demonstrates that the XGBoost model performs well in distinguishing cosmic and neutrino events. XGBoost was chosen due its fast prediction times on the CPUs available to the ProtoDUNE DAQ. The XGBoost model was trained and then exported as compilable C++ code that was directly built into the DUNE DAQ software.

Figure 39a shows the probability of neutrino selection as a function of the trigger rate due to the cosmic-ray background. The trained XGBoost model is compared with applying a threshold on the total charge in a 0.3 ms time window, which is the basis of the best currently available trigger algorithm for a neutrino and BSM search at ProtoDUNE. The XGBoost model outperforms the charge threshold across all potential trigger rates.

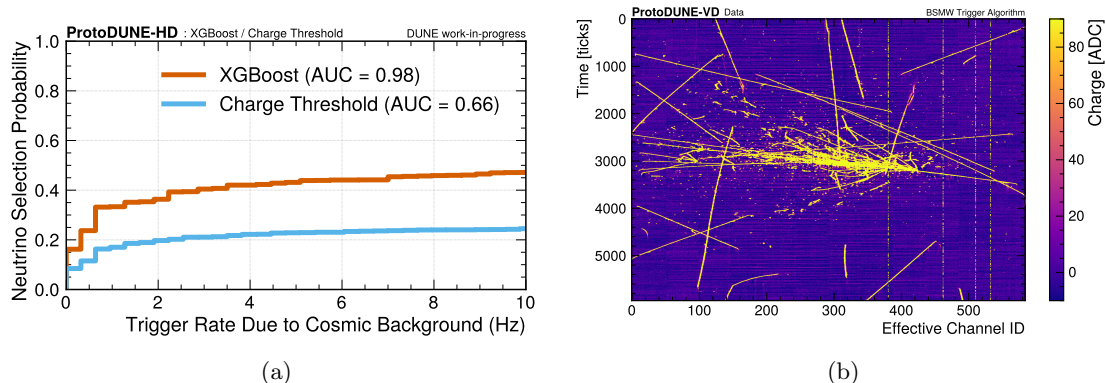


Figure 39: Figure 39a shows the neutrino selection probability as a function of the trigger rate at ProtoDUNE-HD due to cosmic-ray background. Figure 39b shows an event display from ProtoDUNE-VD data taken during a test of the XGBoost-based trigger algorithm.

The XGBoost-based algorithm was implemented in the DUNE DAQ software, allowing a live test at ProtoDUNE-VD to be carried out. ProtoDUNE-VD successfully took data using this algorithm at a stable trigger rate of approximately 5 Hz. Figure 39b shows an example ProtoDUNE-VD event captured during this data run. It is therefore possible to trigger for neutrinos at ProtoDUNE using an XGBoost-based algorithm with efficiencies of approximately 30% or higher. It should be noted that the future DUNE underground detectors will be shielded from cosmic rays, allowing 100% trigger efficiency for high-energy events without the need for ML algorithms. Nonetheless, this can be viewed as a feasibility case study, well-motivated for rare event searches at surface detectors such as ProtoDUNE, demonstrating that ML algorithms can be deployed in the online DUNE DAQ whilst meeting strict latency requirements.

### 3.3.4 Real-time Anomaly Detection in DUNE

**Contributors:** Sunny Seo, Loredana Gastaldo, Doojin Kim, Alex Sousa

#### Anomaly Detection Method

DUNE’s DAQ and online event selection system is designed to meet the experiment’s physics requirements. To further accelerate discoveries through dedicated data streams with improved signal-to-background ratio, we proposed an anomaly detection approach in DUNE’s AI/ML kick-off workshop in early 2025 [203], which addresses three goals: searching for BSM physics signatures, detecting supernova burst (or pre-supernova) neutrinos, and monitoring detector malfunctions—all in real time using raw data. To accomplish this, we have been developing a CNN-based autoencoder (AE) model. Autoencoders are well-suited to this task because they learn, in an unsupervised manner, to compress input data into a compact latent representation and then reconstruct it. The model optimizes by minimizing the reconstruction loss—the difference between the original and reconstructed images. Crucially, when the trained model encounters data that differs from what it learned as “normal,” the reconstruction degrades, flagging potential anomalies.

#### Initial Study

We conducted a proof-of-concept (PoC) study targeting supernova burst neutrino detection in

summer 2025 [204]. We trained an AE model exclusively on radiological backgrounds, the dominant background source for supernova burst neutrino searches. We then evaluated the model on three distinct datasets: two supernova burst neutrino interactions (charged current and elastic scattering) on top of radiological backgrounds, and a held-out sample of radiological backgrounds-only not used during training, and obtained promising preliminary results [204]. The mean squared error distributions revealed clear separation between radiological backgrounds (i.e., nominal events) and supernova burst neutrinos (i.e., anomalies), demonstrating the model’s ability to distinguish genuine signals from nominal detector activity.

### Next Steps

Upon the success of the PoC study, we are now working to develop more realistic training datasets. These will incorporate not only increased radiological background samples, but also solar neutrinos and cosmic muons—events that should be treated as nominal rather than anomalous. We will also explore the model’s sensitivity to lower-energy neutrino sources, including solar and pre-supernova [205] neutrinos, by varying the training dataset composition. In parallel, we will simulate detector-malfunction scenarios (i.e., unresponsive channels or any physical/environmental causes that change detector responses over time) to ensure the model can serve as a reliable monitoring tool, ultimately aiming to build an agentic AI monitoring and/or shift system.

In parallel, we will evaluate the AE model on BSM physics signatures, including cosmogenic boosted dark matter, millicharged particles, dark-sector tridents, as well as magnetic monopoles and atmospheric long-lived particles, which are expected to produce atypical energy deposition patterns or topologies that differ from standard neutrino interactions. Depending on the model’s sensitivity to these signatures, we may fine-tune the architecture or adjust anomaly thresholds for specific signal classes. Since DUNE is under construction, the current anomaly detection study is carried out using simulated data. However, once data is taken by the DUNE detectors, the model needs to be retrained on good quality real data. In the meantime, we are also considering using real datasets taken by the ProtoDUNE and/or Near Detector prototype (ND 2x2).

Once validated on continuous data streams, we plan to deploy the optimized AE model on FPGAs in the DAQ path using frameworks such as HLS4ML [170, 28] or CGRA4ML [206], with model compression through pruning and quantization to meet the power and latency constraints of the underground environment. As an alternative deployment path, the model could also operate on DAQ servers using trigger primitives as input.

In addition to the DUNE’s TPC detector system, we also plan to develop a real-time anomaly detection system using DUNE’s photon detector system.

### 3.3.5 Real-time AI for Data Selection in DUNE

**Contributor: Georgia Karagiorgi, Seokju Chung, Michael H.L. S. Wang**

Real-time and efficient identification of rare and low-energy physics signals among electronics noise and radiological backgrounds, needed to enable an expanded astro-particle physics program in DUNE, faces stringent constraints on latency, power, and computational resources in front-end electronics. ML integrated directly into front-end data paths provides a promising path for increased intelligence and efficiency gains in data selection, compression, and anomaly detection, especially when combined with techniques and architectures that allow for reduced resource utilization. Below, we summarize key developments in applying ML to LArTPC front-end

electronics, with a focus on recent contributions demonstrating feasibility for FPGA implementations in DUNE.

### **ML for Real-Time Data Selection in LArTPCs**

Deep neural networks (DNNs) have proven effective at classifying raw LArTPC wire-time readouts, greatly reducing data volumes while preserving physics-rich information. As demonstrated in [207, 195, 196], convolutional neural networks (CNNs) can achieve high accuracy for selecting rare astro-particle and Beyond-Standard Model (BSM) signals in DUNE over a wide energy range, or identifying regions of interest of low-energy signals with increased accuracy. These methods could complement existing trigger algorithms by improving performance in the low-energy regime ( $\sim 10$  MeV and below), where achieving high efficiency is challenging due to overwhelming radiological background rates, provided overall trigger rates can be maintained at the required level. Furthermore, such 1D or 2D CNNs can be accelerated on resource-constrained hardware such as FPGAs. Refinement using tools such as `hls4ml` [170] enables deployment of quantized networks onto FPGAs under strict resource, latency, and power constraints, in a way that is compatible with the operational environment and performance needs of DUNE's front-end electronics.

### **Real-Time Anomaly Detection at the Front End**

Beyond supervised classification, anomaly detection can be a game-changer for identifying rare or unexpected data patterns. LArTPC waveform denoising and low-energy signal identification using autoencoders have been explored in [208, 209]. A recent study [210] introducing autoencoder-based anomaly detection in LArTPC wire-time data, combined with knowledge distillation to allow the model's execution on FPGAs, has also shown that unsupervised identification of outlier behavior such as high-multiplicity interactions in streaming LArTPC data is possible. This offers opportunities to expand front-end ML capabilities not only to adaptive data selection but also rare-event triggering and potentially to detector monitoring.

### **Integration into Front-End Electronics**

In DUNE, ML-augmented front-end systems can interface with modular trigger architectures to make early, physics-informed decisions and reduce data rates by orders of magnitude. Integrating ML into DUNE front-end electronics requires models that are: quantized and compressed for FPGA implementation; optimizable for tens of  $\mu$ s to ms latency inference; robust under continuous, zero-deadtime operation; and power-efficient for deployment in deep underground environments. Co-design of ML models and hardware architectures, aided by tools like `hls4ml`, is essential.

Machine learning for front-end electronics is emerging as a promising approach for next-generation LArTPC detectors. Demonstrations of FPGA deployment of CNNs and anomaly detection networks suggest that real-time ML-enabled data selection can be implemented within representative latency and resource constraints relevant to DUNE's front-end environment. While these studies demonstrate compatibility with FPGA-level resource and timing budgets, full system-level validation, including integration with the broader DUNE data selection architecture, as well as power, cooling, and sustained trigger-rate constraints, remains an important area for continued R&D. Future work should explore alternate network architectures, pursue full-system integration and demonstration in currently operating LArTPC detectors or prototypes such as SBND [211] or ProtoDUNE [212], and develop shared community infrastructure for ML model training and deployment.

### 3.3.6 Smart Time Projection Chamber

**Contributor: Sunny Seo**

The Smart TPC project [203] investigates whether simple ML-based pattern recognition deployed at the front-end electronics level can improve triggering and filtering for LArTPC data volume reduction by enhancing signal-to-background ratio before data reaches the DAQ.

DUNE’s baseline cold electronics [213] transmit all digitized data to DAQ servers without zero suppression or compression, where software-based algorithms generate trigger primitives and perform data selection. This design is expected to meet DUNE’s physics requirements. Smart TPC explores whether performing simple pattern recognition earlier in the readout chain directly on digitized waveforms could reject dominant radiological backgrounds closer to the source, lowering energy threshold, reducing downstream data volume and potentially improving sensitivity to low-energy signals. Optionally, TPC charge and photon detector light coincidences currently performed only in offline software could be moved into the electronics for further background rejection if the physics case warrants it.

We propose two complementary pathways. The near-term approach deploys lightweight classifiers such as Boosted Decision Trees, which have been demonstrated within embedded FPGA resource constraints with sub-100 ns inference [170, 55], on existing warm-side FPGAs (WIB and DAPHNE). The longer-term approach explores similar classifiers on custom cold ASICs operating at 87 K inside the cryostat, building on the CMS Smart Pixel group’s demonstration of BDT-based inference on 28 nm CMOS front-end ASICs for HL-LHC tracking [214, 215]. The FPGA pathway serves as a near-term demonstrator and risk reduction for the ASIC approach.

This project partners with microelectronics engineers and the CMS Smart Pixel group. Partnership with the LArPix [216] and Q-Pix [217] groups would be pretty useful to leverage complementary expertise in low-power on-detector inference and self-triggered readout architectures. The primary question Smart TPC aims to answer is whether ML-based pattern recognition at the electronics level can meaningfully improve lowering energy threshold and increasing signal-to-background ratio for low-energy physics including solar and supernova neutrinos, beyond what software-based data selection alone achieves.

### 3.3.7 LArTPC Calibration Using Pre-Trigger Data

**Contributors: Sunghin Oh, Linyan Wan, Aobo Li**

Many existing LArTPC calibration strategies rely heavily on abundant cosmic-ray muons. For deep-underground detectors such as the DUNE far detector, the cosmic-muon flux is strongly suppressed, significantly reducing the availability of steady, high-statistics calibration samples. While dedicated calibration systems—such as laser and LED systems—are designed to mitigate this limitation, they require specialized data-taking runs with data-acquisition configurations that differ from standard physics operations and are mostly having limited spatial coverage except special devices such as pulse neutron sources [218, 219]. As a result, a continuous, spatially distributed probe that samples detector conditions uniformly over time is highly desirable.

Commercial atmospheric argon contains  $^{39}\text{Ar}$  at an activity of order 1 Bq/kg, producing a persistent and uniform  $\beta$ -decay source throughout the detector volume with a well-defined low-energy

spectrum at  $\mathcal{O}(100 \text{ keV})$  [218]. This intrinsic radioactivity can therefore serve as a continuous calibration handle for both the TPC readout chain and the photon-detection system (PDS). However, relevant data are typically discarded or only minimally exploited due to the prohibitive computing and storage costs associated with processing untriggered, continuous waveforms at the full  $^{39}\text{Ar}$  rate.

A promising path is to move the  $^{39}\text{Ar}$  calibration upstream, computing compact summary features directly from digitized data prior to triggering. This can be enabled by the processing capabilities in front-end electronics such as field-programmable gate arrays (FPGAs). Machine-learning approaches such as compact convolutional encoders are ideal candidates for these feature extraction tasks with low resource footprint constraints. Deployed as resource-aware inference models, they can provide calibration proxies for the overall charge scale, light yield, their corresponding local nonuniformities, and the gain and timing response of individual electronics channels. Propagating only these lightweight metrics downstream preserves the near-continuous, high-granularity information while avoiding the storage and processing burden of full untriggered waveforms, eventually paving the way towards a time-dependent calibration and reduced detector systematics in physics. In addition, such automated calibration capability could release pressure to experiments for taking data dedicated to calibration purposes and personpower for analyzing the data to monitor the detector status. This helps for experiments to focus more on scientific goals and accelerates the scientific discovery process.

### 3.3.8 ML-based self-trigger for the COHERENT experiment for supernova burst and BSM searches

**Contributors:** Zepeng Li, Kate Scholberg

The COHERENT collaboration has measured coherent elastic neutrino-nucleus scattering (CEvNS) at the Spallation Neutrino Source (SNS) [220, 221, 222], establishing a powerful neutral-current neutrino probe sensitive to all neutrino flavors. Tonne-scale CEvNS detectors offer a unique opportunity to detect neutrinos from a Galactic core-collapse supernova, with few to  $\mathcal{O}(10)$  events per tonne expected for a 10-kpc collapse. However, because COHERENT detectors have little overburden, the expected supernova neutrino signal is overwhelmed by steady-state detector backgrounds by several orders of magnitude. We describe an example machine learning (ML) trigger on front-end electronics to enable supernova neutrino detection for next-generation COHERENT detectors [223].

Core-collapse supernovae release neutrinos with energies up to tens of MeV over a timescale of  $\sim 10 \text{ s}$  [224]. While next-generation neutrino detectors, such as JUNO [225], Hyper-Kamiokande [226], and DUNE [227] are primarily sensitive to  $\nu_e$  and  $\bar{\nu}_e$  via charged-current interactions, CEvNS provides a flavor-blind measurement of the total neutrino flux. This makes CEvNS detectors uniquely robust against uncertainties from neutrino oscillations in dense supernova environments.

Because the CEvNS cross section scales approximately as  $N^2$ , compact detectors with heavy nuclei can achieve relatively high interaction rates compared with charged-current interactions. The diverse target materials across the COHERENT array enable cross-validation of signals and constraints on systematic uncertainties, enhancing confidence in a potential supernova neutrino observation. COHERENT CEvNS targets currently deployed or planned for the near future include Ar, Ge, NaI, and cryogenic CsI. In the following, we take a future potential upgrade of CsI as a concrete example; however the implementation of an ML-based self-trigger can be applied for any COHERENT subsystem.

Cryogenic CsI scintillators exhibit high light yield and low intrinsic radioactivity, enabling sensitivity to few-keV nuclear recoils for CEvNS detection. For beam-triggered mode, the SNS duty factor provides a factor of  $10^3 - 10^4$  background suppression. In self-trigger mode, a cryogenic CsI detector would have background rates of approximately  $7 \text{ kg}^{-1} \text{ s}^{-1}$ , dominated by natural radioactivity and cosmic muons [228]. Extrapolated to a tonne-scale detector, this corresponds to raw trigger rates of  $\mathcal{O}(10^4)$  Hz, far exceeding the expected supernova signal rate. Backgrounds can be broadly categorized into high-energy events from radioactivity and cosmic muons, as well as low-energy instrumental backgrounds, dominated by scintillation afterglow and PMT dark noise. An effective trigger must suppress both classes while maintaining high efficiency for CEvNS-like events. We consider a multi-stage trigger architecture suitable for implementation in front-end electronics.

A strong correlation exists between deposited energy and waveform maximum amplitude. Applying an upper cut on the waveform maximum efficiently suppresses high energy backgrounds, reducing the event rate by one to two orders of magnitudes without impacting CEvNS sensitivity. A lower bound on the waveform integral is also applied to reject coincident PMT dark-noise triggers. After these selections, the remaining waveforms are sparse and low-amplitude, greatly reducing computational load for subsequent processing.

At low energies, the dominant background arises from CsI scintillation afterglow, which exhibits a distinct temporal structure compared to genuine energy-deposition events. To exploit this difference, we developed a lightweight PointNet-based neural network [229] that operates on sparse waveform representations. Each event is encoded using the time indices and amplitudes of waveform samples exceeding a small threshold, preserving pulse-shape information while minimizing data volume. The network achieves strong separation power, rejecting over 90% of afterglow-induced events at a signal efficiency of approximately 85%. This corresponds to an additional order-of-magnitude reduction in the trigger rate. The trained PointNet model was synthesized into FPGA firmware using the `hls4ml` framework [15, 16]. Hardware tests confirm excellent agreement between FPGA inference and software validation, with an inference latency of  $\sim 10 \mu\text{s}$ . This demonstrates that ML-based pulse-shape discrimination can be integrated directly into front-end electronics without compromising real-time operation.

The combination of the waveform-integral cut and the PointNet-based afterglow rejection model provides a highly effective multi-stage background suppression strategy for the cryogenic CsI detector. Each stage targets distinct sources of background, leveraging both simple pulse-amplitude correlations and advanced ML techniques to achieve efficient signal purification while maintaining high CEvNS detection efficiency. We note that self-trigger methods can be used also for other searches for beam-correlated BSM signals outside of the standard beam-trigger window.

### 3.3.9 Real-Time, Low-Power Machine Learning for Neutrino Telescopes

**Contributors:** Miao Chen Jin, Carlos Argüelles

**Motivation:**

Next-generation large-scale neutrino telescopes will operate at data rates and detector scales that increasingly strain traditional trigger and data-handling architectures. These experiments are located in resource-scarce environments, where per-module power budgets are typically at the level of a few watts, limiting the usage of machine-learning techniques. Together, these constraints will force current CPU-based real-time, in-situ reconstruction and triggering to discard a large fraction of data to satisfy data-transmission limits.

Recent advances in Edge Machine Learning hardware motivate a re-examination of this

paradigm [230, 231, 232]. In the context of neutrino telescopes, Ref. [233] presents the first demonstration that machine-learning-based neutrino event reconstruction can be performed on Edge devices such as *Tensor Processing Units* (TPUs) [234, 235, 236]. These could be installed within each detector module, within a power envelope of only a few watts, while surpassing the accuracy of currently deployed real-time methods. This contribution summarizes the key technical challenges inherent to this problem and the workarounds that make such an approach viable today.

A critical enabler of this effort is the availability of open-source, community-developed software. On the physics side, all detector simulation and data generation were performed using Prometheus [237], an open-source neutrino telescope simulation framework. On the hardware and software side, there also exist communities actively developing software foundations for the hardware architectures [238, 239, 240].

### Core Challenges for Edge ML in Neutrino Experiments and Design Strategies:

Deploying machine learning models on ultra-low-power edge devices introduces several fundamental challenges that differ qualitatively from conventional GPU-accelerated workflows, mainly:

- **Power Constraints.** Edge accelerators suitable for in-detector deployment operate at  $\mathcal{O}(1 - 3) W$ , orders of magnitude below GPUs typically used for ML inference.
- **Limited Numerical Precision.** The Google Edge TPU [236] used in Ref. [233], like many other Edge computing platforms across different hardware architecture designs, requires fully integer (`uint8`) inference, eliminating floating-point arithmetic.
- **Architectural Constraints.** Supported operations are limited: tensor dimensionality is capped, three-dimensional convolutions are disallowed, and only a restricted set of neural network layers can be executed efficiently. This goes against the traditional 4-dimensional convolutions or graph neural networks [241, 242] design strategies for neutrino telescopes.

To address these challenges, the reconstruction pipeline needs to be co-designed with the hardware, rather than adapted post hoc. For example, in the implementation presented in Ref. [233] the following key features of design were introduced:

- **Time-Series Reformulation.** Instead of conventional convolution-style algorithms, the data can be processed using an early language-model-type approach via RNN. In this encoding, detector photon hits are discretized into a sequence of temporal snapshots. Similar snapshot techniques could be used in other experiments where coarse time-graining can be used. The use of RNNs fits the more limited TPU architecture.
- **Hybrid CNN–RNN Architecture.** Hybrid architectures can be used to encode all available information. For example, TPUs allow for 2-dimensional convolutions. Thus, one can perform low-dimensional CNN convolutions that serve as encoders to the RNN backbone. In the application given in Ref. [233], two-dimensional convolutional encoders extract spatial features from each time slice, while a recurrent (LSTM) network integrates temporal information—avoiding unsupported 3D convolutions while retaining sensitivity to event signature. This technique can also be used in fine-grain detectors, for example, a tracker could be split into various planes, where each plane is processed first through a two-dimensional convolution, and then an RNN acts on the whole event.
- **Quantization-Aware Data Encoding.** Aside from problem formulation, quantization-aware data pre-processing is also performed. Inputs are constructed to be integer-valued by design, enabling full-network `uint8` quantization. A staged quantization and retraining procedure mitigates accuracy loss from reduced numerical precision.

Though some of these are specific to neutrino telescopes, many of the insights here can be extended to other neutrino experiments.

### Physics Performance, Power Efficiency, and Outlook:

Despite these constraints, the fully quantized edge-deployed network introduced in Ref. [233] achieves median angular reconstruction errors of approximately  $6^\circ$  in ice and  $7\text{--}8^\circ$  in water, significantly outperforming currently used real-time CPU-based reconstruction algorithms, which typically achieve  $\sim 10^\circ$  resolution at trigger level, with their performance limited by the power constraint introduced in real-time processing. These first results make TPU-enhanced event reconstruction an interesting avenue of future investigation.

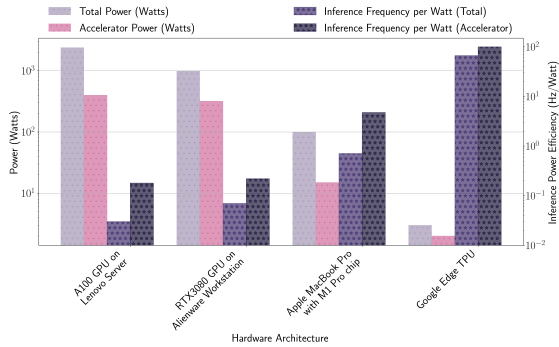


Figure 40: Inference power efficiency for single-event neutrino reconstruction on different hardware architectures. Edge ML devices achieve the highest inference-per-watt performance, despite operating at drastically lower absolute power.

Most importantly, this improvement is achieved at dramatically higher energy computational efficiency, see Figure 40 (adapted from Fig. 6 of Ref [233]). For single-event inference—the relevant regime for real-time triggering—edge ML devices outperform GPUs by orders of magnitude in power efficiency, enabling real-time inference at  $\mathcal{O}(100)$  Hz/W.

It is worth noting that angular regression is neither an ideal task nor a commonly desired one for quantized inference. Nevertheless, the results strongly motivate future efforts focused on classification, triggering, and intelligent data reduction, where edge ML is expected to perform even more effectively. More broadly, this proof-of-concept highlights the importance of hardware–algorithm co-design and open simulation tools in enabling the next generation of intelligent, resource-aware particle physics experiments.

### 3.3.10 Efficient Neural Network Architectures for Real-Time Neutrino Telescope Data Processing

**Contributors:** Carlos Argüelles, Nicholas Kamp, Jeffrey Lazar, Felix Yu

#### Introduction and Motivation:

The transition to the big data frontier in particle physics demands new approaches to real-time inference, intelligent data reduction, and computational efficiency. As experiments scale to unprecedented detector volumes and data rates, the development of machine learning architectures that can operate within the power, latency, and bandwidth constraints of edge computing environments becomes essential.

Neutrino telescopes offer a particularly instructive case study, as they confront many of these challenges in an especially resource-constrained setting. Detectors such as IceCube [243], KM3NeT [244], and the forthcoming IceCube-Gen2 [245] instrument cubic-kilometer-scale volumes with thousands of optical modules, generating trigger rates on the order of kilohertz while searching for rare astrophysical signals. Real-time reconstruction is critical for background rejection and for enabling rapid alerts that support multi-messenger astronomy campaigns [246]. IceCube operates at the geographic South Pole, where computing resources and data transmission bandwidth are severely limited, making it a natural testbed for developing efficient inference methods.

Beyond the environmental constraints, the data produced by neutrino telescopes exhibit properties shared by many next-generation detectors: extreme sparsity, irregular detector geometries, high dimensionality from nanosecond-resolution timing, and substantial variance across many orders of magnitude in energy. To address these challenges, recent work has explored architectural innovations, including sparse convolutions and learned data compression, enabling high-performance real-time computing suitable for deployment in these resource-constrained environments.

#### **Sparse Submanifold Convolutions for Trigger-Level Reconstruction:**

Ref. [247] demonstrated sparse submanifold convolutional neural networks (SSCNNs) for event reconstruction in neutrino telescopes. Traditional CNNs prove highly inefficient on sparse data, performing operations across the entire input volume regardless of occupancy. SSCNNs, originally developed for computer vision applications [248], restrict convolution operations to non-zero elements while preserving input sparsity across network depth, maintaining efficiency in deep architectures. This approach has already demonstrated success in liquid argon time projection chamber experiments [249, 250].

The SSCNN approach achieves angular reconstruction at rates exceeding 9.9 kHz on an NVIDIA A100 GPU, representing approximately a 16-fold speedup compared to traditional CNNs [251] and substantially exceeding the roughly 3 kHz trigger rates of current neutrino telescopes. This throughput enables real-time processing at the detector site for improved trigger-level background rejection and rapid alert systems. The architecture naturally accommodates irregular detector geometries by operating on spatial coordinates directly, enabling straightforward adaptation to diverse detector configurations, including water-based telescopes such as KM3NeT and P-ONE [252].

#### **Learned Representations for Data Compression and Downstream Efficiency:**

Complementing the sparse convolution approach Ref. [253] developed `om2vec`, a transformer-based variational autoencoder that learns compact latent representations of photon arrival time distributions (PATDs) recorded by individual optical modules. Raw PATDs span thousands of nanosecond-resolution time bins with highly variable photon counts, requiring careful handling to preserve physics-relevant features such as the “double-bang” signatures characteristic of tau neutrino interactions.

The `om2vec` architecture encodes arbitrary PATDs into fixed-length latent vectors of 32–128 dimensions while retaining sufficient information for accurate reconstruction. Compared to traditional asymmetric Gaussian mixture model fitting approaches [254], `om2vec` achieves order-of-magnitude speedups on CPU and two-order-of-magnitude speedups on GPU, with substantially lower failure rates. The learned representations enable downstream reconstruction networks to achieve performance comparable to models operating on full timing information while reducing input dimensionality and simplifying model pipelines. This approach integrates naturally with community tools such as GraphNeT [255], facilitating adoption across the neutrino telescope

community.

### **Implications for Edge and Heterogeneous Computing:**

These architectural developments have direct implications for edge computing deployment. The SSCNN’s ability to process events at trigger-level rates on GPU hardware, combined with comparable single-core CPU performance to traditional likelihood methods, suggests viable deployment scenarios ranging from GPU-accelerated processing at detector sites to CPU-based reconstruction in bandwidth-limited environments. The `om2vec` representations offer an additional pathway for data reduction by replacing high-dimensional PATDs with compact latent vectors early in the processing chain, potentially relaxing throughput constraints that currently limit timing resolution.

The self-supervised nature of the variational autoencoder framework also enables training directly on detector data without labeled simulation, supporting robust performance despite simulation-data discrepancies. These software-focused approaches could naturally complement hardware-oriented research aimed at leveraging efficient edge computing platforms [256], such as FPGAs or TPUs.

### **3.3.11 Accelerating KamLAND2-Zen’s Search for Majorana Neutrino with Hardware AI Codesign**

**Contributors:** Zepeng Li, Aobo Li, Christopher Grant, Koji Ishidoshiro, Hideyoshi Ozaki

#### **Executive Overview**

KamLAND-Zen currently sets the world-leading limit of neutrinoless double beta decay ( $0\nu\beta\beta$ ) and is the first experiment to probe a portion of the Inverted Mass Ordering parameter space for a subset of nuclear matrix element calculations [257]. With the forthcoming KamLAND2-Zen upgrade, the experiment is positioned to refresh the world leading sensitivity to  $0\nu\beta\beta$  in the coming decade [258].

This white paper outlines a hardware-AI codesign strategy that enables the deployment of machine-learning (ML) algorithms directly on the field-programmable gate arrays (FPGAs) in the KamLAND2-Zen data acquisition (DAQ). By enabling real-time, position-aware adaptive triggering, this approach will enhance the experiment’s sensitivity to  $0\nu\beta\beta$  signatures by suppressing background events.

#### **Motivation and challenges**

The main motivation for hardware-AI codesign in KamLAND2-Zen is to enhance the tagging of long-lived spallation isotopes, the major background in  $0\nu\beta\beta$  region of interest. Current KamLAND-Zen trigger system employs a simple, fixed-threshold hardware trigger. Therefore, many valuable low-energy events, particularly those relevant for long-lived spallation isotope tagging, are discarded before detailed analysis. To fully exploit the upgraded detector’s capabilities, KamLAND2-Zen requires a shift from static, threshold-based triggers to intelligent, low-latency, physics-aware triggering.

**Preliminary Demonstration: PointNet on RFSoc** As an initial proof of concept, PointNet was successfully deployed on RFSoc to reconstruct event position and energy using KamLAND-Zen Point Cloud data [259]. PointNet was chosen because of its distributed nature: it applies the same multilayer perceptron layers to each point individually before global aggregation. This

design perfectly matches the KamLAND-Zen DAQ system, where 130 boards each can only access up to 16 points. The results show that PointNet can achieve 20 cm position resolution and a 0.06 MeV energy resolution [260]. Comparing PointNet to KamLAND-Zen’s offline reconstruction

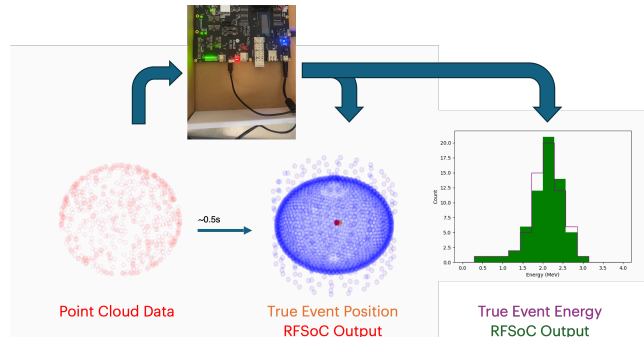


Figure 41: Demonstration of event reconstruction with the PointNet model achieving  $\mathcal{O}(s)$  latency on a RFSoc board.

tion method, while the position resolution is modestly degraded relative to offline reconstruction, the energy resolution is improved. The `cgra4m1` framework [261] was used to deploy the PointNet model onto a RFSoc heterogeneous computing system. As shown in Figure 41, the model was able to reconstruct event position and energy with a 0.5 second latency. While this is still much longer than the desired latency for KamLAND2-Zen, it serves as the first successful demonstration of the feasibility of real-time event reconstruction on RFSoc.

**Real-time Event Reconstruction:** Building on this foundation, the proposed KamLAND2-Zen trigger architecture centers on ultra-fast reconstruction using Ridge Regression implemented directly on front-end FPGAs. Ridge regression has been demonstrated to accurately reproduce the KamLAND-Zen offline reconstruction [262] while requiring orders of magnitude fewer parameters than neural networks. This approach reproduces the behavior of established vertex fitters with orders-of-magnitude fewer parameters, making it well suited for low-latency hardware deployment.

The development program includes:

- **Front-end feature extraction:** real-time charge integration to extract PMT charge and timing information on RFSoc boards.
- **Event-level inference:** a trained Ridge Regression model mapping PMT-level features to event energy and spatial coordinates  $(x, y, z)$  within nanoseconds.
- **Validation and robustness studies:** systematic evaluation of reconstruction accuracy as a function of energy and position, including tolerance to compromised PMT channels.
- **Interpretability analysis:** leveraging model linearity to quantify the influence of individual PMTs and ensure physics transparency.

**Software Trigger:** The key physics motivation of fast machine learning on RFSoc is long-lived spallation product rejection. The 2.2 MeV neutron capture events — the event when neutron is captured by hydrogen items and emit a 2.2 MeV photon, are one of the most important handle for rejecting the long-lived spallation backgrounds which dominate the  $0\nu\beta\beta$  region of interest [263].

However, these events cannot be completely triggered by the fixed-threshold hardware trigger in current generation DAQ. To address this challenge, the collaboration plans to train and deploy a binary classification neural network that distinguishes neutron capture events from the abundant PMT afterpulses, and then perform software trigger based on the neutron capture score.

Moreover, the abovementioned real-time event reconstruction could provide additional handles in rejecting long-lived spallation product. The reconstructed position information allows us to trigger more frequently in the xenon-loaded fiducial volume while maintaining acceptable overall data rates; moreover, real-time energy and position information enables efficient triggering on other short-lived spallation products following cosmic muons, events that are largely missed under the current trigger scheme. Capturing these signals provides critical input for off-line ML-based coincidence tagging, significantly improving suppression of long-lived spallation backgrounds.

### **Conclusion**

The implementation of real-time event reconstruction and an integrated software trigger is foundational to achieving the target sensitivity for neutrinoless double-beta decay in KamLAND2-Zen. By embedding machine learning algorithms into the earliest stages of the data acquisition pipeline, the experiment transcends traditional passive data collection, evolving into an adaptive, physics-driven “intelligent detector.” This transformation is also vital for physics beyond neutrinoless double-beta decay. The ability to perform high-fidelity reconstruction in real time enables the rapid identification of transient astrophysical phenomena, such as the initial stages of a supernova neutrino burst. Furthermore, the framework allows for the autonomous and dynamic adjustment of trigger thresholds, ensuring that the detector can handle the extreme flux of a nearby supernova without compromising data integrity.

More broadly, this hardware-AI codesign provides a robust, interpretable blueprint for next-generation rare-event searches. As experiments scale in complexity, the ability to manage massive data volumes while maximizing physics reach is no longer optional, but essential. From a core machine learning perspective, our work addresses the core ML4FE challenge of deploying distributed, interpretable inference under extreme latency and bandwidth constraints. By introducing tools like `cgra4ml` and a concrete testbed for hardware/ML co-design, this work establishes a new standard for scientific instrumentation.

## **3.4 Quantum Sensors & Experiments**

**Contributors:** Christian Boutan, Tom Braine, Talal Ahmed Chowdhury, Chance Desmet, Stephen Jones, Andreas Jung, Doojin Kim, Kyoungchul Kong, Benedikt Maier, Mark Neubauer, Santosh Parajuli, Myeonghun Park, Cristián Peña, Noah Singer, Michael Spannowsky, Daniel Tapia Takaki, Simon Williams

### **3.4.1 Continuous-variable photonic quantum extreme learning machines for fast collider-data selection**

Recent work has demonstrated that continuous-variable (CV) photonic quantum extreme learning machines (QELMs) provide a compelling hardware-native approach to low-latency machine learning for collider experiments [264]. In this architecture, schematically shown in Figure 42, classical event features are encoded as quadrature displacements across multiple optical modes

and propagated through a fixed-depth Gaussian photonic circuit acting as a random nonlinear feature map. The resulting high-dimensional feature representation is read out via Gaussian-compatible measurements, either photon-number-resolving or, more practically, homodyne detection, followed by a purely linear classifier trained analytically via ridge or logistic regression. Only the linear readout is trained, allowing retraining through a single deterministic linear solve rather than iterative gradient descent.

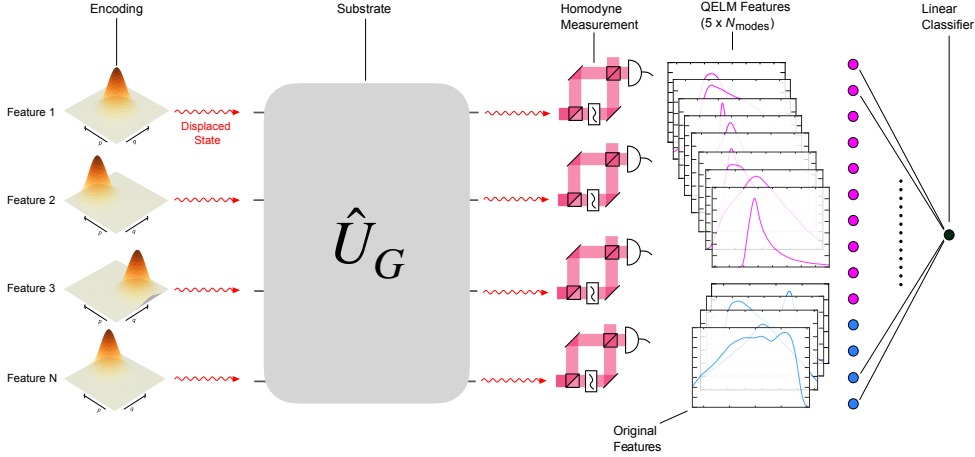


Figure 42: Visualisation of the QELM. The features of the data get encoded onto qumodes via displacement operations. A fixed-time Gaussian quantum substrate  $\hat{U}_G$  followed by Gaussian-compatible measurements creates a random, high-dimensional feature map, which is used, together with the original data, in a linear classifier.

This approach is particularly well matched to the constraints of front-end collider data processing and trigger systems. Inference latency is set by the optical path length and detector response and is therefore fixed, deterministic, and on nanosecond scales, independent of event complexity. Furthermore, photonic devices operate at room temperature and do not require cryogenic cooling, whilst benefiting from long decoherence times. The absence of back-propagation, learning-rate tuning, or stochastic optimisation greatly simplifies deployment and rapid adaptation to changing detector conditions, calibration drifts, or domain shifts in the data stream.

Benchmark studies on representative collider classification tasks, including top-jet tagging and Higgs boson identification, show that CV-QELMs consistently outperform parameter-matched classical multilayer perceptrons and match or exceed wider networks at larger training set sizes, despite training far fewer parameters [264]. Selected results are shown in Figure 2. Notably, the QELM exhibits significantly lower variance across runs, reflecting the stability of fixed photonic random features and analytic readout training. These results indicate that Gaussian photonic substrates can supply compact yet expressive random feature maps without requiring quantum computational advantage, positioning CV-QELMs as a realistic hardware ML primitive for online data selection, and potentially even first-level trigger integration, at future collider experiments.

### 3.4.2 Particle Tracking and Active Particle Sensing via Quantum Devices

Prior work on quantum annealing for track clustering illustrates one of the earliest applications of quantum optimization to a core reconstruction task in collider physics [265], even valid more

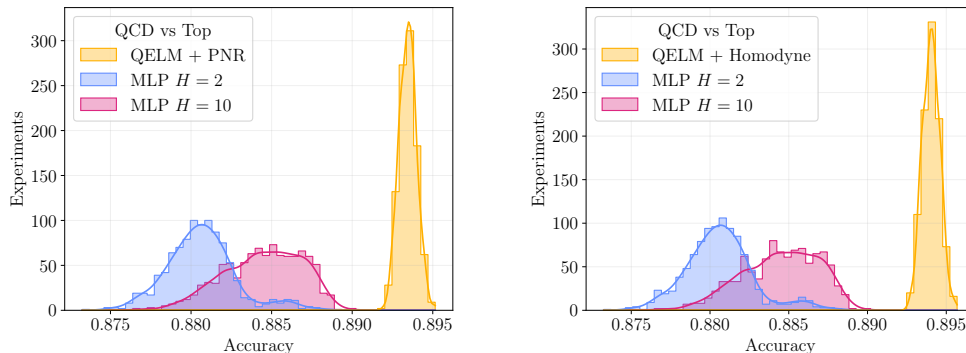


Figure 43: QCD versus Top jet classification with  $F = 16$  features and  $n_{\text{samples}} = 105$  from the HLS4ML dataset [100] using logistic regression on the CV-QELM outputs. Photon-number-resolving (PNR) measurements (left) and homodyne measurements (right). Accuracy distributions are compared against MLP baselines with  $H = 2$  and  $H = 10$ . The CV-QELM achieves higher mean accuracy and substantially lower variance than both MLP baselines.

generally for particle tracking and reconstruction. Therein the problem of clustering charged particle tracks to identify primary interaction vertices along the beam axis is formulated as a binary optimization problem that is amenable to solution on a quantum annealing device. Using a D-Wave quantum annealer, we embed track clustering onto the device’s hardware graph, optimize annealing parameters, and benchmark performance against classical simulated and deterministic annealing under equivalent time budgets. Although current hardware limitations constrain the size and connectivity of instances that can be directly mapped, the results demonstrate a measurable performance gain for quantum annealing in modestly sized problems and establish practical strategies for embedding, parameter tuning, and hybrid workflows. By validating this approach on realistic collider topologies, the study provides a foundational proof of concept for quantum-accelerated reconstruction in high-pileup environments expected at the high-luminosity LHC. This approach can be extrapolated to other future collider facilities and their environmental conditions. Furthermore, quantum tomography can provide an efficient method for extracting angular distribution and quantum correlations among the final-state particles from collider data, as demonstrated in Ref. [266].

Building on this foundation, we propose two complementary research directions that extend the scope and impact of quantum methods in experimental particle physics. While using different methods, these are synergistic to each other.

First, we aim to extend the vertex clustering paradigm from one-dimensional beam-axis clustering to **full three-dimensional tracking**. The comprehensive 3D reconstruction of charged particle trajectories within complex detector geometries is among the most computationally challenging tasks in high-energy physics. By casting full track finding and fitting as a global optimization over hit associations and track hypotheses, and expressing this as a form suitable for quantum annealers or hybrid quantum-classical solvers, we seek to exploit global search capabilities to navigate the combinatorial complexity inherent in tracking. Key aspects of this extension include embedding detailed detector geometry and spatial correlations into the optimization representation, integrating physical constraints given by e.g. magnetic fields, and developing scalable embedding strategies that leverage next-generation annealing hardware.

Second, we propose to explore the use of **arrays of qubits in gate-based quantum processors as direct sensors** for weakly interacting or non-photon-interacting particles, including

dark matter candidates. In this conceptual framework, qubits are repurposed from purely computational roles to act as highly sensitive detectors, where rare interactions with passing particles could induce perturbations in qubit states that are amplified and read out with high fidelity. Gate-based architectures, such as superconducting circuits or trapped ions, inherently support high coherence times and precision control, enabling quantum sensing protocols that surpass classical limits. By engineering tunable coupling between qubit arrays and external fields or novel sensing media, and by leveraging entanglement and error-mitigated readout schemes, such systems could probe minute energy depositions or decoherence signatures indicative of interactions with hidden-sector fields. This direction positions quantum processors not just as accelerators of existing algorithms, but as transformative hardware for particle detection and fundamental physics discovery. Limited access to gate-based systems will allow to establish figure-of-merits for expected sensitivities in given noisy realm of gate-based systems.

### 3.4.3 Quantum-Enhanced Graph Neural Networks for Particle Tracking in High-Energy Physics

Charged-particle tracking at the HL-LHC presents unprecedented computational challenges. With proton–proton collisions occurring at bunch-crossing rates up to 40 MHz and pile-up approaching  $\mathcal{O}(200)$  interactions per crossing [267], tracking detectors generate extremely dense hit patterns that lead to a combinatorial explosion in candidate hit-to-hit connections.

Graph Neural Networks (GNNs) offer an attractive approach by reformulating tracking as a graph learning problem: detector hits become nodes, candidate connections become edges, and the reconstruction task reduces to edge classification. While recent GNN-based tracking pipelines demonstrate strong performance, they typically require dense multilayer perceptrons (MLPs) with wide hidden dimensions and numerous message-passing iterations, resulting in substantial parameter counts and computational overhead [268, 269].

Quantum Machine Learning (QML) presents a complementary paradigm through parameterized quantum circuits that can represent nonlinear transformations in high-dimensional Hilbert spaces using relatively few trainable parameters [270]. Motivated by the potential for parameter-efficient expressivity, in [271] we explore a hybrid quantum–classical GNN architecture for edge classification in TrackML graphs [272]. In our approach, variational quantum circuits replace some classical linear layers in encoders, networks and decoder. We implement quantum modules using PennyLane [273] integrated into an Interaction Network [269] baseline via the ACORN framework [274].

The hybrid architecture shown in Fig. 44 was implemented in which quantum circuits serve as drop-in replacements for classical linear layers within node encoders, edge encoders, message-passing functions, and the final edge classifier. The approach integrates PennyLane-based quantum modules into a classical GNN framework using ACORN and PyTorch Geometric, enabling end-to-end training on TrackML graphs. Quantum circuits with between two and eight qubits are evaluated, using angle encoding, entangling layers, and Pauli- $Z$  measurements to produce classical outputs.

Performance is evaluated using standard TrackML metrics, including ROC AUC, edge-level efficiency, and purity. The results shown in 1 demonstrate that low-qubit quantum models can achieve performance comparable to classical baselines while substantially reducing the total number of trainable parameters. Quantum circuits operate in  $2^n$ -dimensional Hilbert spaces, which enables compact representations. In our 8-qubit model, the quantum circuit components contribute 320 trainable parameters out of a total of 2553 parameters in the full model. This compares to the classical baseline with 2485 total parameters, all of which are in classical layers. The 2-qubit configuration achieves the most dramatic parameter reduction, with only 711 total

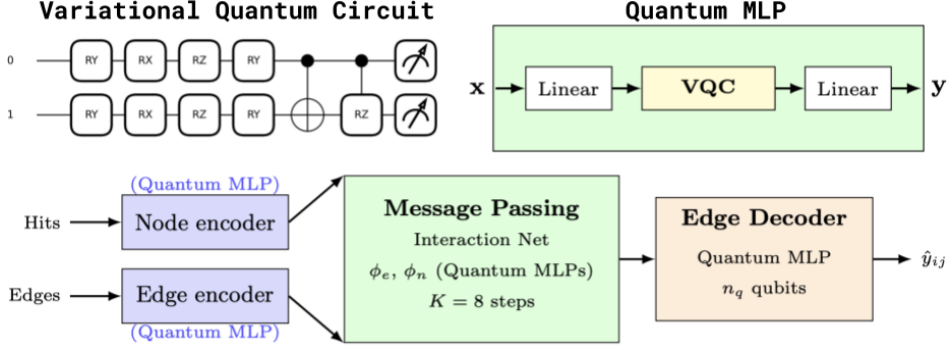


Figure 44: Hybrid quantum–classical GNN pipeline. All MLPs (node encoder, edge encoder, message passing  $\phi_e$  and  $\phi_n$ , and edge decoder) use quantum circuits in the hybrid model [269, 273].

| Model         | Hidden Dim | Qubits | Total Params | Quantum Params | AUC (%) | Eff (%) | Purity (%) |
|---------------|------------|--------|--------------|----------------|---------|---------|------------|
| Classical GNN | 32         | —      | 2485         | 0              | 92.1    | 76.92   | 66.09      |
| Quantum GNN   | 16         | 2      | 711          | 80             | 91.6    | 77.80   | 63.52      |
| Quantum GNN   | 16         | 4      | 1325         | 160            | 93.2    | 79.17   | 66.67      |
| Quantum GNN   | 16         | 8      | 2553         | 320            | 95.3    | 84.45   | 69.97      |

Table 1: Performance across model configurations [273].

parameters (80 quantum) versus 2485 in the classical baseline and achieves similar classification accuracy with more than a factor of three reduction in parameter count. The larger quantum circuits (four and eight qubits) exceed the classical baseline across multiple metrics. The role of entangling gates in creating feature correlations for edge classification warrants further investigation.

This study shows that hybrid quantum–classical GNNs are a promising direction for future investigation in particle tracking, particularly as quantum hardware and hybrid computing infrastructures mature. While the current results rely on classical simulation of quantum circuits and are limited to modest system sizes, the study provides an early demonstration of how quantum machine learning techniques may contribute to parameter efficiency and expressivity in high-energy physics reconstruction pipelines.

### 3.4.4 Quantum Sensing Radiative Decays of Neutrinos and Dark Matter Particles

Dark matter remains undiscovered despite extensive searches, and the cosmic neutrino background (C $\nu$ B)—a cornerstone prediction of Big Bang cosmology—has never been directly detected due to its ultra-low energy ( $\sim 10^{-6}$ – $10^{-4}$  eV). Meanwhile, quantum sensing has advanced rapidly, with qubits achieving unprecedented sensitivity to weak electromagnetic fields. This convergence motivates a new possibility: elusive particle decays might produce electromagnetic fields strong enough to be detected by quantum devices, opening unexplored regions of parameter space.

We propose a new strategy to detect radiative decays of extremely weakly interacting particles—specifically dark matter (DM) and the C $\nu$ B—using the extraordinary sensitivity of quan-

tum devices such as superconducting transmon qubits and trapped ions [275]. Radiative decays generate extremely faint photons. Although far too weak for traditional detectors, these photons can induce measurable transitions in carefully engineered quantum systems.

A radiative decay  $X_2 \rightarrow X_1 + \gamma$  from DM or neutrinos produces a coherent photon that induces an effective electric field. This field drives a transition in the quantum device from its ground state to an excited state. Placing the device inside a highly reflective cavity causes the decay photon to become trapped, enhancing the probability of interaction. Two experimental platforms are considered: (i) transmon qubits with tunable GHz resonators and well-understood noise properties, and (ii) trapped ions with long coherence times and complementary frequency ranges.

The study of dark matter radiative decay considers a two-component scenario with a small mass splitting. Using realistic quantum device parameters, the analysis shows that current devices already probe significant regions of dark matter parameter space. Reinterpreting the DarQ experiment [276] sets an upper bound of  $m_2 \lesssim 4 \times 10^{-5}$  eV for fixed  $\Delta m^2/m_2$ , and constrains the dark matter–photon coupling  $\mu$ . Discovery and exclusion contours indicate sensitivity to new mass-splitting regimes for transmon frequencies in the 1–10 GHz range, with trapped ions offering complementary reach in long-coherence regimes [275].

For the  $C\nu B$ , radiative neutrino decays depend on extremely small transition magnetic moments  $\mu$ . Current devices cannot detect the induced qubit excitations, but even next-generation architectures with dramatically improved coherence and scalability may reach existing reactor bounds on the transition magnetic moment. Nonetheless, this work establishes the first constraint on neutrino magnetic moments using a quantum device and presents a scalable pathway toward future quantum-based  $C\nu B$  detection [275].

Overall, this work establishes quantum sensing as a powerful emerging tool for exploring physics beyond the Standard Model. Quantum sensing represents a promising new frontier for fundamental physics, with several avenues for dramatic sensitivity improvements, including longer coherence times, higher-frequency qubits in the 10–100 GHz range (albeit with increased decoherence challenges), large entangled qubit arrays, and expanded cavity volumes.

### 3.4.5 Axion DM Searches: Quantum Amplifier auto-tuning

Parametric amplification is a generic phenomenon that occurs when strong and weak waves interact in a nonlinear medium: energy from a strong “pump” tone is transferred to a weak “signal,” resulting in gain. Quantum Parametric amplifiers serve as the first stage of amplification in an ultralow noise receiver, largely determining the noise performance of the system. Unfortunately, optimal performance can only be reached when the operating parameters of the sensitive amplifier are precisely tuned, and automated tuning is currently a time-consuming iterative process. For example, the ADMX receiver relies upon a Josephson Parametric Amplifier (JPA) as its primary amplifier, and as a result, the experiment’s dead-time in data collection is dominated by amplifier re-biasing.

Looking to hasten discovery, we demonstrate a Reinforcement Learning (RL) solution for “auto-tuning” quantum amplifiers. An agent was trained to autonomously tune a Kinetic Inductance Traveling Wave Parametric Amplifier (KITWPA). It controlled the system in real time, by adjusting 3 parameters: bias current, pump frequency, pump power. The agent received a reward proportional to achieved gain measured. The system was sometimes intentionally hamstrung and forced to use a fixed value for one of the parameters; preliminary results suggest that the RL is able to swiftly recover. Future reward shaping work will explore: SNR, fast tuning, minimal heating, and bias point stability.

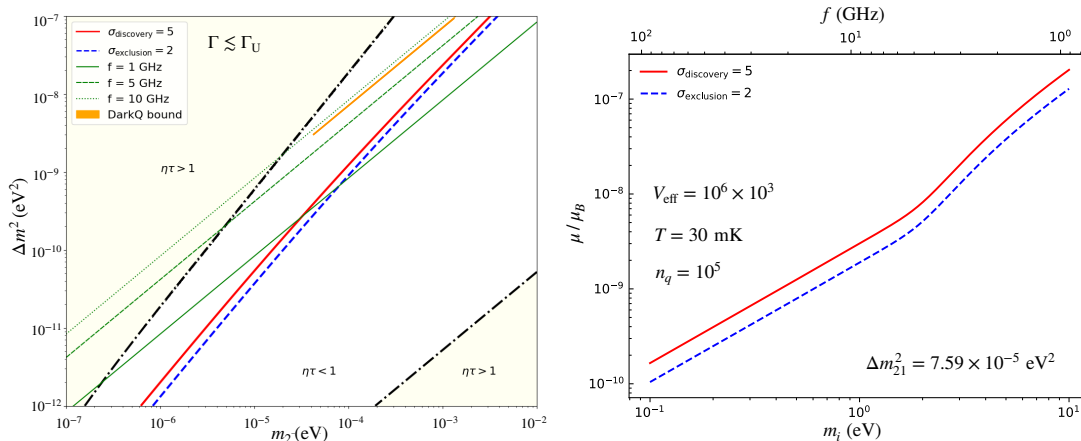


Figure 45: (*Left*)  $5\sigma$  discovery (red, solid) and  $2\sigma$  exclusion (blue, dashed) contours for dark matter radiative decay in the  $(m_2, \Delta m^2)$  plane, assuming the maximum allowed coupling, a coherence time of  $100 \mu\text{s}$  for a single qubit, and the experimental parameters described in the text. (*Right*) Corresponding sensitivity to the neutrino transition magnetic moment  $\mu$  for  $\Delta m_{12}^2 = 7.59 \times 10^{-5} \text{eV}^2$ , assuming  $10^5$  qubits and an effective volume  $V_{\text{eff}} = 10^6 \times 10^3$ . A data collection time of 14s per frequency and a temperature of  $T = 30$  mK are assumed to estimate the dark-count background.

### 3.4.6 The Advent of Superconducting Microwire Single Particle Detectors

HEP mission to explore the fundamental nature of matter relies heavily on the evolution of detector technologies capable of operating in increasingly hostile and high-precision environments. For decades, silicon-based sensors have been the workhorse of High Energy Physics (HEP) detection. However, as we look toward the next generation of facilities – including the Electron-Ion Collider (EIC), the High-Luminosity LHC, Future Circular Collider (FCC), and the proposed Muon Collider – traditional silicon is reaching its physical limits regarding radiation hardness, power dissipation, and timing resolution. Recent breakthroughs documented in [277, 278] present a transformative alternative: the Superconducting Microwire Single Photon Detector (SMSPD). These papers document the successful migration of superconducting sensor technology from small-scale laboratory quantum optics to large-area, high-energy particle tracking, signaling a “quantum leap” in instrumentation that aligns with the P5 (Particle Physics Project Prioritization Panel) strategic roadmap.

The first major milestone, detailed in [277], addresses the primary historical bottleneck of superconducting sensors: the scale-up problem. While Superconducting Nanowire Single Photon Detectors (SNSPDs) have long been the gold standard for infrared photon detection, their micrometer-scale active areas made them impractical for HEP tracking. This research team successfully characterized a  $2 \times 2 \text{mm}^2$  SMSPD array using high-energy particle beams (120 GeV protons and 8 GeV electrons/pions) at the Fermilab Test Beam Facility. This work proved that “microwires”—which are significantly wider than traditional nanowires—can maintain the Cooper-pair breaking sensitivity required to detect minimum ionizing particles (MIPs). By achieving stable detection and a time resolution of 1.15 ns across a larger active area, this study provided the first definitive proof-of-concept that superconducting films could be scaled into architectures suitable for global tracking systems in collider experiments.

Building rapidly upon this foundation, the research presented in [278] demonstrates the ac-

celerated maturation of the technology. Conducted at the CERN SPS H6 beamline, this study optimized the sensor geometry and utilized a 4.7 nm thick Tungsten Silicide (WSi) film to achieve unprecedented performance metrics. The results were twofold: first, the device achieved a 75% fill-factor-normalized efficiency for muons, marking the first time this specific particle species – central to the physics goals of any future lepton collider – was detected with such high efficiency by a microwire array (see Figure 46). Second, the time resolution was improved by nearly an order of magnitude, reaching approximately 130 ps. This rapid improvement in temporal precision is critical; it suggests that SMSPDs are on a trajectory to provide 4D tracking capabilities, where spatial hits are coupled with picosecond-level timing to resolve the extreme event pile-up expected in future high-luminosity environments.

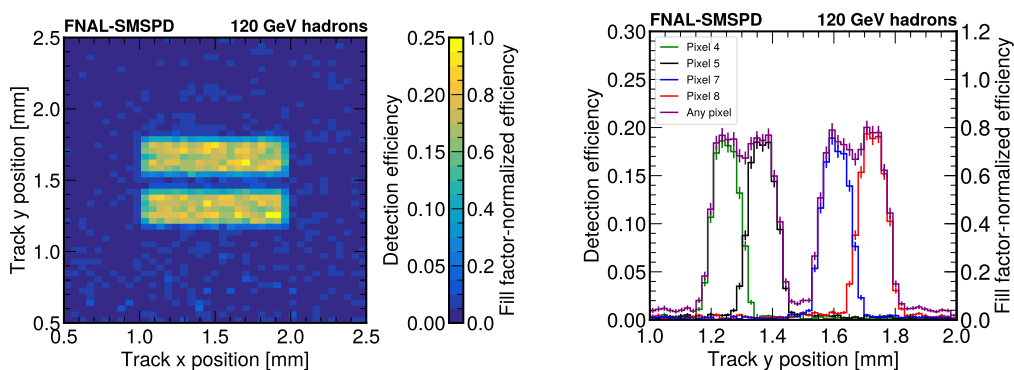


Figure 46: The (fill factor-normalized) detection efficiency of the four SMSPD pixels are shown. The efficiency as a function of the incident track position in the x and y directions (left) and in the y direction only (right) while integrating along the x-axis a 0.7 mm length from the center of each SMSPD pixel. The data in both plots were recorded with the pixels 4, 5, 7, and 8 operating at 8.7, 9.1, 8.8, and  $9.1\mu\text{A}$ , respectively. The gap observed between pixel 5 and pixel 7 is expected and due to the fact that pixel 6 in between was not read out. Both figures are taken from [278].

These advancements offer a compelling case for an advanced research and development program (R&D) in Superconducting Tracking Systems (STS). Besides the superior performance metric another advantage of the SMSPD is its inherent radiation hardness. Unlike silicon, which suffers from bulk displacement damage that degrades signal-to-noise ratios over time, superconducting thin films are remarkably resilient to the high-fluence environments of the innermost tracking layers. Furthermore, because these sensors operate at cryogenic temperatures with nearly zero dissipation in the quiescent state, they offer a pathway to reducing the massive thermal management and cooling services that currently dominate the material budget of modern trackers. Reducing this "dead material" is essential for improving momentum resolution and meeting the physics requirements of the EIC and other precision-frontier experiments.

Furthermore, the implications for the proposed Muon Collider are particularly profound. One of the primary technical hurdles for a muon collider is the Beam-Induced Background (BIB), a "halo" of secondary particles that can blind traditional detectors. The 130 ps (and improving) timing resolution demonstrated, which intrinsically can be made sub-10 ps, in the second paper provides a powerful tool for BIB suppression, allowing physicists to use narrow time-gating to separate primary collision products from background noise. As the DOE seeks to maintain US leadership in accelerator-based physics, the development of SMSPDs represents a unique synergy between the Office of High Energy Physics and the National Quantum Initiative. Funding the transition from these successful test-beam prototypes to wafer-scale production and integrated

cryogenic readout electronics (such as cryo-CMOS) will be essential to scale both the pixel count and sensitive area required for the next decade of HEP instrumentation.

In conclusion, the research across these two articles moves SMSPD technology from a high-risk R&D concept to a viable, high-performance candidate for future collider subsystems. The leap from nanosecond to picosecond timing in a single year of testing underscores the rapid development cycle of this technology. For the HEP community, prioritizing the scale-up and systems-integration of these superconducting sensors will ensure that the next generation of discovery machines is equipped with detectors that are not just incrementally better, but fundamentally more capable than the silicon-based technologies of the past half-century. These papers serve as the technical foundation for a new era of "Quantum-Enabled" particle physics, where the sensitivity of a single-particle detector is harnessed to enhance our discovery potential.

### 3.5 Accelerators

**Contributors:** Niels Bidault, Huaijin Chen, Auralee Edelen, Siqi Li, Yanwen Sun

#### 3.5.1 Physics-Informed AI for Ultrafast X-Ray Diffraction at SLAC's LCLS

The recently launched *Genesis Mission* is a national initiative to enhance scientific discovery and innovation through artificial intelligence (AI). This proposed project advances that vision by developing a physics-informed AI framework capable of interpreting the massive, high-throughput imaging data produced by the fastest X-ray facilities in the United States.

State-of-the-art instruments such as SLAC's Linac Coherent Light Source (LCLS) produce imaging data at extreme rates, enabled by MHz-class detectors and coherent scattering geometries [279]. Techniques like X-ray Photon Correlation Spectroscopy (XPCS) record speckle patterns that capture nanoscale, femtosecond-nanosecond material dynamics [280, 281]. However, interpreting these patterns using conventional molecular-dynamics simulations requires modeling  $10^{11}$  atoms, far beyond modern HPC limits [282]. This data-computation gap necessitates next-generation AI tools that combine physical modeling with scalable learning.

This project introduces a three-part physics-informed AI framework:

**Latent Alignment of MD and Experimental Speckles** Using DINOv2 [283] and CLIP [284], we construct a shared latent space aligning coarse molecular-dynamics (MD) simulations ( $\sim 10^4$  atoms) with experimental speckle patterns. The resulting representation is designed to reveal physically interpretable structure—relaxation modes, spatial heterogeneity, and symmetry features—embedded within high-dimensional diffraction data.

**Diffusion-Based Speckle Simulation with Physics Constraints** Leveraging latent diffusion models [285] and flow-matching generators [286], we develop a simulation engine that produces physically realistic speckle patterns conditioned on MD embeddings and experiment metadata. Physics-based self-supervision losses [287] ensure that outputs remain consistent with known scattering laws, enabling high-fidelity simulation without the prohibitive cost of atomistic computation.

**Automated Comparison, Anomaly Detection, and VLM-Guided Reasoning** Multimodal AI systems such as Flamingo [288] and BLIP-2 [289] automatically compare simulated and observed speckles, identify mismatches, and generate natural-language hypotheses regarding

underlying molecular processes. This establishes an AI-augmented scientific pipeline for ultrafast imaging experiments, directly aligned with the goals of the Genesis Mission.

A key application domain is the glass transition, one of the most important unresolved problems in condensed matter physics [290, 291]. Recent XPCS studies have revealed ultrafast relaxation pathways in glass-forming liquids [292], but extracting mechanistic insight requires a unifying computational framework across experiment and simulation—precisely the capability enabled by physics-informed AI.

By integrating physics-grounded AI with world-leading X-ray infrastructure, this work advances the Genesis Mission’s vision of accelerating scientific discovery through artificial intelligence.

### 3.5.2 AI/ML for Beam Optimization at the UH Accelerator and FEL Facility

The University of Hawai’i (UH) accelerator and free-electron laser (FEL) facility includes a microwave thermionic gun, a 2.856 GHz RF linac, an infrared FEL oscillator, and an inverse Compton scattering (ICS) X-ray beamline. The beamline is compact and densely instrumented with steering magnets, quadrupoles, spectrometers, wire scanners, beam position monitors, and optical diagnostics. Previously demonstrated operating parameters include 50–60 pC micropulses,  $\sim 2$  ps pulse duration,  $\sim 5$   $\mu$ s macropulse lengths, and beam energies near 40 MeV. The FEL produces  $\sim 3$   $\mu$ m IR radiation and the ICS chamber generates  $\sim 10$  keV X-rays [293].

Start-to-end beam dynamics simulations using ASTRA [294], GPT [295], ELEGANT [296], GINGER [297], and GENESIS [298] characterize transport from the cathode to the FEL and ICS interaction points. These simulations track transverse and longitudinal phase space, emittance growth, and timing sensitivity throughout the beamline. Even small variations in injector phase, magnet strengths, or cathode conditions lead to large downstream changes in beam quality, illustrating the highly coupled, high-dimensional, and nonlinear nature of the system. The machine therefore presents an ideal environment for data-driven optimization, where simulation-informed models can complement sparse experimental measurements.

Recent recommissioning work [299] has focused on establishing a stable operational baseline: repairing a major vacuum leak, installing a newly fabricated cathode, and retesting RF power delivery. Ongoing physics studies, such as FEL phase coherence and oscillator desynchronization [300], underscore the sensitivity of cavity performance to arrival-time jitter, energy chirp, and emittance, further motivating algorithmic control strategies capable of maintaining tight synchronization.

At this facility, opportunities for AI and machine learning span injector optimization, beam transport, lattice matching, undulator performance, and cavity tuning. Injector optimization involves adjusting heater power, RF phase, and solenoid fields to maximize current without inducing excessive beam loading or cathode back-heating. ML-based surrogate models or Bayesian optimization can map the high-dimensional response surface, enabling faster and safer tuning than grid scans or manual iteration.

Longitudinal phase-space control represents another major opportunity. Electron beam properties at the linac exit determine FEL performance and ICS spectral quality; machine learning can help maintain minimal energy spread and compensate for drifts in RF amplitude or phase. Reinforcement learning or adaptive control algorithms could learn corrective actions based on diagnostics such as spectrometers.

Transverse matching to the undulator and ICS point is similarly suitable for ML-driven optimization. Quadrupole settings, chicane strengths, and steering corrections can be tuned using surrogate-assisted multi-objective methods that account for emittance, Twiss parameters, orbit stability, and radiation output simultaneously.

Finally, FEL performance can benefit from ML-guided optimization of cavity alignment, interferometer settings, and cavity length detuning. These adjustments traditionally rely on operator experience, but machine learning can search parameter space more systematically, maintain stability over long timescales, and adapt to thermal or mechanical drifts.

Overall, the UH accelerator provides a rich, controllable, and diagnostics-constrained environment ideally suited for AI/ML-enabled beam optimization and autonomous accelerator operation.

### 3.5.3 Combining System Models and ML-based Control to Enable New Capabilities in Beam Tuning for Accelerators

Particle accelerators are essential tools in modern science, and they have numerous applications in medicine and industry. Emerging applications require increasing degrees of precision and rapid on-demand customization of beams, sometimes with increasingly challenging-to-control characteristics (e.g. higher charge and energy, shorter duration). At present, the operation of these machines is handled by expert human operators and simple control algorithms (e.g. standard PID feedback, corrections based on linear physics models). There is substantial room for improvement in both the efficiency and quality of beam tuning.

In the past decade, the suite of AI/ML techniques that have successfully been applied to accelerators has grown dramatically (see [301, 302, 303, 304] for overviews). At SLAC, substantial effort has been devoted to novel algorithm development for improved modeling and control of accelerators, open-source software development, and deployment of AI/ML tools into operations. A priority has been placed on developing tools that can aid fast beam customization for the many different operating modes of SLAC's scientific user facilities, such as FACET-II, MeV-UED, and the free electron laser (FEL) at LCLS. To address the associated challenges, researchers at SLAC initially took two complementary paths: (1) they targeted ML-based optimization algorithms that could learn on-the-fly from limited measurements, to optimize a given configuration without the need for sophisticated system models or large amounts of previous data, and (2) they targeted methods to improve start-to-end modeling of accelerator systems, including hybrid physics and ML modeling approaches.

SLAC produced some of the first successful uses of Bayesian optimization (BO) for accelerators [305] and subsequently demonstrated many improvements, such as inclusion of learned output constraints (e.g. for avoiding beam losses), smoother local sampling (to avoid wasting time as variables settle), and trust region-based search for gradually exploring large parameter spaces (important, for example, in maintaining FEL pulse intensity while respecting constraints such as beam losses) [306, 301]. SLAC researchers and collaborators have also demonstrated several approaches for using physics and ML-based system models to provide a jump start to optimizers (warm starts, physics-model informed kernels, and system models as priors) [307, 308, 309]. SLAC has also pioneered the use of methods for efficient exploration of parameter spaces in accelerators, such as Bayesian Exploration [306]. In an example at FACET-II, SLAC researchers were able to get an 8x more efficient characterization of the injector system by using Bayesian Exploration instead of standard N-D parameter scans. This data was then ready and well-distributed for putting into an ML-based system model of the injector. SLAC has also developed approaches that combine on-the-fly system modeling and information-based sampling for multi-point optimization problems, such as emittance tuning; the team found that this resulted in a nearly 20 times speedup in emittance tuning [310].

Turning to digital twins and online modeling, SLAC was an early leader in the development of ML-based surrogate models of accelerator systems based on both physics simulations and measurements [311, 312, 313]. The eventual aim is to produce digital twins of the accelerator that

can aid operators in the control room by providing more insight into machine behavior, provide models to be used to jump start tuning, and provide models that can be used for experiment planning prior to beam times. SLAC produced several early demonstrations of physics and ML based digital twins for sub-sections of LCLS, including linking live-updating particle-in-cell physics simulations to control room operation [313]. For example, SLAC physicists used a physics simulation for the LCLS-II injector that was running live on the SLAC HPC cluster to provide insight into accelerator behavior that normally is not measurable. This helped the physicists to identify different settings of the injector to try to get to higher beam quality. They then fine-tuned the solution with BO, resulting in the best emittance that had been seen at that time during the LCLS-II injector commissioning, despite extensive previous tuning by hand. SLAC is continuing to expand this work toward a full digital twin of its facilities, both in terms of associated ML techniques and overarching software workflows. There is substantial ongoing collaboration between SLAC, LBNL, and other DOE partners in this space.

Alongside R&D, SLAC has also been developing software tools that are open source and can be used at a wide variety of particle accelerator facilities. For example, Badger and Xopt have been used in the control room of many facilities for online optimization (e.g. see Ref. [314]), and the LUME software ecosystem for start-to-end physics simulations and ML-enhanced digital twins has been used worldwide [315]. These tools have been used on various problems with demonstrated improvements; just a few examples include sextupole tuning at FACET-II resulting in a 2x improvement in acceleration efficiency, emittance tuning with a 20x improvement in tuning speed, a storage lifetime record at ESRF [316], and improvement in FEL pulse intensity at LCLS (percent improvement is still highly variable, but 15-20% improvement has been observed). Current work focuses on making these software tools and algorithms more robust and user-friendly, and relies heavily on feedback from the accelerator community.

We envision having accurate, fast-executing digital twins that adapt to the machine over time, provide initial settings, and can be used in model-based control. When exploring very new beam configurations for which there is little data, BO can provide an advantage in the initial search without the need for previous data. As data is collected, the digital twin can be updated to accurately model the new configuration. Finally, RL and other data-intensive control techniques can then be brought into play for faster / continuous control for configurations where there is more data and accurate models are available. We envision these techniques will all be used in tandem during different types of operational states. Eventually, we also envision the accelerator and photon beamlines for LCLS being more closely linked in the modeling and tuning process, enabling the whole facility to be adjusted on-the-fly to better meet demands of scientific users and to take advantage of more subtle correlations across the whole facility [317].

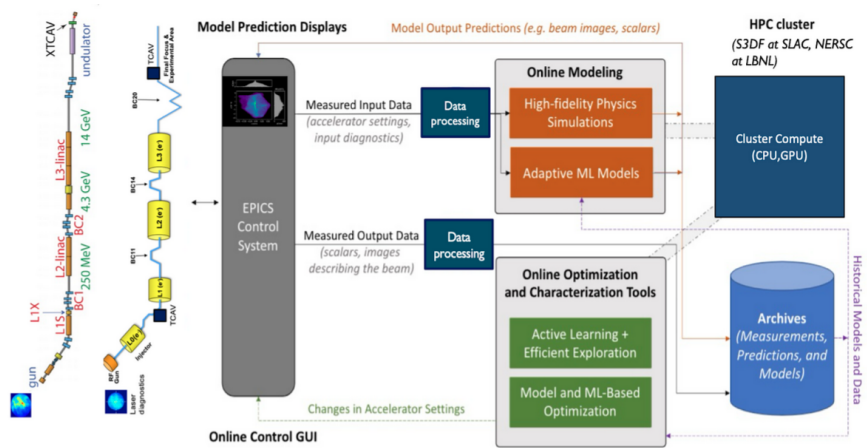


Figure 47

## 4 Community & Education

**Contributors:** Julia Gonski, Philip Harris, Bo-Cheng Lai, Mark Neubauer, Giordon Stark, Ioannis Xiotidis, Keisuke Yoshihara

### 4.1 Related Organizations and Initiatives

The advent of ML-HEQUPP into the sciences has taken off across all subfields on an international scale; for example, the 2026 International Conference on High Energy Physics (ICHEP) is the first in the series to have a dedicated track on “Artificial Intelligence, Machine Learning, and Quantum Computing in HEP” <sup>6</sup>. As a result, organic collaborations have emerged that aim to fully harness and democratize the use of these technologies in modern particle physics experiments. In the US, pre-existing organizations such as the Division of Particles and Fields of the American Physical Society, particularly the Coordinating Panel on Advanced Detectors (CPAD) <sup>7</sup>, can act as facilitators. Significant overlaps also exist with physics organizations dedicated to specific current or future facilities, as these are the ultimate clients of ML-HEQUPP research. Details on several specific organizations follow below.

#### 4.1.1 Accelerated AI Algorithms for Data-Driven Discovery (A3D3)

The Accelerated Artificial Intelligence Algorithms for Data-Driven Discovery (A3D3) Institute represents a large-scale, multi-institutional effort to enable real-time scientific discovery through the integration of domain science, advanced artificial intelligence algorithms, and specialized computing hardware Figure 48. As scientific experiments increasingly confront extreme data volumes and stringent latency requirements—exemplified by the Large Hadron Collider (LHC), where streaming rates reach terabytes per second and raw data bandwidths extend to the petabyte-per-second regime—the need for tightly co-designed AI and hardware solutions has become imperative. A3D3 addresses this challenge by uniting 21 partner institutions and more than 170 members across high energy physics, multi-messenger astronomy, neuroscience, and computer science and engineering. This interdisciplinary structure provides a collaborative environment for developing next-generation algorithms and acceleration strategies tailored to the unique constraints of real-time data-intensive applications.

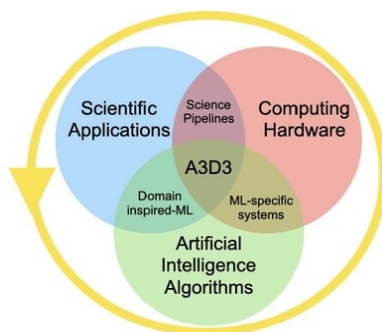


Figure 48: A3D3: an NSF HDR Institute to enable real-time artificial intelligence at scale to advance scientific knowledge and accelerate discovery.

<sup>6</sup>[ichep2026.org](http://ichep2026.org)

<sup>7</sup><https://cpad-dpf.org/>

Here we share an experience of research collaboration between NYCU (National Yang Ming Chiao Tung University, Taiwan) and the A3D3 ecosystem. We focus on FPGA-based acceleration of graph neural networks (GNNs), neural decoding models, and high-throughput particle tracking pipelines. The collaborative workflow emphasizes iterative engagement with domain experts, including problem definition, algorithmic evaluation, software-hardware architectural design, prototyping, performance analysis, and model refinement. This approach has facilitated the creation of several end-to-end hardware-accelerated systems that bridge scientific needs with efficient ML-driven computation.

Beyond high energy physics, the collaboration also developed an FPGA-accelerated deployment of the Latent Factor Analysis via Dynamical Systems (LFADS) model for real-time neuroscience experiments. By extending the `hls4ml` framework, applying quantization-aware training, and designing a multi-model dataflow architecture, the system achieved sub-millisecond latency and preserved the result quality. These results demonstrate the generality of A3D3 methodology for applications requiring both low latency and high computational efficiency.

In addition to research, A3D3 promotes community engagement through workshops, conferences, summer schools, and ML hardware design competitions, strengthening cross-institutional training and collaboration. The recent admission of National Yang Ming Chiao Tung University (NYCU) as a Technical Associate Institute of ATLAS further highlights the growing international role of Taiwan’s scientific computing efforts.

Overall, the work presented here illustrates the transformative potential of coordinated AI-hardware co-design in addressing the demands of real-time scientific data processing. Through deep integration of algorithms, domain expertise, and specialized accelerators, A3D3 provides a blueprint for future breakthroughs in data-driven discovery.

#### 4.1.2 Next Generation Triggers (NGT)

The Next Generation Triggers project [318] at CERN is an on-going project that officially has started in January 2024. It’s a cross experimental community engulfing most CERN departments (Experimental Physics, Theory, Information Technology), the two main experiments (ATLAS and CMS) and external collaborators. The main objective of the project focuses on extracting more physics information from the upcoming HL-LHC upgrade by developing neural network based solutions. Due to the unprecedented conditions of HL-LHC such algorithms target different deployment algorithms from Application Specific Integrated Circuits (ASIC)s, to Field-Programmable-Gate-Arrays (FPGA)s all the way to Quantum Computing based solutions. The project is funded for 5-years from the Eric and Wendy Schmitt foundation.

As part of the mandate the project also evaluates novel technologies from the industry that could provide important performance upgrades for hardware based trigger system. With that technologies like the AMD AI-Engines are being explored in different ATLAS and CMS sub-systems aiming to enhance the processing power of custom FPGA based hardware boards. In addition NGT provides a platform for Machine Learning (ML) model R&D for the challenging conditions of HL-LHC. Industry based developed models and techniques are tested in edge conditions allowing for a thorough survey of cutting edge ML technologies.



Figure 49: NextGen Triggers (NGT): a cross experiment CERN based initiative aiming for enhancing the HL-LHC program.

### 4.1.3 FastML Community

The Fast Machine Learning (FastML) community [5] is a research collective of physicists, engineers, and computer scientists focused on deploying machine learning algorithms for challenging scientific applications requiring low latency and high throughput. The community’s projects span from real-time, on-detector inference to high-throughput heterogeneous computing. A broad range of scientific domains are covered, ranging from particle physics to include multi-messenger astrophysics, quantum computing, astrophysics, neuroscience, and many more. The key driver within FastML is need to for hardware optimized algorithms to ensure either low latency, low power, or high throughput. ML with its intrinsic parallelizability, resulting from matrix multiply, when combined with heterogeneous computing, ends up often being the core element of optimization within FastML

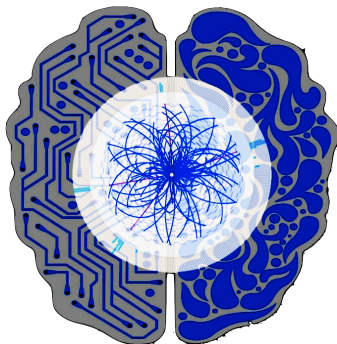


Figure 50: Logo for the Fast Machine Learning Community

Central to the FastML ecosystem for latency and power optimized deployment of ML models is the `hls4ml` library [16, 138, 28], an open-source Python package that translates trained machine learning models into FPGA firmware using high-level synthesis (HLS). The library enables scientists to deploy neural networks, boosted decision trees, and other ML architectures with nanosecond-scale latency while fitting within the strict resource constraints of detector front-ends. The `hls4ml` framework supports multiple HLS backends (including AMD/Xilinx Vitis, Intel Quartus, Catapult HLS, and others) and has been extended to support quantization-aware training through integration with QKeras and QONNIX, enabling systematic optimization of bit-width configurations for hardware deployment.

For high throughput systems, the FastML community focuses on the integration of inference-as-a-service as a paradigm for high throughput computation. Much of this work centers around the Super Services for Optimized Network in Coprocessors (SONIC) framework, which provides an optimized toolkit for efficient resource and scaling of heterogeneous computing targeting large-scale high throughput scientific workflows. These scientific workflows are often found in later stages of the data acquisition chain of large scale experiments, and typically exploit GPU, and CPU computation.

The FastML community organizes annual workshops that bring together domain scientists with ML and hardware experts, the first of the annual workshops happening in 2019[319]. Recent editions include the 2024 workshop hosted by Purdue University and the 2025 conference at ETH Zurich, featuring presentations on topics ranging from graph neural networks for tracking to online deployment of real-time systems including anomaly detection at the Large Hadron Collider, and Multi-messenger alerts at LIGO, to include novel architectures like Kolmogorov-Arnold Networks on FPGAs[320, 321, 322]. These workshops serve as forums for sharing best

practices in codesign methodologies and fostering collaborations between experiments. Furthermore, these meetings aim to broaden collaboration with computing communities allowing for new connections, and extended features in core software packages.

Beyond workshops, the community maintains extensive educational resources including tutorial notebooks, summer schools, and documentation. The `hls4ml` Summer School, supported by the NSF POSE program, provides hands-on training for students in hardware-accelerated ML, addressing the critical workforce development need for specialists who can bridge ML algorithms with FPGA implementation. Additionally, the community maintains a Slack space to enable collaboration. With over 2000 members on the Slack, the FastML community's open-source tools and collaborative culture have made it a cornerstone of the broader effort to embed intelligent processing at the edge of scientific experiments.

#### 4.1.4 U.S. Higgs Factory Circular Collider Organization

Guided by P5 recommendations, the U.S. Department of Energy (DOE) established the Higgs Factory Circular Collider (HFCC) organization to provide a strategic U.S. role in the planning and research for a future Higgs factory, specifically the FCC-ee (electron-positron Future Circular Collider) under study at CERN. This organization brings together national laboratories and universities to coordinate U.S. contributions in physics studies, accelerator design, detector R&D, software, computing, and collaboration planning with international partners. Its mission is to help shape the technical and scientific groundwork needed for meaningful U.S. participation in the FCC program, from pre-project R&D to long-term experimental contributions, and to ensure alignment with the broader global particle physics community.

Within the HFCC structure, the AIM initiative focuses on three cross-cutting areas crucial for next-generation collider detectors: artificial intelligence and machine learning (AI/ML), integrated detector concepts, and microelectronics development. This group evolved from earlier detector electronics and ASIC efforts and now coordinates R&D that spans from smart readout to ML-optimized detector design and open-source tools. Its goals include developing AI/ML approaches suitable for complex detector systems (such as on-detector data processing), optimizing whole-detector concepts through simulation and design tools, and driving innovations in microelectronics (e.g., high-performance ASICs, integrated sensors, silicon photonics, and advanced integration techniques) that are essential to meet the extreme performance requirements of future FCC-ee experiments. The introduction of AIM to the US detector R&D planning process highlights the importance of these critical emerging technologies and a holistic full-detector perspective in delivering on physics goals.



Figure 51: AIM (AI, Integrated Detector Concepts, Microelectronics) initiative of the US Higgs Future Circular Collider organization.

### 4.1.5 Quantum Computing for High-Energy Physics

The intersection of quantum computing and high-energy physics represents an emerging frontier with potential implications for both theoretical simulations and experimental data analysis. Several community initiatives are coordinating efforts in this space, complementing the classical ML and FPGA-focused work described elsewhere in this whitepaper.

**QC4HEP Working Group** The Quantum Computing for High-Energy Physics (QC4HEP) Working Group [323], organized by CERN, DESY, and IBM Quantum, brings together experts from academic and research institutions across four continents to explore quantum computing’s potential as a transformative technology for the field. The working group’s 2024 roadmap paper identified two core areas where quantum computing may impact HEP: algorithms for modeling high-energy physics problems (including lattice gauge theory simulations) and numerical methods for analyzing experimental results (including quantum machine learning approaches for event classification and reconstruction). The group holds annual meetings and actively develops benchmark applications targeting near-term quantum hardware.

**CERN Quantum Technology Initiative (QTI)** CERN’s Quantum Technology Initiative [324] provides a platform for collaboration between the HEP and quantum technology communities. Phase II of CERN QTI (launched January 2024) focuses on identifying applications of quantum computing and quantum sensing to deliver “quantum advantage” within CERN’s physics program. The initiative offers extensive training resources, including online courses on quantum computing, the QTI Journal Club, and schools and workshops that have trained thousands of participants from the HEP community.

**Relevance to Front-End ML** While quantum computing remains in early stages for practical HEP deployment, several connections to front-end ML merit attention: quantum machine learning algorithms are being explored for pattern recognition tasks such as tracking; hybrid quantum-classical workflows may eventually complement edge computing architectures; and quantum sensing technologies may inform future detector designs. As quantum hardware matures, the codesign principles developed for FPGA-based ML—including quantization, resource optimization, and latency-aware design—may prove valuable for quantum-classical hybrid systems.

## 4.2 Workforce Development

The demand for researchers who can develop low-latency, hardware-aware machine learning (ML) has grown rapidly across both industry and experimental physics. Even as the general AI/ML workforce expands, there remains a critical shortage of people who can work at the intersection of ML algorithms, FPGAs/ASICs, firmware, and front-end electronics. Real-time triggering, intelligent data reduction, and high-throughput readout are now central to modern experiments, and they require a workforce that understands both algorithmic design and hardware constraints. Developing this expertise is therefore an urgent community priority.

A major challenge is that most physics students begin without prior training in digital electronics or FPGA programming. In practice, it takes focused instruction, covering topics such as combinational and sequential logic, HDL coding, and vendor toolchains (e.g., AMD/Xilinx Vivado or Vitis, many of whose advanced synthesis and IP-core features require commercial licenses), as well as hands-on work with FPGA, before students can meaningfully contribute to front-end R&D. Model development itself is relatively accessible thanks to open-source ML templates in Keras, PyTorch, scikit-learn, XGBoost, and others; however, understanding how to

convert these models into low-latency hardware implementations requires additional, specialized guidance.

A practical way to address these needs is to integrate electronics, ML, and hardware–software co-design directly into training programs. For example, the modern electronics course at the University of Hawai‘i at Mānoa provides hands-on instruction in digital circuit design with FPGAs and in deploying AI/ML models on hardware using HLS tools such as `hls4ml`. Through this type of curriculum, students learn to build low-latency inference pipelines under real detector constraints, including resource usage, timing closure, synchronization, and power. After such training, students can immediately apply these skills in collider experiments, for example in beam anomaly detection, waveform feature extraction, and other intelligent front-end tasks.

Similar efforts at KEK, particularly within the E-Sys group, involve students directly in firmware development, real-time ML for front-end systems, and mixed-signal design for instrumentation. Recent programs also incorporate AMD Versal architecture, giving trainees exposure to advanced computational engines such as the AI Engine and Deep-Learning Processing Unit (DPU), which are increasingly relevant for ML inference in next-generation readout systems. These initiatives demonstrate that effective education must be closely coupled to ongoing detector R&D, ensuring that trainees work with actual hardware, realistic latency constraints, and modern heterogeneous computing resources.

Beyond individual institutions, community-level initiatives play a critical role. The HEP community is uniquely positioned to serve as a hub for broader workforce development. By coordinating training materials, sharing curricula, and creating cross-institutional research opportunities, the community can accelerate the cultivation of specialists capable of advancing low-latency ML and intelligent front-end systems for future experiments while also contributing to the national need for a technically skilled workforce.

**Emerging Training Needs: Quantum and Analog Computing** As the field moves toward heterogeneous computing architectures that may eventually include quantum processors and analog accelerators, workforce development must anticipate these emerging technologies. The CERN Quantum Technology Initiative offers introductory courses on quantum computing that have reached thousands of participants, providing a model for community-wide training. Similarly, the QC4HEP Working Group’s activities help build familiarity with quantum algorithms among HEP researchers.

For analog computing approaches discussed in Section 2.4.2, specialized training is needed to bridge the gap between traditional digital design and emerging paradigms such as in-memory computing, optical neural networks, and mixed-signal processing. While dedicated curricula for analog ML in HEP do not yet exist, the foundational skills developed through FPGA and ASIC training—including understanding of noise, precision trade-offs, and hardware–software codesign—provide a starting point. As analog computing matures for scientific applications, the community should consider developing targeted educational materials that address the unique challenges of deploying ML on these platforms.

### 4.3 Interdisciplinary Impacts

**Contributors: Shiva Abbaszadeh, Praveen Gurunath Bharathi, Angela Di Fulvio, Sara Pozzi**

Real-time machine learning (ML) implemented on field-programmable gate arrays (FPGAs) [325, 326, 327] has emerged as a natural solution to ultra-low-latency problems. In high-energy physics (HEP), the need to reduce event rates by orders of magnitude within micro or nanoseconds has driven a co-design culture in which compact ML models are optimized jointly with

FPGA firmware [328, 169]. Demonstrations of deep autoencoders, boosted decision trees, and other compact architectures on production-class FPGAs show that unsupervised anomaly detection can be executed in tens to hundreds of nanoseconds while fitting strict power and resource limits, enabling model-agnostic searches for rare signals directly at the trigger level [329, 330]. This body of work established FPGAs as a mature and reliable substrate for deterministic, high-frequency ML inference [331, 44, 332, 138] — the same class of requirements encountered in Biology-guided radiotherapy (BgRT)’s positron emission tomography (PET)-driven control cycle.

The impact of these HEP-driven developments extends far beyond particle physics, offering interdisciplinary benefits in fields where high throughput, tight latency bounds, and limited power are equally critical. Medical imaging is one of the most direct beneficiaries. Here, low-latency edge inference enables closed-loop applications such as intra-operative imaging [333], adaptive filtering, and frame-rate enhancement in ultrasound/computed tomography (CT) [334], as well as on-device prescreening when data transmission is impractical. FPGAs have also been shown to support full image-reconstruction pipelines directly on hardware. For example, gamma-ray imaging systems have demonstrated filtered back projection (FBP) and maximum-likelihood expectation maximization (MLEM) implemented and optimized on low-cost FPGA platforms using high-level synthesis (HLS), achieving multi-fold speedups while preserving image contrast despite reduced numerical precision. Such results highlight the feasibility of real-time or near-real-time reconstruction and localization on embedded FPGA hardware, reinforcing their suitability for advanced radiation-detection and imaging systems[335].

Numerous studies show that FPGA-accelerated image analysis pipelines achieve significant improvements in throughput and energy efficiency compared to CPU/GPU approaches, making FPGA ML an attractive technology for embedded clinical systems [333]. Modern FPGA-based PET electronics now integrate real-time signal processing, high-throughput data acquisition, and ML-enhanced reconstruction within tight resource budgets. In particular, systems combining custom front-end designs (e.g., delta-sigma ADC-based SiPM readouts) with deep neural networks synthesized via the `hls4ml` library demonstrate how pruning, quantization, and co-design can deliver low-latency, resource-efficient performance suitable for real-time PET imaging[336, 337]. These trends align closely with the requirements of image-guided radiotherapy, where real-time reconstruction and decision-making must be both fast and predictable [338, 339]. Tracking the tumor in real time [340, 341] is crucial in radiotherapy, where external radiation beams must remain precisely aligned with a moving biological target. BgRT [342] represents a major advance toward this goal by integrating a linear accelerator (LINAC) with PET [343, 344], enabling radiation delivery guided directly by emissions originating inside the patient. For BgRT to function safely and effectively, a demanding control loop must be executed every 100 ms [345]. Extreme temporal constraints mirror the real-time challenges seen in HEP, where detectors must extract salient information from massive data rates on sub-microsecond timescales.

Beyond medical imaging, related advances in aerospace [346], industrial sensing [347], and hyperspectral imaging [348] further demonstrate the versatility of FPGA-based anomaly detection. Implementations combining autoencoders with sequence models have enabled real-time anomaly detection across thousands of flight-test channels with orders-of-magnitude improvements in latency and power [349]. Closely related work in radiation detection shows that artificial neural networks implemented on FPGAs can classify high-rate detector pulses in real time, even in the presence of severe pile-up. By recovering and classifying individual neutron and gamma events at MHz-scale rates with microsecond-level latency, these systems illustrate how FPGA-based ML can operate reliably in intense radiation environments, a regime that shares important characteristics with nuclear imaging and radiotherapy instrumentation[350].

Similar results exist for Radio Frequency (RF) and hyperspectral pipelines, where continuous-

stream detection at high sample rates supports safety-critical operations such as structural health monitoring and fault prediction [351]. These examples reinforce a broader pattern: when data rates are extreme and latency budgets unforgiving, FPGAs provide a uniquely capable platform for real-time ML. Cybersecurity and network monitoring [352, 353] also exploit this paradigm. High-throughput FPGA architectures hosting neural-network-based anomaly detectors [354, 355, 331] achieve line-rate processing of network traffic, enabling ML-driven intrusion detection that complements traditional signature-based systems. The deterministic timing, field-updatability, and multi-model flexibility of FPGAs make them ideal for deploying adaptive anomaly-detection pipelines in rapidly evolving threat landscapes [356]. These characteristics parallel medical and HEP needs, where algorithms must be both robust and reconfigurable as detectors or clinical protocols evolve.

Real-time or near-real-time ML applied to post-silicon bug diagnosis offers a powerful new way to enhance complex hardware systems by identifying anomalous behavior and localizing faults during validation [357, 358, 359]. By combining lightweight on-chip observability with FPGA-based analysis pipelines, these approaches accelerate failure localization and reliability validation in modern SoCs [359, 360, 361]. This convergence between microarchitectural debugging, HEP trigger systems, and medical-imaging pipelines illustrates the increasingly universal role of hardware-accelerated ML: it enables domain-specific intelligence to move closer to the data source, making real-time decision-making feasible in settings where software-only solutions cannot meet the timing constraints.

Taken together, these developments underscore the growing importance of edge-AI as a unifying paradigm for real-time decision-making in data-intensive, latency-critical systems. By moving intelligence closer to the data source, FPGA-based ML enables deterministic performance, reduced data movement, and energy-efficient operation that cannot be achieved with software-centric approaches alone.

## 5 Key R&D Topics

Fully developing aforementioned technologies and realizing their potential to enhance physics experiments requires considerable R&D in both existing and fundamentally new directions. The ML4FE community drafted a series of prioritized R&D topics at the conclusion of the workshop, which have been expanded and refined following considerable scope expansion and input during the white paper process. These topics follow below, with emphasis both on the core technology and the follow-on implications for physics experiments and related infrastructure.

1. **Facilitating codesign** through continued cross-frontier opportunities for collaboration between scientists, engineers, technicians
2. **Development of open source interdisciplinary benchmarking data/simulation sets for electronics design;**  
e.g. “AI-Ready Data”, including digitization-level detector simulations, readout demonstrators, end-to-end test benches, etc.
3. **Identify areas of greatest impact for hardware-based ML via classical vs. ML benchmarking;**  
e.g. comparative studies of performance, resource efficiency, and scalability with and without AI/ML-based workflows, in order to guide targeted optimization efforts
4. **Resource planning** for US analysis facilities, namely considering GPUs and other accelerators, FPGA development environments, inference-as-a-service infrastructure, automation/validation tools, and quantum processors
5. **End-to-end differentiable DAQ/heterogenous pipeline open source optimization tools;**  
addressing need for multi-stage instrument design and ML operations considering data rates, costs, and system boundaries
6. Design and fabrication of **smart ASICs and/or embedded FPGAs;**  
including 3D integration of advanced sensors + embedded intelligence, towards self-driving/real-time-capable instruments and/or real-time training
7. **Expand open source tools to synthesize advanced ML for hardware implementation;**  
e.g. streaming, structured pruning, high-granularity quantization, quantum algorithms for complex inference at trigger/DAQ level
8. **Intelligence in cold electronics;**  
for real-time applications with LAr time projection chambers/calorimeters, quantum devices/sensors
9. **Analog compute;**  
towards the frontier of fast and low-power computation needs for advanced detectors (4D tracking, 5D high-granularity calorimetry, streaming)
10. **Tracking and incorporating advances in commercial technology;**  
e.g. performance comparisons on new industrial hardware for modern physics applications and challenges
11. **Filling essential workforce development gaps** with key emerging technologies at the university and post-graduate levels

## 6 Conclusions

The onset of the AI/ML era has set fundamental scientific research at an inflection point. The introduction of cutting-edge technologies related to AI/ML, microelectronics, high-performance computing, and quantum processors is essential to deliver an ever more ambitious physics program intent on discovering new physics and measuring the Standard Model to extreme precision. However, the novelty of these technologies means that such an introduction must be done carefully and intentionally to avoid compromising the quality and integrity of experimental and theoretical scientific pursuits. Continued community-centered conversations across science, engineering, government, and industry, supported by a robust and purposeful basic research funding program in the US, is the key to success in this process. With such a system in place, the US scientific community can look forward to yet unimaginable advances in enabling technologies and scientific efforts, on a global scale defined by US leadership, with an era-changing long-term outlook for our understanding of the universe.

## References

- [1] Joel N. Butler et al. *Report of the 2021 U.S. Community Study on the Future of Particle Physics (Snowmass 2021) Summary Chapter*. 2023. arXiv: 2301.06581 [hep-ex]. URL: <https://arxiv.org/abs/2301.06581>.
- [2] Hitoshi Murayama et al. *Exploring the Quantum Universe: Pathways to Innovation and Discovery in Particle Physics*. Tech. rep. <http://dx.doi.org/10.2172/2368847>. Office of Scientific and Technical Information (OSTI), June 2023. DOI: 10.2172/2368847.
- [3] *Basic Research Needs for High Energy Physics Detector Research & Development*. Dec. 2019. URL: <https://science.osti.gov/-/media/hep/pdf/Reports/2020/DOE%5C%5FBasic%5C%5FResearch%5C%5FNeeds%5C%5FStudy%5C%5Fon%5C%5FHigh%5C%5FEnergy%5C%5FPhysics.pdf>.
- [4] Thea Klæboe Aarrestad et al. *Building an AI-native Research Ecosystem for Experimental Particle Physics: A Community Vision*. 2026. arXiv: 2602.17582 [hep-ex]. URL: <https://arxiv.org/abs/2602.17582>.
- [5] Allison McCarn Deiana et al. “Applications and Techniques for Fast Machine Learning in Science”. In: *Frontiers in Big Data* 5 (Apr. 2022), p. 787421. ISSN: 2624-909X. DOI: 10.3389/fdata.2022.787421. arXiv: 2110.13041 [cs.LG]. URL: <http://dx.doi.org/10.3389/fdata.2022.787421>.
- [6] S. Mandal et al. “A Smart Readout ASIC with Real-Time Digital Waveform Processing and Machine Learning”. In: *2024 IEEE Nuclear Science Symposium (NSS), Medical Imaging Conference (MIC) and Room Temperature Semiconductor Detector Conference (RTSD)*. 2024, pp. 1–1. DOI: 10.1109/NSS/MIC/RTSD57108.2024.10656168.
- [7] Grzegorz W. Deptuch et al. “Pixel detectors with built-in signal processing and bandwidth-efficient data transmission”. In: *10th International Workshop on Semiconductor Pixel Detectors for Particles and Imaging*. 2022.
- [8] Soumyajit Mandal et al. “A 12-bit 50 MS/s Hybrid ADC for Waveform Sampling, Data Streaming, and Sparse Readout”. In: *2022 IEEE Nuclear Science Symposium and Medical Imaging Conference (NSS/MIC)*. 2022, pp. 1–2. DOI: 10.1109/NSS/MIC44845.2022.10399146.

- [9] Sandeep Miryala et al. “Peak Prediction Using Multi Layer Perceptron (MLP) for Edge Computing ASICs Targeting Scientific Applications”. In: *2022 23rd International Symposium on Quality Electronic Design (ISQED)*. 2022, pp. 1–6. DOI: 10.1109/ISQED54688.2022.9806285.
- [10] Suyog Gupta et al. *Deep Learning with Limited Numerical Precision*. 2015. arXiv: 1502.02551 [cs.LG]. URL: <https://arxiv.org/abs/1502.02551>.
- [11] Shubha R. Kharel et al. *Automated and Holistic Co-design of Neural Networks and ASICs for Enabling In-Pixel Intelligence*. 2024. arXiv: 2407.14560 [cs.LG]. URL: <https://arxiv.org/abs/2407.14560>.
- [12] Benjamin Parpillon, Amit Ranjan Trivedi, and Farah Fahim. “Readout IC with 40 MSPS in-pixel ADC for future vertex detector upgrades of Large Hadron Collider”. In: *2023 IEEE International Symposium on Circuits and Systems (ISCAS)*. 2023, pp. 1–5. DOI: 10.1109/ISCAS46773.2023.10182033.
- [13] B. Parpillon. *Radiation-hard smart-pixel detector ASIC readout with digital AI in 28 nm*. Poster presentation at TWEPP 2024, Topical Workshop on Electronics for Particle Physics. 30 September–4 October 2024. Glasgow, United Kingdom, Sept. 2024.
- [14] Benjamin Parpillon et al. *Smart Pixels: In-pixel AI for on-sensor data filtering*. 2024. arXiv: 2406.14860 [physics.ins-det]. URL: <https://arxiv.org/abs/2406.14860>.
- [15] FastML Team. *fastmachinelearning/hls4ml*. Version v1.0.0. 2024. DOI: 10.5281/zenodo.1201549. URL: <https://github.com/fastmachinelearning/hls4ml>.
- [16] Javier Duarte et al. “Fast inference of deep neural networks in FPGAs for particle physics”. In: *JINST* 13.07 (2018), P07027. DOI: 10.1088/1748-0221/13/07/P07027. arXiv: 1804.06913 [physics.ins-det]. URL: <https://doi.org/10.1088/1748-0221/13/07/P07027>.
- [17] Siemens EDA. *Catapult HLS*. Online. 2025. URL: <https://eda.sw.siemens.com/en-US/ic/catapult-high-level-synthesis>.
- [18] S Di Giacomo et al. “Implementing an integrated neural network for real-time position reconstruction in emission tomography with monolithic scintillators”. In: *IEEE transactions on radiation and plasma medical sciences* 8.5 (2024), pp. 501–510.
- [19] S Di Giacomo et al. “Experimental Validation of ANNA: Analog Neural Network ASIC for Event Positioning in Monolithic Scintillation Detectors”. In: *IEEE Transactions on Radiation and Plasma Medical Sciences* (2025).
- [20] M Ronchi et al. “Design, Implementation, and Analysis of an Integrated Switched Capacitor Analog Neuron for Edge Computing AI Accelerators”. In: *IEEE Transactions on Circuits and Systems I: Regular Papers* (2025).
- [21] Luca Buonanno et al. “Gamma: A 16-channel spectroscopic asic for sipms readout with 84-db dynamic range”. In: *IEEE Transactions on Nuclear Science* 68.10 (2021), pp. 2559–2572.
- [22] I D’Adda et al. “SITH: a SiPM Readout ASIC for Prompt Gamma-Ray Detection in Hadrontherapy Applications”. In: *IEEE Transactions on Nuclear Science* (2024).
- [23] M Amadori et al. “A Compact Neuron Implementation for a Capacitive Analog Neural Network for In-Sensor Processing”. In: *2024 31st IEEE International Conference on Electronics, Circuits and Systems (ICECS)*. IEEE. 2024, pp. 1–4.

- [24] Tutu Ajayi et al. “INVITED: Toward an Open-Source Digital Flow: First Learnings from the OpenROAD Project”. In: *Proceedings of the 56th Annual Design Automation Conference (DAC)*. New York, NY, USA: Association for Computing Machinery, 2019, pp. 1–4. DOI: 10.1145/3316781.3326334.
- [25] Andrew B. Kahng and Tom Spyrou. “The OpenROAD Project: Unleashing Hardware Innovation”. In: *Proceedings of the Government Microcircuit Applications and Critical Technology Conference (GOMACTech)*. 2021, pp. 1–6.
- [26] Nicolas Bohm Agostini et al. “Bridging Python to Silicon: The SODA Toolchain”. In: *IEEE Micro* 42.5 (2022), pp. 78–88. DOI: 10.1109/MM.2022.3178580. URL: <https://doi.org/10.1109/MM.2022.3178580>.
- [27] Pacific Northwest National Laboratory. *End-to-end Co-design for Performance, Energy Efficiency, and Security in AI-enabled Computational Science (ENCODE)*. <https://www.pnnl.gov/projects/encode>. DOE Advanced Scientific Computing Research Competitive Portfolio Program. 2025.
- [28] Jan-Frederik Schulte et al. “hls4ml: A Flexible, Open-Source Platform for Deep Learning Acceleration on Reconfigurable Hardware”. In: (Dec. 2025). arXiv: 2512.01463 [cs.AR].
- [29] Claudionor N. Coelho et al. “Automatic heterogeneous quantization of deep neural networks for low-latency inference on the edge for particle detectors”. In: *Nature Mach. Intell.* 3 (2021), p. 675. DOI: 10.1038/s42256-021-00356-5. arXiv: 2006.10159 [physics.ins-det].
- [30] Chang Sun et al. “HGQ: High Granularity Quantization for Real-time Neural Networks on FPGAs”. In: (May 2024). DOI: 10.1145/3748173.3779200. arXiv: 2405.00645 [cs.LG].
- [31] Benjamin Ramhorst, Vladimir Lončar, and George A. Constantinides. “FPGA Resource-aware Structured Pruning for Real-Time Neural Networks”. In: *2023 International Conference on Field Programmable Technology (ICFPT)*. 2023, p. 282. DOI: 10.1109/icfpt59805.2023.00046. eprint: 2308.05170.
- [32] Alessandro Pappalardo et al. “QONNX: Representing Arbitrary-Precision Quantized Neural Networks”. In: *4th Workshop on Accelerated Machine Learning at the High-performance Embedded Architecture and Compilation 2022 Conference*. 2022. arXiv: 2206.07527 [cs.LG]. URL: [https://accml.dcs.gla.ac.uk/papers/2022/4thAccML%5C%5Fpaper%5C%5F1\(12\).pdf](https://accml.dcs.gla.ac.uk/papers/2022/4thAccML%5C%5Fpaper%5C%5F1(12).pdf).
- [33] CMS Collaboration. *2024 Data Collected with AXOL1TL Anomaly Detection at the CMS Level-1 Trigger*. CMS Detector Performance Summary CMS-DP-2024-059. 2024. URL: <https://cds.cern.ch/record/2904695>.
- [34] CMS Collaboration. *Model-Independent Real-Time Anomaly Detection at the CMS Level-1 Calorimeter Trigger with CICADA*. CMS Detector Performance Summary CMS-DP-2024-121. 2024. URL: <https://cds.cern.ch/record/2917884>.
- [35] Edge SpAIce. *Novel Edge-AI system for accurate and near real-time plastic detection and monitoring in marine environment*. 2024. URL: <https://edgespace.eu/>.
- [36] Nicolò Ghielmetti et al. “Real-time semantic segmentation on FPGAs for autonomous vehicles with hls4ml”. In: *Mach. Learn. Sci. Tech.* 3 (2022), p. 045011. DOI: 10.1088/2632-2153/ac9cb5. arXiv: 2205.07690 [cs.CV].
- [37] Giuseppe Di Guglielmo et al. “End-to-End Workflow for Machine-Learning-Based Qubit Readout With QICK and hls4ml”. Jan. 2025. DOI: 10.1109/TQE.2025.3604712. arXiv: 2501.14663 [quant-ph].

- [38] Feroz Ahmed Mian and Saima Zafar. “SoC-Based Implementation of 1-D Convolutional Neural Network for 3-Channel ECG Arrhythmia Classification via HLS4ML”. In: *IEEE Embedded Systems Letters* 16.4 (2024), pp. 429–432. DOI: 10.1109/LES.2024.3354081.
- [39] Giuseppe Di Guglielmo et al. “A Reconfigurable Neural Network ASIC for Detector Front-End Data Compression at the HL-LHC”. In: *IEEE Trans. Nucl. Sci.* 68.8 (2021), pp. 2179–2186. DOI: 10.1109/TNS.2021.3087100. arXiv: 2105.01683 [physics.ins-det].
- [40] Jieun Yoo et al. “Smart pixel sensors: towards on-sensor filtering of pixel clusters with deep learning”. In: *Mach. Learn. Sci. Tech.* 5.3 (Oct. 2024), p. 035047. DOI: 10.1088/2632-2153/ad6a00. arXiv: 2310.02474 [physics.ins-det].
- [41] Benjamin Parpillon et al. “Smart Pixels: In-pixel AI for on-sensor data filtering”. In: *2024 IEEE Nuclear Science Symposium, Medical Imaging Conference, and Room-Temperature Semiconductor Detectors Symposium*. 2024. DOI: 10.1109/NSS/MIC/RTSD57108.2024.10655003. arXiv: 2406.14860 [physics.ins-det].
- [42] G Abarajithan et al. *CGRA4ML: A Hardware/Software Framework to Implement Neural Networks for Scientific Edge Computing*. 2024. arXiv: 2408.15561 [cs.AR]. URL: <https://arxiv.org/abs/2408.15561>.
- [43] Jan-Frederik Schulte et al. *hls4ml: A Flexible, Open-Source Platform for Deep Learning Acceleration on Reconfigurable Hardware*. 2025. arXiv: 2512.01463 [cs.AR]. URL: <https://arxiv.org/abs/2512.01463>.
- [44] Yaman Umuroglu et al. “Finn: A framework for fast, scalable binarized neural network inference”. In: *Proceedings of the 2017 ACM/SIGDA international symposium on field-programmable gate arrays*. 2017, pp. 65–74.
- [45] lowRISC. *Ibex RISC-V Core*. 2025. URL: <https://github.com/lowRISC/ibex>.
- [46] Ryan Herbst et al. *Implementation of a framework for deploying AI inference engines in FPGAs*. 2023. arXiv: 2305.19455 [physics.ins-det]. URL: <https://arxiv.org/abs/2305.19455>.
- [47] Abhilasha Dave et al. “FPGA-accelerated SpeckleNN with SNL for real-time X-ray single-particle imaging”. In: *Frontiers in High Performance Computing Volume 3 - 2025* (2025). ISSN: 2813-7337. DOI: 10.3389/fhpcp.2025.1520151. URL: <https://www.frontiersin.org/journals/high-performance-computing/articles/10.3389/fhpcp.2025.1520151>.
- [48] Hamza Ezzaoui Rahali et al. *Neural Network Acceleration on MPSoC board: Integrating SLAC’s SNL, Rogue Software and Auto-SNL*. 2025. arXiv: 2508.21739 [cs.LG]. URL: <https://arxiv.org/abs/2508.21739>.
- [49] Haoyi Jia et al. *Analysis of Hardware Synthesis Strategies for Machine Learning in Collider Trigger and Data Acquisition*. 2024. arXiv: 2411.11678 [physics.ins-det]. URL: <https://arxiv.org/abs/2411.11678>.
- [50] Abhilasha Dave et al. *FPGA-Accelerated Real-Time Beam Emission Spectroscopy Diagnostics at DIII-D Using the SLAC Neural Network Library for ML Inference*. 2025. arXiv: 2511.21924 [physics.plasm-ph]. URL: <https://arxiv.org/abs/2511.21924>.
- [51] Ilya Tolstikhin et al. *MLP-Mixer: An all-MLP Architecture for Vision*. 2021. arXiv: 2105.01601 [cs.CV]. URL: <https://arxiv.org/abs/2105.01601>.

- [52] Duncan McElfresh et al. “When Do Neural Nets Outperform Boosted Trees on Tabular Data?” In: *Advances in Neural Information Processing Systems*. Ed. by A. Oh et al. Vol. 36. Curran Associates, Inc., 2023, pp. 76336–76369. URL: [https://proceedings.neurips.cc/paper\\_files/paper/2023/file/f06d5ebd4ff40b40dd97e30cee632123-Paper-Datasets%5C%5Fand%5C%5FBenchmarks.pdf](https://proceedings.neurips.cc/paper_files/paper/2023/file/f06d5ebd4ff40b40dd97e30cee632123-Paper-Datasets%5C%5Fand%5C%5FBenchmarks.pdf).
- [53] Léo Grinsztajn, Edouard Oyallon, and Gaël Varoquaux. *Why do tree-based models still outperform deep learning on tabular data?* 2022. arXiv: 2207.08815 [cs.LG]. URL: <https://arxiv.org/abs/2207.08815>.
- [54] Thorben Finke et al. *Back To The Roots: Tree-Based Algorithms for Weakly Supervised Anomaly Detection*. 2023. arXiv: 2309.13111 [hep-ph]. URL: <https://arxiv.org/abs/2309.13111>.
- [55] S. Summers et al. “Fast inference of Boosted Decision Trees in FPGAs for particle physics”. In: *Journal of Instrumentation* 15.05 (May 2020), P05026. DOI: 10.1088/1748-0221/15/05/P05026. URL: <https://doi.org/10.1088/1748-0221/15/05/P05026>.
- [56] T.M. Hong et al. “Nanosecond machine learning event classification with boosted decision trees in FPGA for high energy physics”. In: *Journal of Instrumentation* 16.08 (Aug. 2021), P08016. DOI: 10.1088/1748-0221/16/08/P08016. URL: <https://doi.org/10.1088/1748-0221/16/08/P08016>.
- [57] B.T. Carlson et al. “Nanosecond machine learning regression with deep boosted decision trees in FPGA for high energy physics”. In: *Journal of Instrumentation* 17.09 (Sept. 2022), P09039. DOI: 10.1088/1748-0221/17/09/P09039. URL: <https://doi.org/10.1088/1748-0221/17/09/P09039>.
- [58] S. T. Roche et al. “Nanosecond anomaly detection with decision trees and real-time application to exotic Higgs decays”. In: *Nature Communications* 15.1 (2024), p. 3527. DOI: 10.1038/s41467-024-47704-8. URL: <https://doi.org/10.1038/s41467-024-47704-8>.
- [59] V V Gligorov and M Williams. “Efficient, reliable and fast high-level triggering using a bonsai boosted decision tree”. In: *Journal of Instrumentation* 8.02 (Feb. 2013), P02013. DOI: 10.1088/1748-0221/8/02/P02013. URL: <https://doi.org/10.1088/1748-0221/8/02/P02013>.
- [60] Darin Acosta et al. “Boosted Decision Trees in the Level-1 Muon Endcap Trigger at CMS”. In: *Journal of Physics: Conference Series* 1085.4 (Sept. 2018), p. 042042. DOI: 10.1088/1742-6596/1085/4/042042. URL: <https://doi.org/10.1088/1742-6596/1085/4/042042>.
- [61] David Reikher. “Leveraging Machine Learning for Enhanced FPGA- Based Tau Triggering and Combined  $H \rightarrow (bb/cc)$  Analysis in the ATLAS Experiment”. PhD thesis. July 2025. DOI: 10.17181/dmhbt-mr131. URL: <https://doi.org/10.17181/dmhbt-mr131>.
- [62] Christopher Brown. “CMS Level-1 Track Finder for the Phase-2 Upgrade”. In: *Proceedings of The 32nd International Workshop on Vertex Detectors — PoS(VERTEX2023)*. Vol. 448. 2024, p. 022. DOI: 10.22323/1.448.0022.
- [63] Peter Eduard Meiring. “Low Energy Leptons in High Energy Physics: A Search for Physics beyond the Standard Model with Compressed Mass-Spectra and New Algorithms for Triggering on Electrons at the High Luminosity LHC”. PhD thesis. Aug. 2024. DOI: 10.5167/uzh-263220. URL: <https://doi.org/10.5167/uzh-263220>.

- [64] Noah Clarke Hall and Nikolaos Konstantinidis. “DECADE: Decorrelated anomaly detection triggers to enhance the low-mass discovery potential of the LHC”. In: (Aug. 2025). arXiv: 2508.10224 [hep-ex].
- [65] Fei Tony Liu, Kai Ming Ting, and Zhi-Hua Zhou. “Isolation Forest”. In: *2008 Eighth IEEE International Conference on Data Mining*. 2008, pp. 413–422. DOI: 10.1109/ICDM.2008.17.
- [66] Yun-Tsung Lai. “Implementation of Small-Scale ML in Belle II Chamber Drift Chamber Front-End Electronics for Cross-Talk Noise Reduction”. In: *ML4FE Workshop, University of Hawaii*. Contributed talk, May 20, 2025. Honolulu, HI, USA, May 2025. URL: <https://indico.phys.hawaii.edu/event/2506/contributions/7939/>.
- [67] J. Gonski et al. “Embedded FPGA developments in 130 nm and 28 nm CMOS for machine learning in particle detector readout”. In: *Journal of Instrumentation* 19.08 (Aug. 2024), P08023. DOI: 10.1088/1748-0221/19/08/P08023. URL: <https://doi.org/10.1088/1748-0221/19/08/P08023>.
- [68] Jyothiraj Johnson et al. “Investigating resource-efficient neutron/gamma classification ML models targeting eFPGAs”. In: *Journal of Instrumentation* 19.07 (July 2024), P07034. DOI: 10.1088/1748-0221/19/07/P07034. URL: <https://doi.org/10.1088/1748-0221/19/07/P07034>.
- [69] John Preskill. “Quantum Computing in the NISQ Era and Beyond”. In: *Quantum* 2 (2018), p. 79.
- [70] M. Kjaergaard, M. E. Schwartz, J. Braumüller, et al. “Superconducting Qubits: Current State of Play”. In: *Annual Review of Condensed Matter Physics* 11 (2020), pp. 369–395.
- [71] Frank Arute et al. “Quantum Supremacy Using a Programmable Superconducting Processor”. In: *Nature* 574 (2019), pp. 505–510.
- [72] Youngseok Kim et al. “Evidence for the utility of quantum computing before fault tolerance”. In: *Nature* 618.7965 (2023), pp. 500–505. DOI: 10.1038/s41586-023-06096-3.
- [73] Talal Ahmed Chowdhury et al. “Enhancing quantum utility: Simulating large-scale quantum spin chains on superconducting quantum computers”. In: *Phys. Rev. Res.* 6.3 (2024), p. 033107. DOI: 10.1103/PhysRevResearch.6.033107. arXiv: 2312.12427 [quant-ph].
- [74] Talal Ahmed Chowdhury et al. “Quantum Utility in Simulating the Real-time Dynamics of the Fermi-Hubbard Model using Superconducting Quantum Computers”. In: (Sept. 2025). arXiv: 2509.14196 [quant-ph].
- [75] Austin G. Fowler et al. “Surface codes: Towards practical large-scale quantum computation”. In: *Phys. Rev. A* 86.3 (2012), p. 032324. DOI: 10.1103/physreva.86.032324. arXiv: 1208.0928 [quant-ph].
- [76] Shantanu Debnath et al. “Demonstration of a Small Programmable Quantum Computer with Atomic Qubits”. In: *Nature* 536 (2016), pp. 63–66.
- [77] C. D. Bruzewicz et al. “Trapped-Ion Quantum Computing: Progress and Challenges”. In: *Applied Physics Reviews* 6 (2019), p. 021314.
- [78] M. Saffman, T. G. Walker, and K. Mølmer. “Quantum Information with Rydberg Atoms”. In: *Reviews of Modern Physics* 82 (2010), pp. 2313–2363.
- [79] Antoine Browaeys and Thierry Lahaye. “Many-Body Physics with Individually Controlled Rydberg Atoms”. In: *Nature Physics* 16 (2020), pp. 132–142.

- [80] J. L. O’Brien, A. Furusawa, and J. Vučković. “Photonic Quantum Technologies”. In: *Nature Photonics* 3 (2009), pp. 687–695.
- [81] F. A. Zwanenburg et al. “Silicon Quantum Electronics”. In: *Reviews of Modern Physics* 85 (2013), pp. 961–1019.
- [82] C. Nayak et al. “Non-Abelian Anyons and Topological Quantum Computation”. In: *Reviews of Modern Physics* 80 (2008), pp. 1083–1159.
- [83] Maria Schuld and Nathan Killoran. “Quantum Machine Learning in Feature Hilbert Spaces”. In: *Phys. Rev. Lett.* 122.4 (2019), p. 040504. DOI: 10.1103/PhysRevLett.122.040504. arXiv: 1803.07128 [quant-ph].
- [84] Suguru Endo, Simon C. Benjamin, and Ying Li. “Practical Quantum Error Mitigation for Near-Future Applications”. In: *Phys. Rev. X* 8.3 (2018), p. 031027. DOI: 10.1103/PhysRevX.8.031027. arXiv: 1712.09271 [quant-ph].
- [85] Tadashi Kadowaki and Hidetoshi Nishimori. “Quantum annealing in the transverse Ising model”. In: *Physical Review E* 58.5 (Nov. 1998), pp. 5355–5363. ISSN: 1095-3787. DOI: 10.1103/physreve.58.5355. URL: <http://dx.doi.org/10.1103/PhysRevE.58.5355>.
- [86] Edward Farhi et al. “A Quantum Adiabatic Evolution Algorithm Applied to Random Instances of an NP-Complete Problem”. In: *Science* 292.5516 (2001), p. 1057726. DOI: 10.1126/science.1057726. arXiv: quant-ph/0104129.
- [87] Hideki Okawa et al. “Quantum-Annealing-Inspired Algorithms for Track Reconstruction at High-Energy Colliders”. In: *Comput. Softw. Big Sci.* 8.1 (2024), p. 16. DOI: 10.1007/s41781-024-00126-z. arXiv: 2402.14718 [quant-ph].
- [88] Souvik Das, Andrew J. Wildridge, and Andreas Jung. “Track clustering with a quantum annealer for primary vertex reconstruction at hadron colliders”. In: (Mar. 2019). arXiv: 1903.08879 [hep-ex].
- [89] Alex Mott et al. “Solving a Higgs optimization problem with quantum annealing for machine learning”. In: *Nature* 550.7676 (Oct. 2017), pp. 375–379. DOI: 10.1038/nature24047. URL: <https://ideas.repec.org/a/nat/nature/v550y2017i7676d10.1038%5C%5Fnature24047.html>.
- [90] William Huggins et al. “Towards quantum machine learning with tensor networks”. In: *Quantum Sci. Technol.* 4.2 (Jan. 2019), p. 024001. ISSN: 2058-9565. DOI: 10.1088/2058-9565/aaea94. URL: <https://doi.org/10.1088/2058-9565/aaea94> (visited on 11/13/2025).
- [91] Shi-Ju Ran and Gang Su. “Tensor Networks for Interpretable and Efficient Quantum-Inspired Machine Learning”. In: *Intelligent Computing* 2 (Nov. 2023), p. 0061. DOI: 10.34133/icomputing.0061. URL: <https://spj.science.org/doi/10.34133/icomputing.0061> (visited on 11/13/2025).
- [92] Hao Chen and Thomas Barthel. “Machine learning with tree tensor networks, CP rank constraints, and tensor dropout”. In: *IEEE Trans. Pattern Anal. Mach. Intell.* 46.12 (Dec. 2024). arXiv:2305.19440 [cs], pp. 7825–7832. ISSN: 0162-8828, 2160-9292, 1939-3539. DOI: 10.1109/TPAMI.2024.3396386. URL: <http://arxiv.org/abs/2305.19440> (visited on 11/20/2025).
- [93] D. Perez-Garcia et al. *Matrix Product State Representations*. arXiv:quant-ph/0608197. Aug. 2007. DOI: 10.48550/arXiv.quant-ph/0608197. URL: <http://arxiv.org/abs/quant-ph/0608197> (visited on 11/13/2025).

- [94] Ignacio Cirac et al. “Matrix Product States and Projected Entangled Pair States: Concepts, Symmetries, and Theorems”. In: *Rev. Mod. Phys.* 93.4 (Dec. 2021). arXiv:2011.12127 [quant-ph], p. 045003. ISSN: 0034-6861, 1539-0756. DOI: 10.1103/RevModPhys.93.045003. URL: <http://arxiv.org/abs/2011.12127> (visited on 11/20/2025).
- [95] Y.-Y. Shi, L.-M. Duan, and G. Vidal. “Classical simulation of quantum many-body systems with a tree tensor network”. In: *Phys. Rev. A* 74.2 (Aug. 2006), p. 022320. DOI: 10.1103/PhysRevA.74.022320. URL: <https://link.aps.org/doi/10.1103/PhysRevA.74.022320> (visited on 11/13/2025).
- [96] Alberto Coppi et al. *Towards Tensor Network Models for Low-Latency Jet Tagging on FPGAs*. 2026. arXiv: 2601.10801 [cs.LG]. URL: <https://arxiv.org/abs/2601.10801>.
- [97] E. Miles Stoudenmire and David J. Schwab. *Supervised Learning with Quantum-Inspired Tensor Networks*. arXiv:1605.05775 [stat]. May 2017. DOI: 10.48550/arXiv.1605.05775. URL: <http://arxiv.org/abs/1605.05775> (visited on 11/13/2025).
- [98] Timo Felser et al. “Quantum-inspired machine learning on high-energy physics data”. en. In: *npj Quantum Inf* 7.1 (July 2021), p. 111. ISSN: 2056-6387. DOI: 10.1038/s41534-021-00443-w. URL: <https://www.nature.com/articles/s41534-021-00443-w> (visited on 11/13/2025).
- [99] Alessio Gianelle et al. “Quantum Machine Learning for  $b$ -jet charge identification”. In: *J. High Energ. Phys.* 2022.8 (Aug. 2022). arXiv:2202.13943 [hep-ex], p. 14. ISSN: 1029-8479. DOI: 10.1007/JHEP08(2022)014. URL: <http://arxiv.org/abs/2202.13943> (visited on 11/13/2025).
- [100] Maurizio Pierini et al. *HLS4ML LHC Jet dataset (150 particles)*. Zenodo, Jan. 2020. DOI: 10.5281/zenodo.3602260. URL: <https://zenodo.org/records/3602260> (visited on 11/20/2025).
- [101] Lorenzo Borella et al. “Tree Tensor Network implemented on FPGA as ultra-low latency binary classifiers”. In: *PoS ICHEP2024* (2025), p. 1004. DOI: 10.22323/1.476.1004.
- [102] Lorenzo Borella et al. “Ultra-low latency quantum-inspired machine learning predictors implemented on FPGA”. en. In: *Mach. Learn.: Sci. Technol.* 6.4 (Dec. 2025). Publisher: IOP Publishing, p. 045062. ISSN: 2632-2153. DOI: 10.1088/2632-2153/ae25b5. URL: <https://doi.org/10.1088/2632-2153/ae25b5> (visited on 12/16/2025).
- [103] CMS Collaboration. “The CMS trigger system”. en. In: *J. Inst.* 12.01 (Jan. 2017), P01020. ISSN: 1748-0221. DOI: 10.1088/1748-0221/12/01/P01020. URL: <https://doi.org/10.1088/1748-0221/12/01/P01020> (visited on 11/20/2025).
- [104] Chang Sun et al. “Fast jet tagging with MLP-Mixers on FPGAs”. In: *Machine Learning: Science and Technology* 6.3 (Aug. 2025), p. 035025. DOI: 10.1088/2632-2153/adf596. URL: <https://doi.org/10.1088/2632-2153/adf596>.
- [105] Lauri Laatu, Chang Sun, et al. *Sub-microsecond Transformers for Jet Tagging on FPGAs*. 2025. arXiv: 2510.24784 [physics.ins-det]. URL: <https://arxiv.org/abs/2510.24784>.
- [106] Miguel Caçador Peixoto et al. “Fitting a collider in a quantum computer: tackling the challenges of quantum machine learning for big datasets”. In: *Front. Artif. Intell.* 6 (2023), p. 1268852. DOI: 10.3389/frai.2023.1268852. arXiv: 2211.03233 [hep-ph].
- [107] Vasilis Belis et al. “Quantum anomaly detection in the latent space of proton collision events at the LHC”. In: *Commun. Phys.* 7.1 (2024), p. 334. DOI: 10.1038/s42005-024-01811-6. arXiv: 2301.10780 [quant-ph].

- [108] Vasilis Belis et al. “Guided quantum compression for high dimensional data classification”. In: *Mach. Learn. Sci. Tech.* 5.3 (2024), p. 035010. DOI: 10.1088/2632-2153/ad5fdd. arXiv: 2402.09524 [quant-ph].
- [109] Aritra Bal et al. “One particle - one qubit: Particle physics data encoding for quantum machine learning”. In: *Phys. Rev. D* 112.7 (2025), p. 076004. DOI: 10.1103/18y2-87vq. arXiv: 2502.17301 [hep-ph].
- [110] Ville Bergholm et al. “PennyLane: Automatic differentiation of hybrid quantum-classical computations”. In: (Nov. 2018). arXiv: 1811.04968 [quant-ph].
- [111] Marcello Benedetti et al. “Parameterized quantum circuits as machine learning models”. In: *Quantum Sci. Technol.* 4.4 (2019), p. 043001. DOI: 10.1088/2058-9565/ab4eb5. arXiv: 1906.07682 [quant-ph].
- [112] Maria Schuld et al. “Evaluating analytic gradients on quantum hardware”. In: *Phys. Rev. A* 99.3 (2019), p. 032331. DOI: 10.1103/PhysRevA.99.032331. arXiv: 1811.11184 [quant-ph].
- [113] David Wierichs et al. “General parameter-shift rules for quantum gradients”. In: *Quantum* 6 (2022), p. 677. DOI: 10.22331/q-2022-03-30-677. arXiv: 2107.12390 [quant-ph].
- [114] Jarrod R. McClean et al. “Barren plateaus in quantum neural network training landscapes”. In: *Nature Commun.* 9 (2018), p. 4812. DOI: 10.1038/s41467-018-07090-4. arXiv: 1803.11173 [quant-ph].
- [115] Dirk Koch et al. “FABulous: An Embedded FPGA Framework”. In: *The 2021 ACM/SIGDA International Symposium on Field-Programmable Gate Arrays*. FPGA ’21. Virtual Event, USA: Association for Computing Machinery, 2021, pp. 45–56. ISBN: 9781450382182. DOI: 10.1145/3431920.3439302. URL: <https://doi.org/10.1145/3431920.3439302>.
- [116] Xifan Tang et al. “OpenFPGA: An Opensource Framework for Agile Prototyping Customizable FPGAs”. In: *IEEE Micro* PP (May 2020), pp. 1–1. DOI: 10.1109/MM.2020.2995854.
- [117] Juan J. Manfredi et al. “The single-volume scatter camera”. In: *Hard X-Ray, Gamma-Ray, and Neutron Detector Physics XXII*. Ed. by Arnold Burger, Stephen A. Payne, and Michael Fiederle. Vol. 11494. International Society for Optics and Photonics. SPIE, 2020, p. 114940V. DOI: 10.1117/12.2569995. URL: <https://doi.org/10.1117/12.2569995>.
- [118] B. Boxer et al. “Studies in pulse shape discrimination for an optimized ASIC design”. In: *Journal of Instrumentation* 18.01 (Jan. 2023), P01020. DOI: 10.1088/1748-0221/18/01/P01020. URL: <https://doi.org/10.1088/1748-0221/18/01/P01020>.
- [119] Bernhard Murmann, Michiel Verhelst, and Yiannis Manoli. “Analog-to-Information Conversion”. In: *NANO-CHIPS 2030*. Ed. by Bernhard Murmann and Bernd Hoefflinger. Springer, 2020.
- [120] David A. Villamizar et al. “An 800 nW Switched-Capacitor Feature Extraction Filterbank for Sound Classification”. In: *IEEE Transactions on Circuits and Systems I* 68.4 (Apr. 2021), pp. 1578–1588.
- [121] Christopher Young et al. “A Data-Compressive 1.5/2.75-bit Log-Gradient QVGA Image Sensor With Multi-Scale Readout for Always-On Object Detection”. In: *IEEE Journal of Solid-State Circuits* 54.11 (Nov. 2019), pp. 2932–2946.
- [122] Qi Lu and Bernhard Murmann. “Enhancing the Energy Efficiency and Robustness of tinyML Computer Vision Using Log-Gradient Images”. In: *ACM Transactions on Embedded Computing Systems* (May 2024), pp. 1–20.

- [123] Michiel Verhelst and Bernhard Murmann. “Machine Learning at the Edge”. In: *NANO-CHIPS 2030*. Ed. by Bernhard Murmann and Bernd Hoefflinger. Springer, 2020.
- [124] Bernhard Murmann. “Mixed-Signal Computing for Deep Neural Network Inference”. In: *IEEE Transactions on Very Large Scale Integration (VLSI) Systems* 29.1 (Jan. 2021), pp. 3–13.
- [125] et al. Doshi. “Medusa: A 0.83/4.6  $\mu$ J /Frame 86/91.6%-CIFAR-10 TinyML Processor with Pipelined Pixel Streaming of Bottleneck Layers in 28nm CMOS”. In: *2024 IEEE Symposium on VLSI Technology and Circuits*. June 2024, pp. 1–2.
- [126] Pacific Northwest National Laboratory. *Democratization of Co-design for Energy-Efficient Heterogeneous Computing (DeCoDe)*. <https://www.pnnl.gov/projects/decode>. DOE Advanced Scientific Computing Research, Microelectronics Science Research Center project. 2025.
- [127] Chris Lattner et al. “MLIR: Scaling Compiler Infrastructure for Domain Specific Computation”. In: (2021), pp. 2–14. DOI: 10.1109/CG051591.2021.9370308.
- [128] Erdal Mutlu et al. “COMET: A Domain-Specific Compilation of High-Performance Computational Chemistry”. In: *Languages and Compilers for Parallel Computing*. Ed. by Barbara Chapman and José Moreira. Cham: Springer International Publishing, 2022, pp. 87–103.
- [129] Ruiqin Tian et al. “A High Performance Sparse Tensor Algebra Compiler in MLIR”. In: *2021 IEEE/ACM 7th Workshop on the LLVM Compiler Infrastructure in HPC (LLVM-HPC)*. 2021, pp. 27–38. DOI: 10.1109/LLVMHPC54804.2021.00009.
- [130] Nicolas Bohm Agostini et al. “An MLIR-Based Compiler Flow for System-Level Design and Hardware Acceleration”. In: *Proceedings of the 41st IEEE/ACM International Conference on Computer-Aided Design*. ICCAD ’22. San Diego, California: Association for Computing Machinery, 2022. ISBN: 9781450392174. DOI: 10.1145/3508352.3549424.
- [131] Fabrizio Ferrandi et al. “Invited: Bambu: an Open-Source Research Framework for the High-Level Synthesis of Complex Applications”. In: *2021 58th ACM/IEEE Design Automation Conference (DAC) (2021)*, pp. 1327–1330. DOI: 10.1109/DAC18074.2021.9586110.
- [132] Tutu Ajayi et al. “Toward an Open-Source Digital Flow: First Learnings from the OpenROAD Project”. In: *Proceedings of the 56th Annual Design Automation Conference 2019*. DAC ’19. Las Vegas, NV, USA: Association for Computing Machinery, 2019. ISBN: 9781450367257. DOI: 10.1145/3316781.3326334. URL: <https://doi.org/10.1145/3316781.3326334>.
- [133] Cheng Tan et al. “OpenCGRA: An Open-Source Unified Framework for Modeling, Testing, and Evaluating CGRAs”. In: *2020 IEEE 38th International Conference on Computer Design (ICCD)*. 2020, pp. 381–388. DOI: 10.1109/ICCD50377.2020.00070.
- [134] Cheng Tan et al. “DRIPS: Dynamic Rebalancing of Pipelined Streaming Applications on CGRAs”. In: *2022 IEEE International Symposium on High-Performance Computer Architecture (HPCA)*. 2022, pp. 304–316. DOI: 10.1109/HPCA53966.2022.00030.
- [135] D. Ciangottini et al. “Analysis Facilities for the HL-LHC White Paper”. In: *Comput. Softw. Big Sci.* 9.1 (2025). Ed. by L. Heinrich, p. 14. DOI: 10.1007/s41781-025-00133-8. arXiv: 2404.02100 [hep-ex].
- [136] NVIDIA Corporation. *Triton Inference Server: An Optimized Cloud and Edge Inferencing Solution*. URL: <https://github.com/triton-inference-server/server>.

- [137] Dmitry Kondratyev et al. “SuperSONIC: Cloud-Native Infrastructure for ML Inferencing”. In: *Practice and Experience in Advanced Research Computing 2025: The Power of Collaboration*. PEARC ’25. Association for Computing Machinery, 2025. ISBN: 9798400713989. DOI: 10.1145/3708035.3736049. URL: <https://doi.org/10.1145/3708035.3736049>.
- [138] Thea Aarrestad et al. “Fast convolutional neural networks on FPGAs with hls4ml”. In: *Machine Learning: Science and Technology* 2.4 (2021), p. 045015.
- [139] Andy Buckley et al. *Enabling stable preservation of ML algorithms in high-energy physics with petrifyML*. 2025. arXiv: 2509.11830 [hep-ph]. URL: <https://arxiv.org/abs/2509.11830>.
- [140] Jennet Dickinson et al. “Smartpixels: Towards on-sensor inference of charged particle track parameters and uncertainties”. In: (Dec. 2023). arXiv: 2312.11676 [hep-ex].
- [141] Benjamin Parpillon et al. “In-pixel integration of signal processing and AI/ML based data filtering for particle tracking detectors”. In: (Oct. 2025). arXiv: 2510.07485 [physics.ins-det].
- [142] Danush Shekar et al. *Sensor Co-design for smartpixels*. 2025. arXiv: 2510.06588 [physics.ins-det]. URL: <https://arxiv.org/abs/2510.06588>.
- [143] Jieun Yoo et al. *Smart pixel sensors: towards on-sensor filtering of pixel clusters with deep learning*. 2023. arXiv: 2310.02474 [physics.ins-det]. URL: <https://arxiv.org/abs/2310.02474>.
- [144] A. Accardi et al. “Electron Ion Collider: The Next QCD Frontier: Understanding the glue that binds us all”. In: *Eur. Phys. J. A* 52.9 (2016). Ed. by A. Deshpande, Z. E. Meziani, and J. W. Qiu, p. 268. DOI: 10.1140/epja/i2016-16268-9. arXiv: 1212.1701 [nucl-ex]. URL: <https://doi.org/10.1140/epja/i2016-16268-9>.
- [145] The ALICE Collaboration. *Technical Design report for the ALICE Inner Tracking System 3 - ITS3 ; A bent wafer-scale monolithic pixel detector*. Tech. rep. Co-project Manager: Magnus Mager. Geneva: CERN, 2024. URL: <https://cds.cern.ch/record/2890181>.
- [146] G. Alimonti et al. “RD53 pixel readout integrated circuits for ATLAS and CMS HL-LHC upgrades”. In: *JINST* 20.03 (2025), P03024. DOI: 10.1088/1748-0221/20/03/P03024. URL: <https://doi.org/10.1088/1748-0221/20/03/P03024>.
- [147] “Technical Design Report for the ATLAS Inner Tracker Pixel Detector”. In: (2017). DOI: 10.17181/CERN.FOZZ.ZP3Q. URL: <https://doi.org/10.17181/CERN.FOZZ.ZP3Q>.
- [148] W. Adam et al. “The CMS Phase-1 Pixel Detector Upgrade”. In: *JINST* 16.02 (2021), P02027. DOI: 10.1088/1748-0221/16/02/P02027. arXiv: 2012.14304 [physics.ins-det]. URL: <https://doi.org/10.1088/1748-0221/16/02/P02027>.
- [149] P. Dorosz. “Data transmission architecture of the ALICE ITS3 stitched sensor prototype MOSAIX”. In: *JINST* 19.04 (2024), p. C04050. DOI: 10.1088/1748-0221/19/04/C04050. URL: <https://doi.org/10.1088/1748-0221/19/04/C04050>.
- [150] M. Abbrescia et al. “The IDEA detector concept for FCC-ee”. In: (Feb. 2025). arXiv: 2502.21223 [physics.ins-det].
- [151] Carlotta Accettura et al. “Towards a muon collider”. In: *Eur. Phys. J. C* 83.9 (2023). [Erratum: *Eur.Phys.J.C* 84, 36 (2024)], p. 864. DOI: 10.1140/epjc/s10052-023-11889-x. arXiv: 2303.08533 [physics.acc-ph].
- [152] S. Jindariani et al. “Promising Technologies and R&D Directions for the Future Muon Collider Detectors”. In: (Mar. 2022). DOI: 10.2172/1881962. arXiv: 2203.07224 [physics.ins-det].

- [153] Charles Bell et al. “MAIA: A new detector concept for a 10 TeV muon collider”. In: (Jan. 2025). arXiv: 2502.00181 [physics.ins-det].
- [154] Paolo Andreetto et al. “MUSIC: A Multi-Purpose Detector Concept for Physics at the 10 TeV Muon Collider”. In: (Nov. 2025). arXiv: 2511.23273 [hep-ex].
- [155] Morris Swartz. “A Detailed Simulation of the CMS Pixel Sensor”. In: (July 2002).
- [156] Danush Shekar et al. “Sensor Co-design for *smartpixels*”. In: (Oct. 2025). arXiv: 2510.06588 [physics.ins-det].
- [157] Deniz Yilmaz, Liangyu Wu, and Julia Gonski. “Edge Machine Learning for Cluster Counting in Next-Generation Drift Chambers”. In: *39th Annual Conference on Neural Information Processing Systems: Includes Machine Learning and the Physical Sciences (ML4PS)*. Nov. 2025. arXiv: 2511.10540 [physics.ins-det].
- [158] Sandvine. *The Global Internet Phenomena Report*. [https://www.applogicnetworks.com/hubfs/Sandvine\\_Redesign\\_2019/Downloads/2024/GIPR/GIPR%202024.pdf](https://www.applogicnetworks.com/hubfs/Sandvine_Redesign_2019/Downloads/2024/GIPR/GIPR%202024.pdf). Accessed: 2025-09-03. Mar. 2024.
- [159] A. M. Sirunyan et al. “Particle-flow reconstruction and global event description with the CMS detector”. In: *JINST* 12.10 (2017), P10003. DOI: 10.1088/1748-0221/12/10/P10003. arXiv: 1706.04965 [physics.ins-det].
- [160] Giuseppe Di Guglielmo et al. “A Reconfigurable Neural Network ASIC for Detector Front-End Data Compression at the HL-LHC”. In: *IEEE Trans. Nucl. Sci.* 68.8 (2021), pp. 2179–2186. DOI: 10.1109/TNS.2021.3087100. arXiv: 2105.01683 [physics.ins-det].
- [161] Kihyuk Sohn, Honglak Lee, and Xinchun Yan. “Learning Structured Output Representation using Deep Conditional Generative Models”. In: *Advances in Neural Information Processing Systems*. Ed. by C. Cortes et al. Vol. 28. Curran Associates, Inc., 2015. URL: <https://proceedings.neurips.cc/paper/2015/file/8d55a249e6baa5c06772297520da2051-Paper.pdf>.
- [162] Rohan Shenoy et al. “Differentiable Earth mover’s distance for data compression at the high-luminosity LHC”. In: *Mach. Learn. Sci. Tech.* 4.4 (2023), p. 045058. DOI: 10.1088/2632-2153/ad1139. arXiv: 2306.04712 [hep-ex].
- [163] N. Akchurin et al. “Hadron and jet detection with a dual-readout calorimeter”. In: *Nucl. Instrum. Meth. A* 537 (2005), pp. 537–561. DOI: 10.1016/j.nima.2004.07.285.
- [164] Sehwook Lee, Michele Livan, and Richard Wigmans. “Dual-Readout Calorimetry”. In: *Rev. Mod. Phys.* 90.2 (2018), p. 025002. DOI: 10.1103/RevModPhys.90.025002. arXiv: 1712.05494 [physics.ins-det].
- [165] N. Akchurin et al. “On the use of neural networks for energy reconstruction in high-granularity calorimeters”. In: *JINST* 16.12 (2021), P12036. DOI: 10.1088/1748-0221/16/12/P12036. arXiv: 2107.10207 [physics.ins-det].
- [166] James Brau et al. “The SiD Digital ECal Based on Monolithic Active Pixel Sensors”. In: *EPJ Web of Conferences* 315 (Dec. 2024), p. 03005. DOI: 10.1051/epjconf/202431503005.
- [167] M. Breidenbach et al. *Updating the SiD Detector concept*. Oct. 2021. DOI: 10.48550/arXiv.2110.09965.
- [168] *Framework TDR for the LHCb Upgrade II*. Tech. rep. Geneva: CERN, 2021. DOI: <https://doi.org/10.17181/CERN.NTVH.Q21W>.
- [169] Javier Duarte et al. “Fast inference of deep neural networks in FPGAs for particle physics”. In: *Journal of instrumentation* 13.07 (2018), P07027.

- [170] Farah Fahim et al. *hls4ml: An Open-Source Codesign Workflow to Empower Scientific Low-Power Machine Learning Devices*. 2021. arXiv: 2103.05579 [cs.LG].
- [171] Martín Abadi et al. *TensorFlow: Large-Scale Machine Learning on Heterogeneous Systems*. Software available from tensorflow.org. 2015. URL: <https://www.tensorflow.org/>.
- [172] Francois Chollet et al. *Keras*. 2015. URL: <https://github.com/fchollet/keras>.
- [173] Claudionor N. Coelho et al. “Automatic heterogeneous quantization of deep neural networks for low-latency inference on the edge for particle detectors”. In: (2020). DOI: 10.48550/ARXIV.2006.10159. URL: <https://arxiv.org/abs/2006.10159>.
- [174] W. McDonald D. Gedecke. “A constant fraction of pulse height trigger for optimum time resolution”. In: *Nuclear Instruments and Methods* 55 (1967), p. 377. DOI: [https://doi.org/10.1016/0029-554X\(67\)90145-0](https://doi.org/10.1016/0029-554X(67)90145-0).
- [175] A. Gandrakota and CMS Collaboration. “Real-time Anomaly Detection at the L1 Trigger of CMS Experiment”. In: *Proceedings of Science (ICHEP2024)*. PoS ICHEP2024 (2025) 1025. 2025, p. 1025.
- [176] *Trigger monitoring and rate predictions using Enhanced Bias data from the ATLAS Detector at the LHC*. Tech. rep. All figures including auxiliary figures are available at <https://atlas.web.cern.ch/Atlas/GROUPS/PHYSICS/PUBNOTES/ATL-DAQ-PUB-2016-002>. Geneva: CERN, 2016. URL: <https://cds.cern.ch/record/2223498>.
- [177] Kai Lukas Unger et al. “A multi-Hough-based displaced vertex track trigger for the Belle II experiment”. In: *Journal of Instrumentation* 20.02 (Feb. 2025), p. C02051. DOI: 10.1088/1748-0221/20/02/C02051. URL: <https://doi.org/10.1088/1748-0221/20/02/C02051>.
- [178] D. S. Akerib et al. *Snowmass2021 Cosmic Frontier Dark Matter Direct Detection to the Neutrino Fog*. 2022. arXiv: 2203.08084 [hep-ex]. URL: <https://arxiv.org/abs/2203.08084>.
- [179] Katherine Freese, Mariangela Lisanti, and Christopher Savage. “Colloquium: Annual modulation of dark matter”. In: *Rev. Mod. Phys.* 85 (4 Nov. 2013), pp. 1561–1581. DOI: 10.1103/RevModPhys.85.1561. URL: <https://link.aps.org/doi/10.1103/RevModPhys.85.1561>.
- [180] Jonathan H. Davis. “Dark matter vs. neutrinos: the effect of astrophysical uncertainties and timing information on the neutrino floor”. In: *Journal of Cosmology and Astroparticle Physics* 2015.03 (Mar. 2015), p. 012. DOI: 10.1088/1475-7516/2015/03/012. URL: <https://dx.doi.org/10.1088/1475-7516/2015/03/012>.
- [181] Yi Zhuang et al. “Prospects for measuring the time variation of astrophysical neutrino sources at dark matter detectors”. In: *Phys. Rev. D* 110 (4 Aug. 2024), p. 043037. DOI: 10.1103/PhysRevD.110.043037. URL: <https://link.aps.org/doi/10.1103/PhysRevD.110.043037>.
- [182] J.S. Wilson et al. “The level-1 trigger for the SuperCDMS experiment at SNOLAB”. In: *Journal of Instrumentation* 17.07 (July 2022), P07010. ISSN: 1748-0221. DOI: 10.1088/1748-0221/17/07/p07010. URL: <http://dx.doi.org/10.1088/1748-0221/17/07/P07010>.
- [183] H. Meyer zu Theenhausen, B. von Krosigk, and J. S. Wilson. “Neural-network-based level-1 trigger upgrade for the SuperCDMS experiment at SNOLAB”. In: *JINST* 18.06 (2023), P06012. DOI: 10.1088/1748-0221/18/06/P06012. arXiv: 2212.07864 [physics.ins-det].

- [184] Mark R Anderson et al. “Performance of a convolutional autoencoder designed to remove electronic noise from p-type point contact germanium detector signals”. en. In: *Eur. Phys. J. C Part. Fields* 82.12 (Dec. 2022), p. 1084. ISSN: 1434-6044,1434-6052. DOI: 10.1140/epjc/s10052-022-11000-w.
- [185] Tongyao Pang et al. “Recorrputed-to-Recorrputed: Unsupervised Deep Learning for Image Denoising”. In: *2021 IEEE/CVF Conference on Computer Vision and Pattern Recognition (CVPR)*. 2021, pp. 2043–2052. DOI: 10.1109/CVPR46437.2021.00208.
- [186] Andrew Engel, Thomas Braine, and Christian Boutan. “Identifying environmentally induced calibration changes in cryogenic RF axion detector systems using deep neural networks”. In: *Review of Scientific Instruments* 96.12 (Dec. 2025), p. 123102. DOI: 10.1063/5.0272636. URL: <https://doi.org/10.1063/5.0272636>.
- [187] J. I. Crespo-Anadón. “The MicroBooNE Continuous Readout Stream for Detection of Supernova Neutrinos”. In: *J. Phys. Conf. Ser.* 1312.1 (2019), p. 012006. DOI: 10.1088/1742-6596/1312/1/012006. arXiv: 1907.02195 [physics.ins-det].
- [188] Antony Earle, Konstantinos Manolopoulos, and Ivana HRISTOVA. “Trigger Primitive Generation using FELIX FPGA system: A Case Study for DUNE”. In: *PoS ICHEP2024* (2025), p. 1139. DOI: 10.22323/1.476.1139.
- [189] P. Abratenko et al. “Demonstration and performance of an online data selection algorithm for liquid argon time projection chambers using MicroBooNE”. In: (Feb. 2026). arXiv: 2602.11138 [hep-ex].
- [190] Adam Abed Abud. *Real-time Hit Finding for the DUNE Experiment using AVX2 SIMD Intrinsic*. Talk presented on behalf of the DUNE collaboration at the 6th International Conference on Technology and Instrumentation in Particle Physics (TIPP 2023), Cape Town, South Africa. Sept. 2023. URL: <https://indico.tlabs.ac.za/event/112/contributions/2813/>.
- [191] Matthew D. Kistler, Wick C. Haxton, and Hasan Yüksel. “Tomography of Massive Stars from Core Collapse to Supernova Shock Breakout”. In: *Astrophys. J.* 778 (2013), p. 81. DOI: 10.1088/0004-637X/778/1/81. arXiv: 1211.6770 [astro-ph.CO].
- [192] S. Al Kharusi et al. “SNEWS 2.0: a next-generation supernova early warning system for multi-messenger astronomy”. In: *New J. Phys.* 23.3 (2021), p. 031201. DOI: 10.1088/1367-2630/abde33. arXiv: 2011.00035 [astro-ph.HE].
- [193] Adam Abed Abud et al. “Supernova pointing capabilities of DUNE”. In: *Phys. Rev. D* 111.9 (2025), p. 092006. DOI: 10.1103/PhysRevD.111.092006. arXiv: 2407.10339 [hep-ex].
- [194] Michael H. L. S. Wang. “Machine Learning-Based Extreme Data Reduction for Prompt Supernova Pointing at DUNE”. In: *IEEE Trans. Nucl. Sci.* 72.3 (2025), pp. 678–683. DOI: 10.1109/TNS.2024.3521357.
- [195] Yeon-jae Jwa et al. “Real-Time Inference With 2D Convolutional Neural Networks on Field Programmable Gate Arrays for High-Rate Particle Imaging Detectors”. In: *Front. Artif. Intell.* 5 (2022), p. 855184. DOI: 10.3389/frai.2022.855184. arXiv: 2201.05638 [physics.ins-det].
- [196] Lorenzo Ubaldi et al. “Extracting low energy signals from raw LArTPC waveforms using deep learning techniques — A proof of concept”. In: *Nucl. Instrum. Meth. A* 1028 (2022), p. 166371. DOI: 10.1016/j.nima.2022.166371. arXiv: 2106.09911 [physics.ins-det].

- [197] DUNE Collaboration, Babak Abi, et al. “Deep Underground Neutrino Experiment (DUNE), Far Detector Technical Design Report, Volume II: DUNE Physics”. In: (Feb. 2020). arXiv: 2002.03005 [hep-ex].
- [198] Luis Manzanillas. “Status of ProtoDUNE-II”. In: *Proceedings of 42nd International Conference on High Energy Physics — PoS(ICHEP2024)*. Vol. 476. 2024, p. 219. DOI: 10.22323/1.476.0219.
- [199] Pilar Coloma et al. “New physics searches using ProtoDUNE and the CERN SPS accelerator”. In: *Journal of High Energy Physics* 2024.1 (2024), pp. 1–18.
- [200] Christos Touramanis. *NP04 Annual Status Report to the SPSC, 2025*. Tech. rep. Geneva: CERN, 2025. URL: <https://cds.cern.ch/record/2932871>.
- [201] Tianqi Chen and Carlos Guestrin. “XGBoost: A Scalable Tree Boosting System”. In: *Proceedings of the 22nd ACM SIGKDD International Conference on Knowledge Discovery and Data Mining*. KDD ’16. ACM, Aug. 2016, pp. 785–794. DOI: 10.1145/2939672.2939785. URL: <http://dx.doi.org/10.1145/2939672.2939785>.
- [202] E.L. Snider and G. Petrillo. “LArSoft: toolkit for simulation, reconstruction and analysis of liquid argon TPC neutrino detectors”. In: *Journal of Physics: Conference Series* 898.4 (Oct. 2017), p. 042057. DOI: 10.1088/1742-6596/898/4/042057. URL: <https://dx.doi.org/10.1088/1742-6596/898/4/042057>.
- [203] S. Seo. *Anomaly Detection & Smart TPC*. DUNE AI/ML Kick-off Workshop. FERMILAB-SLIDES-25-0081-PPD; see also S. Seo, “Smart TPC: Feasibility Study” Fermilab LDRD pre-proposal (2024). Apr. 2025.
- [204] E. Novello, S. Seo, and M. Wang. *Real-Time Anomaly Detection in DUNE Raw Data*. Tech. rep. FERMILAB-PUB-25-0505-STUDENT. Fermilab, July 2025.
- [205] C. Kato, K. Ishidoshiro, and T. Yoshida. “Theoretical prediction of pre-supernova neutrinos and their detection”. Version v2. In: (2020). arXiv: 2006.02519 [astro-ph.HE].
- [206] G. Abarajithan et al. *CGRA4ML: A Framework to Implement Modern Neural Networks for Scientific Edge Computing*. 2024. arXiv: 2408.15561 [cs.AR].
- [207] Yeon-Jae Jwa et al. “Accelerating Deep Neural Networks for Real-time Data Selection for High-resolution Imaging Particle Detectors”. In: *2019 New York Scientific Data Summit: Data-Driven Discovery in Science and Industry*. June 2019. DOI: 10.1109/NYSDS.2019.8909784. arXiv: 2201.04740 [physics.ins-det].
- [208] J. Mitrevski. “Low energy LArTPC signal detection using anomaly detection”. Fast Machine Learning for Science Workshop, 2023. [Online]. Available: <https://indico.cern.ch/event/1283970/contributions/5550632/>. URL: [%7Bhttps://indico.cern.ch/event/1283970/contributions/5550632/](https://indico.cern.ch/event/1283970/contributions/5550632/)%7D.
- [209] V. Lian et al. “Denoising autoencoder for raw wireplane waveforms in dune’s LArTPC detector”. NSF HDR Postbaccalaureate Workshop 2023. [Online]. Available: <https://indico.cern.ch/event/1253923/contributions/5443551/>. URL: [%7Bhttps://indico.cern.ch/event/1253923/contributions/5443551/](https://indico.cern.ch/event/1253923/contributions/5443551/)%7D.
- [210] S. Chung et al. “Real-time Anomaly Detection for Liquid Argon Time Projection Chambers”. In: (Sept. 2025). arXiv:2509.21817 [hep-ex], submitted to JINST. arXiv: 2509.21817 [hep-ex].
- [211] R. Acciarri et al. “A Proposal for a Three Detector Short-Baseline Neutrino Oscillation Program in the Fermilab Booster Neutrino Beam”. In: (Mar. 2015). arXiv: 1503.01520 [physics.ins-det].

- [212] B. Abi et al. “The Single-Phase ProtoDUNE Technical Design Report”. In: (June 2017). arXiv: 1706.07081 [physics.ins-det].
- [213] Alejandro Yankelevich. “The ICEBERG Test Stand for DUNE Cold Electronics Development”. In: *25th International Workshop on Neutrinos from Accelerators*. Jan. 2025. arXiv: 2501.14838 [physics.ins-det].
- [214] Anthony Badea et al. “Intelligent pixel detectors: towards a radiation hard ASIC with on-chip machine learning in 28nm CMOS”. In: *PoS ICHEP2024* (2025), p. 1074. DOI: 10.22323/1.476.1074. arXiv: 2410.02945 [physics.ins-det].
- [215] Julia Gonski et al. “Embedded FPGA developments in 130 nm and 28 nm CMOS for machine learning in particle detector readout”. In: *JINST* 19.08 (2024), P08023. DOI: 10.1088/1748-0221/19/08/P08023. arXiv: 2404.17701 [cs.AR].
- [216] D. A. Dwyer et al. “LArPix: Demonstration of low-power 3D pixelated charge readout for liquid argon time projection chambers”. In: *JINST* 13.10 (2018), P10007. DOI: 10.1088/1748-0221/13/10/P10007. arXiv: 1808.02969 [physics.ins-det].
- [217] *Q-Pix*. <https://www.qpix.work/>. Accessed: 2026-02-23.
- [218] Babak Abi et al. “Deep Underground Neutrino Experiment (DUNE), Far Detector Technical Design Report, Volume II: DUNE Physics”. In: (Feb. 2020). arXiv: 2002.03005 [hep-ex].
- [219] A. Paudel et al. “Modeling Light Signals Using Data from the First Pulsed Neutron Source Program at the DUNE Vertical Drift ColdBox Test Facility at CERN Neutrino Platform”. In: (Dec. 2025). arXiv: 2512.10790 [hep-ex].
- [220] D. Akimov et al. “Observation of Coherent Elastic Neutrino-Nucleus Scattering”. In: *Science* 357.6356 (2017), pp. 1123–1126. DOI: 10.1126/science.aao0990. arXiv: 1708.01294 [nucl-ex].
- [221] D. Akimov et al. “First Measurement of Coherent Elastic Neutrino-Nucleus Scattering on Argon”. In: *Phys. Rev. Lett.* 126.1 (2021), p. 012002. DOI: 10.1103/PhysRevLett.126.012002. arXiv: 2003.10630 [nucl-ex].
- [222] S. Adamski et al. “First detection of coherent elastic neutrino-nucleus scattering on germanium”. In: (June 2024). arXiv: 2406.13806 [hep-ex].
- [223] D. Akimov et al. “The COHERENT Experimental Program”. In: *Snowmass 2021*. Apr. 2022. arXiv: 2204.04575 [hep-ex].
- [224] Alessandro Mirizzi et al. “Supernova Neutrinos: Production, Oscillations and Detection”. In: *Riv. Nuovo Cim.* 39.1-2 (2016), pp. 1–112. DOI: 10.1393/ncr/i2016-10120-8. arXiv: 1508.00785 [astro-ph.HE].
- [225] Angel Abusleme et al. “JUNO physics and detector”. In: *Prog. Part. Nucl. Phys.* 123 (2022), p. 103927. DOI: 10.1016/j.pnpnp.2021.103927. arXiv: 2104.02565 [hep-ex].
- [226] K. Abe et al. “Hyper-Kamiokande Design Report”. In: (May 2018). arXiv: 1805.04163 [physics.ins-det].
- [227] B. Abi et al. “Supernova neutrino burst detection with the Deep Underground Neutrino Experiment”. In: *Eur. Phys. J. C* 81.5 (2021), p. 423. DOI: 10.1140/epjc/s10052-021-09166-w. arXiv: 2008.06647 [hep-ex].
- [228] Chen’guang Su et al. “Performance of a Large-Volume Cryogenic Pure CsI Detector for CE $\nu$ NS and Low-Energy Rare-Event Searches”. In: (Sept. 2025). arXiv: 2509.17528 [physics.ins-det].

- [229] Charles R Qi et al. “Pointnet: Deep learning on point sets for 3d classification and segmentation”. In: *Proceedings of the IEEE conference on computer vision and pattern recognition*. 2017, pp. 652–660.
- [230] Hsu-Hsun Chin, Ren-Song Tsay, and Hsin-I Wu. *A High-Performance Adaptive Quantization Approach for Edge CNN Applications*. 2021. arXiv: 2107.08382 [cs.CV].
- [231] Clemens JS Schaefer et al. *Edge Inference with Fully Differentiable Quantized Mixed Precision Neural Networks*. 2023. arXiv: 2206.07741 [cs.LG].
- [232] Kyle Hoffpauir et al. “A Survey on Edge Intelligence and Lightweight Machine Learning Support for Future Applications and Services”. In: *ACM Journal of Data and Information Quality* (2023). DOI: 10.1145/3581759.
- [233] Miao Chen Jin, Yushi Hu, and Carlos A. Argüelles. “Two Watts is all you need: enabling in-detector real-time machine learning for neutrino telescopes via edge computing”. In: *JCAP* 06 (2024), p. 026. DOI: 10.1088/1475-7516/2024/06/026. arXiv: 2311.04983 [hep-ex].
- [234] Norman P. Jouppi, Cliff Young, Nishant Patil, et al. *In-Datacenter Performance Analysis of a Tensor Processing Unit*. 2017. arXiv: 1704.04760 [cs.AR].
- [235] Norman P. Jouppi et al. *TPU v4: An Optically Reconfigurable Supercomputer for Machine Learning with Hardware Support for Embeddings*. 2023. arXiv: 2304.01433 [cs.AR].
- [236] Google Coral. *The Edge TPU Dev Board*. <https://coral.ai/products/dev-board>. Retrieved: 05-25-2023.
- [237] Jeffrey Lazar et al. “Prometheus: An Open-Source Neutrino Telescope Simulation”. In: (Apr. 2023). arXiv: 2304.14526 [hep-ex].
- [238] *Tensorflow Lite Library*. <https://www.tensorflow.org/lite>. Retrieved: 04-24-2024.
- [239] *PyCoral EdgeTPU Compiler*. <https://coral.ai/docs/edgetpu/compiler/>. Retrieved: 05-25-2023.
- [240] *PyTorch ExecuTorch*. <https://pytorch.org/executorch-overview>. Retrieved: 10-20-2023.
- [241] Andreas Søgaard et al. “GraphNeT: Graph neural networks for neutrino telescope event reconstruction”. In: *J. Open Source Softw.* 8.85 (2023), p. 4971. DOI: 10.21105/joss.04971. arXiv: 2210.12194 [astro-ph.IM].
- [242] Mirco Huennefeld. “Reconstruction Techniques in IceCube using Convolutional and Generative Neural Networks”. In: *EPJ Web Conf.* 207 (2019). Ed. by C. Spiering, p. 05005. DOI: 10.1051/epjconf/201920705005.
- [243] IceCube Collaboration, M. G. Aartsen, et al. “The IceCube Neutrino Observatory: Instrumentation and Online Systems”. In: *JINST* 12.03 (2017), P03012. DOI: 10.1088/1748-0221/12/03/P03012. arXiv: 1612.05093 [astro-ph.IM].
- [244] S. Adrián-Martínez et al. “Sensitivity of the KM3NeT/ARCA neutrino telescope to point-like neutrino sources”. In: *Astropart. Phys.* 111 (2019), p. 100.
- [245] The IceCube Collaboration et al. “IceCube-Gen2: the Window to the Extreme Universe”. In: *J. Phys. G* 48.6 (2021), p. 060501. DOI: 10.1088/1361-6471/abbd48. arXiv: 2008.04323 [astro-ph.HE].
- [246] IceCube Collaboration, M. G. Aartsen, et al. “Multimessenger observations of a flaring blazar coincident with high-energy neutrino IceCube-170922A”. In: *Science* 361.6398 (2018), eaat1378. DOI: 10.1126/science.aat1378. arXiv: 1807.08816 [astro-ph.HE].

- [247] F. J. Yu, J. Lazar, and C. A. Argüelles. “Trigger-level event reconstruction for neutrino telescopes using sparse submanifold convolutional neural networks”. In: *Phys. Rev. D* 108 (2023), p. 063017.
- [248] B. Graham and L. van der Maaten. “Submanifold Sparse Convolutional Networks”. In: (2017). arXiv: 1706.01307.
- [249] P. Abratenko et al. “Semantic segmentation with a sparse convolutional neural network for event reconstruction in MicroBooNE”. In: *Phys. Rev. D* 103 (2021), p. 052012.
- [250] L. Dominé and K. Terao. “Scalable deep convolutional neural networks for sparse, locally dense liquid argon time projection chamber data”. In: *Phys. Rev. D* 102 (2020), p. 012005.
- [251] M. Hünnefeld. “Online Reconstruction of Muon-Neutrino Events in IceCube using Deep Learning Techniques”. MA thesis. TU Dortmund, 2017.
- [252] M. Agostini et al. “The Pacific Ocean Neutrino Experiment”. In: *Nature Astron.* 4 (2020), p. 913.
- [253] F. J. Yu, N. Kamp, and C. A. Argüelles. “Learning Efficient Representations of Neutrino Telescope Events”. In: *JINST* 20 (2025), P12010.
- [254] R. Abbasi et al. “A muon-track reconstruction exploiting stochastic losses for large-scale Cherenkov detectors”. In: *JINST* 16.08 (2021), P08034. DOI: 10.1088/1748-0221/16/08/P08034. arXiv: 2103.16931 [hep-ex].
- [255] A. Søgaaard et al. “GraphNeT: Graph neural networks for neutrino telescope event reconstruction”. In: *J. Open Source Softw.* 8 (2023), p. 4971.
- [256] M. Jin, Y. Hu, and C. A. Argüelles. “Two Watts is all you need: enabling in-detector real-time machine learning for neutrino telescopes via edge computing”. In: *JCAP* 06 (2024), p. 026.
- [257] S. Abe et al. “Search for Majorana neutrinos with the complete KamLAND-Zen dataset”. In: *Phys. Rev. Lett.* (Oct. 2025). DOI: 10.1103/jkfk6-48j8. URL: <https://link.aps.org/doi/10.1103/jkfk6-48j8>.
- [258] R. Nakamura et al. “Research and development toward KamLAND2-Zen”. In: *Journal of Physics: Conference Series*. Vol. 1468. IOP Publishing, 2020, p. 012256.
- [259] Charles R Qi et al. “Pointnet: Deep learning on point sets for 3d classification and segmentation”. In: *Proceedings of the IEEE conference on computer vision and pattern recognition*. 2017, pp. 652–660.
- [260] Alexander Migala et al. “Real-time Position Reconstruction for the KamLAND-Zen Experiment using Hardware-AI Co-design”. In: *arXiv preprint arXiv:2410.02991* (2024).
- [261] G. Abarajithan et al. “cgra4ml: A Hardware/Software Framework to Implement Neural Networks for Scientific Edge Computing”. In: *ACM Transactions on Reconfigurable Technology and Systems* 1.1 (Nov. 2025), pp. 1–33.
- [262] Zhenghao Fu et al. “Generative models for simulation of KamLAND-Zen”. In: *Eur. Phys. J. C* 84.6 (2024), p. 651. DOI: 10.1140/epjc/s10052-024-12980-7. arXiv: 2312.14372 [physics.data-an].
- [263] S. Abe et al. “Measurement of cosmic-ray muon spallation products in a xenon-loaded liquid scintillator with KamLAND”. In: *Phys. Rev. C* 107.5 (5 May 2023), p. 054612. DOI: 10.1103/PhysRevC.107.054612. arXiv: 2301.09307 [hep-ex]. URL: <https://link.aps.org/doi/10.1103/PhysRevC.107.054612>.

- [264] Benedikt Maier, Michael Spannowsky, and Simon Williams. *Continuous-variable photonic quantum extreme learning machines for fast collider-data selection*. 2025. arXiv: 2510.13994 [quant-ph]. URL: <https://arxiv.org/abs/2510.13994>.
- [265] Debanjan Das, James Wildridge, and Soon-Wook Jung. “Track clustering with a quantum annealer for primary vertex reconstruction at hadron colliders”. In: *arXiv preprint* (2019). arXiv: 1903.08879.
- [266] John C. Martens, John P. Ralston, and J. D. Tapia Takaki. “Quantum tomography for collider physics: Illustrations with lepton pair production”. In: *Eur. Phys. J. C* 78.1 (2018), p. 5. DOI: 10.1140/epjc/s10052-017-5455-8. arXiv: 1707.01638 [hep-ph].
- [267] I. Béjar Alonso et al. *High-Luminosity Large Hadron Collider (HL-LHC): Technical Design Report*. Tech. rep. CERN-2020-010. CERN, 2020.
- [268] X. Ju et al. “Graph Neural Networks for Particle Reconstruction in High Energy Physics Detectors”. In: *arXiv preprint* (2020). arXiv: 2003.11603 [physics.ins-det].
- [269] P. W. Battaglia et al. “Interaction Networks for Learning about Objects, Relations and Physics”. In: *arXiv preprint* (2016). arXiv: 1612.00222 [cs.LG].
- [270] J. Biamonte et al. “Quantum Machine Learning”. In: *Nature* 549 (2017), pp. 195–202.
- [271] Santosh Parajuli. “Quantum-Enhanced Graph Neural Networks for Particle Tracking in High-Energy Physics”. In: *Proceedings of the Connecting the Dots Workshop (CTD 2025)*. PROC-CTD2025-45. CERN, Feb. 2026.
- [272] S. Amrouche et al. “The Tracking Machine Learning Challenge: Accuracy Phase”. In: *arXiv preprint* (2019). arXiv: 1904.06778 [physics.data-an].
- [273] V. Bergholm et al. “PennyLane: Automatic Differentiation of Hybrid Quantum-Classical Computations”. In: *arXiv preprint* (2018). arXiv: 1811.04968 [quant-ph].
- [274] M. J. Atkinson et al. *ACORN: A Charged Object Reconstruction Network*. 2024. DOI: 10.5281/zenodo.14526454.
- [275] Zhongtian Dong et al. “Quantum Sensing Radiative Decays of Neutrinos and Dark Matter Particles”. In: *arXiv preprint* (2025). arXiv: 2508.09139 [hep-ph].
- [276] DarQ Collaboration. “Search for Dark Photon Dark Matter with a Mass around 36.1  $\mu\text{eV}$  Using a Frequency-tunable Cavity Controlled through a Coupled Superconducting Qubit”. In: *arXiv preprint* (2025). arXiv: 2505.15619 [hep-ex].
- [277] Cristián Peña et al. “High energy particle detection with large area superconducting microwire array”. In: *JINST* 20.03 (2025), P03001. DOI: 10.1088/1748-0221/20/03/P03001. arXiv: 2410.00251 [hep-ex].
- [278] Christina Wang et al. “Towards high-efficiency particle detection using superconducting microwire arrays”. In: *JINST* 20.12 (2025), P12033. DOI: 10.1088/1748-0221/20/12/P12033. arXiv: 2510.11725 [physics.ins-det].
- [279] L. Rota et al. “The SparkPix-S ASIC for the sparsified readout of 1 MHz frame-rate X-ray cameras at LCLS-II”. In: *J. Instrum.* 19.1 (2024).
- [280] Y. Sun et al. “Nonuniform flow dynamics probed by nanosecond X-ray speckle visibility spectroscopy”. In: *Phys. Rev. Lett.* 127 (2021).
- [281] Y. Sun et al. “Realizing split-pulse X-ray photon correlation spectroscopy”. In: *Phys. Rev. Research* 2 (2020).
- [282] Y. Sun et al. “Dynamics of nanoscale phase decomposition in laser ablation”. In: *arXiv:2407.10505* (2024).

- [283] M. Oquab et al. “DINOv2: Learning robust visual features without supervision”. In: *TMLR* (2024).
- [284] A. Radford et al. “Learning transferable visual models from natural language supervision (CLIP)”. In: *Proc. ICML*. 2021.
- [285] R. Rombach et al. “High-resolution image synthesis with latent diffusion models”. In: *Proc. IEEE CVPR*. 2022.
- [286] Y. Lipman et al. “Flow matching for generative modeling”. In: *ICLR* (2023).
- [287] H. Chen et al. “Reblur2Deblur: Deblurring videos via self-supervised learning”. In: *Proc. IEEE ICCP*. 2018, pp. 1–9.
- [288] J.-B. Alayrac et al. “Flamingo: A visual language model for few-shot learning”. In: *Adv. Neural Inf. Process. Syst.* 35 (2022), pp. 23716–23736.
- [289] J. Li et al. “BLIP-2: Bootstrapping language-image pre-training”. In: *Proc. ICML*. 2023.
- [290] L. Berthier and G. Biroli. “Theoretical perspective on the glass transition and amorphous materials”. In: *Rev. Mod. Phys.* 83.2 (2011), pp. 587–645.
- [291] G. Biroli and J. P. Garrahan. “Perspective: The glass transition”. In: *J. Chem. Phys.* 138.12 (2013).
- [292] T. Fujita et al. “Directly observing atomic-scale relaxations of a glass-forming liquid using femtosecond XPCS”. In: *arXiv:2312.08613* (2023).
- [293] Pardis Niknejadi et al. “Free-electron laser inverse-Compton interaction x-ray source”. In: *Physical Review Accelerators and Beams* 22.4 (2019), p. 040704.
- [294] K. Floettmann. *A Space Charge Tracking Algorithm ASTRA*. <http://www.desy.de/~mpyf1o/>.
- [295] M. J. De Loos and S. B. Van Der Geer. “General Particle Tracer: A new 3D code for accelerator and beamline design”. In: *5th European Particle Accelerator Conference*. Vol. 1241. 1996.
- [296] Michael Borland. *Elegant: A flexible SDDS-compliant code for accelerator simulation*. Tech. rep. LS-287. Argonne National Lab., IL (US), 2000.
- [297] William M. Fawley. “Algorithm for loading shot noise microbunching in multidimensional, free-electron laser simulation codes”. In: *Physical Review Special Topics-Accelerators and Beams* 5.7 (2002), p. 070701.
- [298] S. Reiche. “Genesis 1.3: a fully 3d time-dependent fel simulation code”. In: *Nuclear Instruments and Methods in Physics Research Section A: Accelerators, Spectrometers, Detectors and Associated Equipment* 429 (1999), p. 243.
- [299] N. Bidault et al. “Recommissioning of the university of hawai’i linac and free electron laser”. In: *16th International Particle Accelerator Conference (JACoW)*. in press. 2025.
- [300] A. Weinberg, N. Bidault, and S. Li. “Research plans for the university of hawai’i accelerator and free-electron laser lab”. In: *16th International Particle Accelerator Conference (JACoW)*. in press. 2025.
- [301] A. L. Edelen et al. “Neural Networks for Modeling and Control of Particle Accelerators”. In: *IEEE Transactions on Nuclear Science* 63.2 (2016). DOI: 10.1109/TNS.2016.2543203. URL: <https://doi.org/10.1109/TNS.2016.2543203>.

- [302] A. Edelen and X. Huang. “Machine Learning for Design and Control of Particle Accelerators: A Look Backward and Forward”. In: *Annual Review of Nuclear and Particle Science* 74 (2024), pp. 557–581. DOI: 10.1146/annurev-nucl-121423-100719. URL: <https://doi.org/10.1146/annurev-nucl-121423-100719>.
- [303] R. Roussel et al. “Bayesian optimization algorithms for accelerator physics”. In: *Physical Review Accelerators and Beams* 27 (2024), p. 084801. DOI: 10.1103/PhysRevAccelBeams.27.084801. URL: <https://doi.org/10.1103/PhysRevAccelBeams.27.084801>.
- [304] K. Rajput et al. “Outlook towards deployable continual learning for particle accelerators”. In: *Machine Learning: Science and Technology* 6 (2025), p. 031001. DOI: 10.1088/2632-2153/adeb45. URL: <https://doi.org/10.1088/2632-2153/adeb45>.
- [305] J. Duris et al. “Bayesian optimization of a free electron laser”. In: *Physical Review Letters* 124 (2020), p. 124801. DOI: 10.1103/PhysRevLett.124.124801. URL: <https://doi.org/10.1103/PhysRevLett.124.124801>.
- [306] R. Roussel et al. “Turn-key constrained parameter space exploration for particle accelerators using Bayesian active learning”. In: *Nature Communications* 12 (2021), p. 5612. DOI: 10.1038/s41467-021-25757-3. URL: <https://doi.org/10.1038/s41467-021-25757-3>.
- [307] A. Scheinker, A. Edelen, et al. “Demonstration of Model-Independent Control of the Longitudinal Phase Space of Electron Beams in the Linac-Coherent Light Source with Femtosecond Resolution”. In: *Physical Review Letters* 121 (2018), p. 044801. DOI: 10.1103/PhysRevLett.121.044801. URL: <https://doi.org/10.1103/PhysRevLett.121.044801>.
- [308] T. Boltz et al. “Leveraging prior mean models for faster Bayesian optimization of particle accelerators”. In: *Scientific Reports* 15 (2025), p. 12232. DOI: 10.1038/s41598-025-95297-z. URL: <https://doi.org/10.1038/s41598-025-95297-z>.
- [309] A. Hanuka et al. “Physics-model informed Gaussian process for online optimization of particle accelerators”. In: *Physical Review Accelerators and Beams* 24 (2021), p. 072802. DOI: 10.1103/PhysRevAccelBeams.24.072802. URL: <https://doi.org/10.1103/PhysRevAccelBeams.24.072802>.
- [310] S. Miskovich et al. “Multipoint-BAX: a new approach for efficiently tuning particle accelerator emittance via virtual objectives”. In: *Machine Learning: Science and Technology* 5 (2024), p. 015004. DOI: 10.1088/2632-2153/ad169f. URL: <https://doi.org/10.1088/2632-2153/ad169f>.
- [311] A. Edelen et al. “Machine learning for orders of magnitude speedup in multiobjective optimization of particle accelerator systems”. In: *Physical Review Accelerators and Beams* 23 (2020), p. 044601. DOI: 10.1103/PhysRevAccelBeams.23.044601. URL: <https://doi.org/10.1103/PhysRevAccelBeams.23.044601>.
- [312] L. Gupta. “Improving surrogate model accuracy for the LCLS-II injector frontend using convolutional neural networks and transfer learning”. In: *Machine Learning: Science and Technology* 2 (2021), p. 045025. DOI: 10.1088/2632-2153/ac27ff. URL: <https://doi.org/10.1088/2632-2153/ac27ff>.
- [313] A. Edelen et al. “Experience integrating online modeling, adaptive digital twin infrastructure, and ML-based tuning for accelerator control at SLAC”. In: *20th International Conference on Accelerator and Large Experimental Physics Control Systems (ICALPCS’25)*. 2025, paper MOCG001. DOI: 10.18429/JACoW-ICALPCS2025-MOCG001. URL: <https://doi.org/10.18429/JACoW-ICALPCS2025-MOCG001>.

- [314] R. Roussel et al. “Xopt and Badger: a machine learning ecosystem for real-time accelerator control and optimization”. In: *20th International Conference on Accelerator and Large Experimental Physics Control Systems (ICALEPCS’25)*. 2025, paper WESV001. URL: <https://epaper.kek.jp/icalepcs2025/pdf/WESV001.pdf>.
- [315] C. Mayes et al. “Lightsource Unified Modeling Environment (LUME), a start-to-end simulation ecosystem”. In: *12th International Particle Accelerator Conference (IPAC’21)*. 2021, paper THPAB217. DOI: 10.18429/JACoW-IPAC2021-THPAB217. URL: <https://doi.org/10.18429/JACoW-IPAC2021-THPAB217>.
- [316] S. Liuzzo et al. “Optimisation of the Touschek Lifetime in Synchrotron Light Sources Using Badger”. In: *18th International Conference on Accelerator and Large Experimental Physics Control Systems (ICALEPCS 2023)*. 2023, paper MO3A001. DOI: 10.18429/JACoW-ICALEPCS2023-MO3A001. URL: <https://doi.org/10.18429/JACoW-ICALEPCS2023-MO3A001>.
- [317] A. Mishra et al. “A Start to End Machine Learning Approach to Maximize Scientific Throughput from the LCLS-II-HE”. In: *Synchrotron Radiation News* 38.4 (2024), pp. 10–17. DOI: 10.1080/08940886.2025.2538420.
- [318] Next Generation Triggers. *Next Generation Triggers - Public proposal*. Dec. 2023. DOI: 10.17181/9jcg-n-r3690. URL: <https://doi.org/10.17181/9jcg-n-r3690>.
- [319] “Fast Machine Learning”. In: Fast machine learning techniques for scientific data analysis. Fermi National Accelerator Laboratory, Batavia, IL, USA, Sept. 2019. URL: <https://indico.cern.ch/event/822126/>.
- [320] “Fast Machine Learning for Science Workshop 2023”. In: Workshop on accelerated machine learning and inference. Imperial College London, UK, Sept. 2023. URL: <https://indico.cern.ch/event/1283970/>.
- [321] “Fast Machine Learning for Science Conference 2024”. In: Hybrid workshop-style conference on machine learning for science. Purdue University, West Lafayette, IN, USA, Oct. 2024. URL: <https://indico.cern.ch/event/1387540/>.
- [322] “Fast Machine Learning for Science Conference 2025”. In: Annual conference on accelerated machine learning methods and scientific applications. ETH Zurich, Zurich, Switzerland, Sept. 2025. URL: <https://indico.cern.ch/event/1496673/>.
- [323] Alberto Di Meglio et al. “Quantum Computing for High-Energy Physics: State of the Art and Challenges. Summary of the QC4HEP Working Group”. In: *PRX Quantum* 5.3 (2024), p. 037001. DOI: 10.1103/PRXQuantum.5.037001. arXiv: 2307.03236 [quant-ph].
- [324] CERN. *CERN Quantum Technology Initiative*. <https://quantum.cern/>. Accessed: 2025. 2024.
- [325] Chen Zhang et al. “Optimizing FPGA-based accelerator design for deep convolutional neural networks”. In: *Proceedings of the 2015 ACM/SIGDA international symposium on field-programmable gate arrays*. 2015, pp. 161–170.
- [326] Jiantao Qiu et al. “Going deeper with embedded FPGA platform for convolutional neural network”. In: *Proceedings of the 2016 ACM/SIGDA international symposium on field-programmable gate arrays*. 2016, pp. 26–35.
- [327] Eriko Nurvitadhi et al. “Can FPGAs beat GPUs in accelerating next-generation deep neural networks?” In: *Proceedings of the 2017 ACM/SIGDA international symposium on field-programmable gate arrays*. 2017, pp. 5–14.

- [328] Tae Min Hong et al. “Nanosecond machine learning event classification with boosted decision trees in FPGA for high energy physics”. In: *Journal of Instrumentation* 16.08 (2021), P08016.
- [329] ST Roche et al. “Nanosecond anomaly detection with decision trees and real-time application to exotic Higgs decays”. In: *Nature Communications* 15.1 (2024), p. 3527.
- [330] BT Carlson et al. “Nanosecond machine learning regression with deep boosted decision trees in FPGA for high energy physics”. In: *Journal of Instrumentation* 17.09 (2022), P09039.
- [331] Yaman Umuroglu et al. “LogicNets: Co-designed neural networks and circuits for extreme-throughput applications”. In: *2020 30th International Conference on Field-Programmable Logic and Applications (FPL)*. IEEE. 2020, pp. 291–297.
- [332] Javier Duarte et al. “Low-latency machine learning inference on FPGAs”. In: *NeurIPS Workshop on Machine Learning and the Physical Sciences (ML4PS)*. 2019.
- [333] Ahmed Sanaullah et al. “Real-time data analysis for medical diagnosis using FPGA-accelerated neural networks”. In: *BMC bioinformatics* 19.Suppl 18 (2018), p. 490.
- [334] Rouzbeh Molaei Imenabadi et al. “FPGA-Accelerated CNN Reconstruction for Low-Power Sparse-Array Ultrasound Imaging”. In: *IEEE transactions on ultrasonics, ferroelectrics, and frequency control* (2025).
- [335] J Leland et al. “Image Reconstruction Algorithms on an FPGA”. In: *2024 IEEE Nuclear Science Symposium (NSS), Medical Imaging Conference (MIC) and Room Temperature Semiconductor Detector Conference (RTSD)*. IEEE. 2024, pp. 1–1.
- [336] Spencer Balliet et al. “Harnessing FPGA for real-time AI-driven PET imaging”. In: *Medical Imaging 2025: Image-Guided Procedures, Robotic Interventions, and Modeling*. Vol. 13408. SPIE. 2025, pp. 439–444.
- [337] Praveen Gurunath Bharathi et al. “Machine learning-assisted event classification in cadmium zinc telluride positron emission tomography detectors leveraging entanglement-informed angular correlations”. In: *Scientific Reports* (2025).
- [338] Yue Yan et al. “Innovative Approaches in Precision Radiation Oncology: Advanced Imaging Technologies and Challenges Which Shape the Future of Radiation Therapy”. In: *Frontiers in Medicine* 12 (2025), p. 1686593.
- [339] Zhiqiang Hu et al. “Image-mode performance characterisation of a positron emission tomography subsystem designed for biology-guided radiotherapy (BgRT)”. In: *The British Journal of Radiology* 96.1141 (2023), p. 20220387.
- [340] Hiroki Shirato et al. “Physical aspects of a real-time tumor-tracking system for gated radiotherapy”. In: *International Journal of Radiation Oncology\*Biophysics* 48.4 (2000), pp. 1187–1195.
- [341] Gregory C Sharp et al. “Prediction of respiratory tumour motion for real-time image-guided radiotherapy”. In: *Physics in Medicine & Biology* 49.3 (2004), p. 425.
- [342] Shervin M Shirvani et al. “Biology-guided radiotherapy: redefining the role of radiotherapy in metastatic cancer”. In: *The British journal of radiology* 94.1117 (2021), p. 20200873.
- [343] Murat Surucu et al. “Commissioning of a novel PET-Linac for biology-guided radiotherapy (BgRT)”. In: *Medical Physics* 51.6 (2024), pp. 4389–4401.
- [344] YANG Xin et al. “Application of PET-LINAC in biology-guided radiotherapy”. In: *Chinese Journal of Medical Instrumentation* 47.3 (2023), pp. 237–241.

- [345] Oluwaseyi M Oderinde et al. “The technical design and concept of a PET/CT linac for biology-guided radiotherapy”. In: *Clinical and translational radiation oncology* 29 (2021), pp. 106–112.
- [346] Qin Liu et al. “Real-time FPGA-based hardware neural network for fault detection and isolation in more electric aircraft”. In: *IEEE Access* 7 (2019), pp. 159831–159841.
- [347] Alexandru Vasilache et al. “Low-Power Vibration-Based Predictive Maintenance for Industry 4.0 using Neural Networks: A Survey”. In: *arXiv preprint arXiv:2408.00516* (2024).
- [348] Julián Caba et al. “Concurrent execution of lossy compression and anomaly detection of hyperspectral images on FPGA devices”. In: *Journal of Real-Time Image Processing* 22.3 (2025), p. 112.
- [349] Milad Memarzadeh et al. “Unsupervised Anomaly Detection in High-Dimensional Flight Data Using Convolutional Variational Auto-Encoder”. In: *26th SIGKDD Conference on Knowledge Discovery and Data Mining*. ARC-E-DAA-TN77606. 2020.
- [350] Noah M Michels et al. “Real-time classification of radiation pulses with piled-up recovery using an FPGA-based artificial neural network”. In: *IEEE Access* 11 (2023), pp. 78074–78083.
- [351] Zhiqiang Que et al. “Real-time anomaly detection for flight testing using AutoEncoder and LSTM”. In: *2019 international conference on field-programmable technology (ICFPT)*. IEEE. 2019, pp. 379–382.
- [352] Abhishek Das et al. “An FPGA-based network intrusion detection architecture”. In: *IEEE Transactions on Information Forensics and Security* 3.1 (2008), pp. 118–132.
- [353] Duc-Minh Ngo et al. “HH-NIDS: Heterogeneous hardware-based network intrusion detection framework for IoT security”. In: *Future Internet* 15.1 (2022), p. 9.
- [354] Muhammad Ali Farooq et al. “High Throughput Neural Network for Network Intrusion Detection on FPGAs: An Algorithm-Architecture Interaction.” In: *ICISSP*. 2024, pp. 423–429.
- [355] Man Wu and Masaaki Kondo. “A High-Throughput Network Intrusion Detection System Using On-Device Learning on FPGA”. In: *2024 IEEE 17th International Symposium on Embedded Multicore/Many-core Systems-on-Chip (MCSoc)*. IEEE. 2024, pp. 426–433.
- [356] Cuong Pham-Quoc, Tran Hoang Quoc Bao, and Tran Ngoc Think. “FPGA/AI-powered architecture for anomaly network intrusion detection systems”. In: *Electronics* 12.3 (2023), p. 668.
- [357] Eshan Singh, Clark Barrett, and Subhasish Mitra. “E-QED: electrical bug localization during post-silicon validation enabled by quick error detection and formal methods”. In: *International Conference on Computer Aided Verification*. Springer. 2017, pp. 104–125.
- [358] Patrick Girard, Shawn Blanton, and Li-C Wang. *Machine Learning Support for Fault Diagnosis of System-on-Chip*. Springer, 2023.
- [359] Andrew DeOrio et al. “Machine learning-based anomaly detection for post-silicon bug diagnosis”. In: *2013 Design, Automation & Test in Europe Conference & Exhibition (DATE)*. IEEE. 2013, pp. 491–496.
- [360] Philipp Wagner, Thomas Wild, and Andreas Herkersdorf. “DiaSys: Improving SoC insight through on-chip diagnosis”. In: *Journal of Systems Architecture* 75 (2017), pp. 120–132.
- [361] Yuting Cao, Hao Zheng, and Sandip Ray. “A communication-centric observability selection for post-silicon system-on-chip integration debug”. In: *20th International Symposium on Quality Electronic Design (ISQED)*. IEEE. 2019, pp. 278–283.